Optimization of Advanced Oxidation Processes for Water Reuse

Effect of Effluent Organic Matter on Organic Contaminant Removal

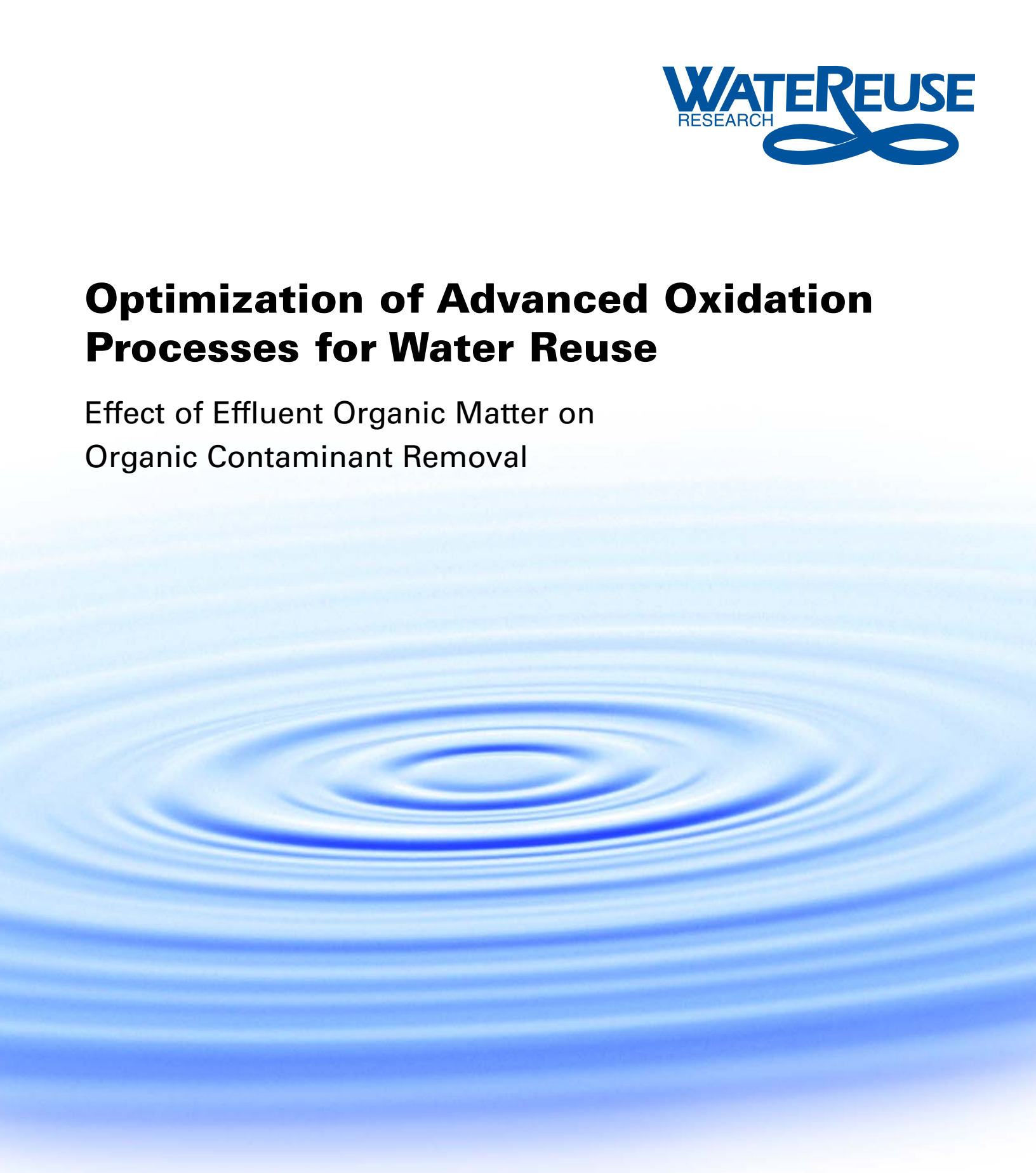

WateReuse Research Foundation

Optimization of Advanced Oxidation Processes for Water Reuse

About the WateReuse Research Foundation

The mission of the WateReuse Research Foundation is to conduct and promote applied research on the reclamation, recycling, reuse, and desalination of water. The Foundation's research advances the science of water reuse and supports communities across the United States and abroad in their efforts to create new sources of high quality water through reclamation, recycling, reuse, and desalination while protecting public health and the environment.

The Foundation sponsors research on all aspects of water reuse, including emerging chemical contaminants, microbiological agents, treatment technologies, salinity management and desalination, public perception and acceptance, economics, and marketing. The Foundation's research informs the public of the safety of reclaimed water and provides water professionals with the tools and knowledge to meet their commitment of increasing reliability and quality.

The Foundation's funding partners include the Bureau of Reclamation, the California State Water Resources Control Board, the California Energy Commission, and the California Department of Water Resources. Funding is also provided by the Foundation's Subscribers, water and wastewater agencies, and other interested organizations.

Optimization of Advanced Oxidation Processes for Water Reuse

Effect of Effluent Organic Matter on Organic Contaminant Removal

Fernando L. Rosario-Ortiz, Eric C. Wert, Shane A. Snyder
Southern Nevada Water Authority

Stephen P. Mezyk
California State University at Long Beach

Cosponsor
Bureau of Reclamation

WateReuse Research Foundation
Alexandria, VA

Disclaimer

This report was sponsored by the WateReuse Research Foundation and cosponsored by the Bureau of Reclamation. The Foundation, its Board Members, and the project cosponsor assume no responsibility for the content of this publication or for the opinions or statements of facts expressed in the report. The mention of trade names of commercial products does not represent or imply the approval or endorsement of the WateReuse Research Foundation, its Board Members, or the cosponsor. This report is published solely for informational purposes.

For more information, contact:
WateReuse Research Foundation
1199 North Fairfax Street, Suite 410
Alexandria, VA 22314
703-548-0880
703-548-5085 (fax)
www.WateReuse.org/Foundation

WateReuse Research Foundation Project Number: WRF-06-012
WateReuse Research Foundation Product Number: 06-012-1

ISBN: 978-1-934183-37-3
Library of Congress Control Number: 2011921781

Printed in the United States of America

Printed on Recycled Paper

CONTENTS

TABLES

FIGURES

ABBREVIATIONS

AOP	Advanced qxidation processes
BTPP	Bench-top pilot plant
C	Concentration
CCWRD	Clark County Water Reclamation District
CRW	Colorado River Water
CT	Ozone exposure (concentration x time)
CVS	Calibration verification samples
d	Polidispersity
Da	Dalton
DEET	N,N-diethyl-3-methylbenzamide
E	Fluence rate
E2	Estradiol
EDCs	Endocrine disrupting compounds
EE2	17α-Ethynylestradiol
EEM	Excitation emission matrix
EfOM	Effluent organic matter
EE_o	Electrical energy per order
ESI	Electrospray ionization
F	Flow
FI	Fluorescence index
gpm	Gallons per minute
H	Fluence
H_2O_2	Hydrogen peroxide
IDL	Instrument detection limit
IOD	Instantaneous ozone demand
IPR	Indirect potable reuse
J	Joule
$k_{EfOM\text{-}OH}$	Reaction rate constant between EfOM and $^{\bullet}OH$
$k_{MP\text{-}OH}$	Reaction rate constant between micropollutant and $^{\bullet}OH$
LACSD	Los Angeles County Sanitation District
LC	Liquid chromatography
LC-UV	Liquid chromatpgraphy with UV detection
LC-MS/MS	Liquid chromatography with tandem mass spectrometry
LP	Low pressure

LVNV	Las Vegas, NV
MDL	Method detection limit
MS	Mass spectrometry
MRL	Method reporting limit
MRM	Multiple reaction monitoring
MW	Molecular weight
MW_W	Weight average molecular weight
MW_N	Number average molecular weight
NDMA	N-nitrosodimethylamine
NOM	Natural organic matter
$^{\bullet}OH$	Hydroxyl radical
$[^{\bullet}OH]_{ss}$	Steady state concentration of hydroxyl radical
OM	Organic matter
O_3	Ozone
P	Rated power
PCFL	Pinellas County, FL
pCBA	para-chlorobenzoic acid
PEG	Polyethylene glycol
PRAM	Polarity rapid assessment method
PFOA	Perfluorooctanoic acid
PFOS	Perfluorooctanesulfonic acid
QA/QC	Quality assurance/quality control
RC	Retention coefficient
R_{CT}	Ratio of $^{\bullet}OH$ exposure to O_3 exposure
$R_{OH,UV}$	Ratio of $^{\bullet}OH$ exposure to fluence
RL	Reporting limit
RMCO	Rocky Mountain region of Colorado
RMCO-N	Rocky Mountain region of Colorado (North)
RMCO-S	Rocky Mountain region of Colorado (South)
SAX	Strong anion exchanger
SEC	Size exclusion chromatography
SNWA	Southern Nevada Water Authority
SPE	Solid phase extraction
SPE-LC-MS/MS	Solid phase extraction and Liquid Chromatography with tandem mass spectrometry
SR	Scavenging rate
SUVA	Specific UV absorbance
TCEP	Tris(2-chloroethyl) phosphate
TCPP	Tris(1-chloro-2-propyl) phosphate
TiO_2	Titanium dioxide
TOC	Total organic carbon
U.S.	United States

UV	Ultraviolet
UVA	UV absorbance
UVT	UV transmittance
WRP	Water reclamation plant
WWTF	Wastewater treatment facility
WWTP	23rd Avenue Wastewater Treatment Plant

FOREWORD

The WateReuse Research Foundation, a nonprofit corporation, sponsors research that advances the science of water reclamation, recycling, reuse, and desalination. The Foundation funds projects that meet the water reuse and desalination research needs of water and wastewater agencies and the public. The goal of the Foundation's research is to ensure that water reuse and desalination projects provide high-quality water, protect public health, and improve the environment.

An Operating Plan guides the Foundation's research program. Under the plan, a research agenda of high-priority topics is maintained. The agenda is developed in cooperation with the water reuse and desalination communities including water professionals, academics, and Foundation subscribers. The Foundation's research focuses on a broad range of water reuse research topics including:

- Defining and addressing emerging contaminants
- Public perceptions of the benefits and risks of water reuse
- Management practices related to indirect potable reuse
- Groundwater recharge and aquifer storage and recovery
- Evaluation and methods for managing salinity and desalination
- Economics and marketing of water reuse

The Operating Plan outlines the role of the Foundation's Research Advisory Committee (RAC), Project Advisory Committees (PACs), and Foundation staff. The RAC sets priorities, recommends projects for funding, and provides advice and recommendations on the Foundation's research agenda and other related efforts. PACs are convened for each project and provide technical review and oversight. The Foundation's RAC and PACs consist of experts in their fields and provide the Foundation with an independent review, which ensures the credibility of the Foundation's research results. The Foundation's Project Managers facilitate the efforts of the RAC and PACs and provide overall management of projects.

The Foundation's primary funding partners include the Bureau of Reclamation, California State Water Resources Control Board, the California Energy Commission, Foundation subscribers, water and wastewater agencies, and other interested organizations. The Foundation leverages its financial and intellectual capital through these partnerships and other funding relationships.

The use of indirect potable reuse (IPR) to augment and sustain water supplies is being actively evaluated to confront availability problems. However, one of the main issues associated with IPR is the presence of micropollutants that are of potential health and ecological concern. The main goal of this study was to evaluate advanced oxidation processes (AOPs) performance from the perspective of the reactivity of $^{\bullet}OH$ toward EfOM and the effects on the efficiency of AOPs for micropollutant oxidation.

Joseph Jacangelo
Chair
WateReuse Research Foundation

G. Wade Miller
Executive Director
WateReuse Research Foundation

ACKNOWLEDGMENTS

This project was funded by the WateReuse Research Foundation in collaboration with the Bureau of Reclamation. The team also acknowledges support from Trojan Technologies, Clark County Water Reclamation District and the Radiation Laboratory, University of Notre Dame. The project team acknowledges the contributions of the following individuals and utilities that participated in this project:

Project Advisory Committee
Dr. Paul Westerhoff, *Arizona State University*
Dr. William Cooper, *University of California, Irvine*
Dr. Ken Ishida, *Orange County Water District*
Dr. Phil Brandhuber, *HDR Engineering*
Saied Delagah, *Bureau of Reclamation*

Principal Investigators
Fernando L. Rosario-Ortiz, *University of Colorado at Boulder (formerly of the Southern Nevada Water Authority)*
Eric C. Wert, *Southern Nevada Water Authority*
Shane A. Snyder, *University of Arizona (formerly of the Southern Nevada Water Authority)*
Stephen P. Mezyk, *California State University at Long Beach*

Other Project Participants
David Rexing, *Southern Nevada Water Authority*
Brett Vanderford, *Southern Nevada Water Authority*
Dr. Douglas Mawhinney, *Southern Nevada Water Authority*
Rebecca Trenholm, *Southern Nevada Water Authority*
Julia Lew, *Southern Nevada Water Authority*
Janie Holady, *Southern Nevada Water Authority*
Mei Xin, *Southern Nevada Water Authority*
Tony Baik, *Southern Nevada Water Authority*
Dr. Mark Benotti, *Southern Nevada Water Authority*
Frankie Lewis, *Southern Nevada Water Authority*
Devin Doud, *California State University, Long Beach*
Dr. Urs von Gunten, *EAWAG*
Dr. Karl Linden, *University of Colorado, Boulder*
Adam Festger, *Trojan Technologies, Ontario, Canada*
Dr. Naoko Munakata, *Sanitation Districts of Los Angeles County*
Dr. Douglas D. Drury, *Clark County Water Reclamation District*
Kevin Freeley, *Metro Wastewater Reclamation District*
Marsha Pryor, *Pinellas County, Florida*
Paul Kinshella, *City of Phoenix, Arizona*

EXECUTIVE SUMMARY

The use of indirect potable reuse (IPR) to augment and sustain water supplies is being actively evaluated to confront availability problems. However, one of the main issues associated with IPR is the presence of micropollutants that are of potential health and ecological concern. The application of advanced oxidation processes (AOPs), including ozone, ozone with hydrogen peroxide (H_2O_2), and UV light with H_2O_2, has been shown to be effective for the removal of micropollutants. The increased effectiveness of AOPs for contaminant removal is due to the formation of hydroxyl radicals ($^{\bullet}OH$), which non-selectively react with a wide range of micropollutants. This reactivity is described by the second-order reaction rate constant between $^{\bullet}OH$ and a specific micropollutant *P* ($k_{P\text{-}OH}$). However, the $^{\bullet}OH$ radical also reacts with water quality components (e.g., alkalinity, total organic carbon [TOC]), limiting AOP effectiveness, a problem commonly referred to as scavenging. An overall calculation of the scavenging is based on the contribution of each of these problematic species, in terms of concentration and reactivity. For instance, the effect of alkalinity can be evaluated utilizing its reactivity with $^{\bullet}OH$ ($k_{Alk.\text{-}OH}$) and its concentration. However, the role of the TOC in wastewater, commonly referred to as effluent organic matter (EfOM), has not been evaluated in detail. This results in an assumption that all TOC will react with $^{\bullet}OH$ equally, although in practice this may not be the case. Detailed information on the specific role of EfOM on the performance of AOPs (i.e., overall scavenging) for water reuse is lacking, resulting in the need to better understand this relationship in order to effectively optimize AOPs for micropollutant removal.

The main goal of this study was to evaluate AOP performance from the perspective of the reactivity of $^{\bullet}OH$ toward EfOM and the effects on the efficiency of AOPs for micropollutant oxidation. The overall $^{\bullet}OH$ scavenging capacity of the EfOM is directly correlated to the second-order reaction rate constant between EfOM and $^{\bullet}OH$ ($k_{EfOM\text{-}OH}$). The magnitude of this parameter will greatly affect overall micropollutant removal. As part of this study, quantification of $k_{EfOM\text{-}OH}$ values was performed using samples collected from different wastewater utilities to evaluate potential variability in EfOM reactivity. Emphasis was placed on the quantification of $k_{EfOM\text{-}OH}$ utilizing non-processed bulk samples. The obtained results indicated that the $k_{EfOM\text{-}OH}$ value varied between sites, from a low value of 0.27×10^9 M_C^{-1} s^{-1} to a high value of 1.21×10^9 M_C^{-1} s^{-1}. This represents a difference of a factor of almost five, which is considerable in terms of the efficiency of micropollutant oxidation at sites with differing wastewater quality and EfOM composition. The differences were attributed to variability in EfOM as a function of background natural organic matter (NOM) as well as in differences in the wastewater treatment process. In addition, quantification of the $k_{EfOM\text{-}OH}$ at one site during two separate sampling events resulted in vastly different values (0.45 and 1.21×10^9 M_C^{-1} s^{-1}). These results suggest that differences in EfOM reactivity could be observed as a function of process variables within a specific treatment process. This conclusion is also supported by the results obtained from the sampling of two parallel treatment trains within a single wastewater facility. In this case, the measured $k_{EfOM\text{-}OH}$ values were 0.27 and 1.02×10^9 M_C^{-1} s^{-1} for each train.

In order to account for variations and to provide a way to predict kinetic values, a model was developed that considered the variability between different sites and related these to specific properties of the EfOM. The model included EfOM polarity, molecular weight, fluorescence

index, and specific UV absorbance. The model was shown to be able to predict the variability in the rate constant values with an R^2>0.99 (n=8). Application of this model would allow utilities to estimate the overall •OH scavenging capacity at a specific site and whether this value would change based on the properties of the EfOM.

The role of differences in EfOM and •OH reactivity, as measured by $k_{EfOM\text{-}OH}$, on the application of AOPs for contaminant removal was also evaluated. Both ozone and UV-based AOPs were tested using samples collected from three wastewater facilities. The efficacy of UV/H_2O_2 for contaminant removal was evaluated at bench-scale using a low pressure UV system. For these experiments, the oxidation of six pharmaceuticals was evaluated. Removal was dependent on the reactivity of •OH with EfOM, as well as on differences in nitrite and alkalinity values, although it was shown that EfOM was the most significant driver for the differences in removal. The three sites evaluated had $k_{EfOM\text{-}OH}$ values ranging between 0.68 and 2.72 x 10^9 M_C^{-1} s^{-1}, as predicted using the developed model. In waters where the overall scavenging rate (including the role of EfOM) was low, higher contaminant removals were observed, indicating that reactivity and concentration of the EfOM is an important factor to consider. In addition, UV/H_2O_2 treatment was evaluated at pilot-scale at one wastewater treatment facility. This facility was chosen based on the lowest expected value for the reactivity between •OH and EfOM. In addition, this facility had low levels of nitrite. The removal of a group of pharmaceuticals was evaluated and, under low flow conditions that represent the highest UV doses, removal of the pharmaceuticals was higher than 90% for 14 out of 20 compounds studied.

The application of ozone was evaluated at both bench-scale and pilot-scale. Results showed that different EfOM composition had a direct impact on O_3 demand, decay rate, and corresponding •OH exposure based on the O_3:TOC ratio. EfOM characterization using size exclusion chromatography (SEC) and specific UV absorbance (SUVA) showed the level of transformation of humic substances with higher molecular weight corresponded well to the amount of O_3 demand. When operating with dosages less than the O_3 demand, minimal •OH was formed for contaminant oxidation. As a result, compounds that react primarily with •OH were less than 30% removed when operating below the O_3 demand of the wastewater. When exceeding the O_3 demand, removal became a function of each individual compound's reactivity with •OH. At higher O_3 dosages, significant •OH exposure was observed in all the wastewaters tested, and under these conditions, removal of micropollutants that are fast-reacting with O_3 was greater than 95%.

The results from this study indicate that, depending on the specific properties of the EfOM (including molecular mass and polarity), AOP treatment could be optimized by varying conditions that are targeted for a specific water quality. The observed variability in EfOM reactivity also suggests that in some cases the efficacy of an AOP for micropollutant removal may be dependent on the changes to the EfOM. Further work should be performed targeting specific treatment of EfOM in order to reduce •OH scavenging and maximize AOP efficiency.

CHAPTER 1

INTRODUCTION

1.1 BACKGROUND

The diminishing availability of freshwater has generated global interest in indirect potable reuse (IPR) as an alternative to augment traditional sources of water. This diminishing availability is due to population growth, drought, climate change, increased pollution of existing supplies, or a combination thereof. These conditions have left many communities in a precarious situation, resulting in the need to expand water sources. Because of limited access to new fresh water resources, many communities are considering IPR to augment existing water supplies.

IPR refers to the use of treated wastewater to enhance existing water supplies (i.e., surface or groundwater augmentation). Because a wastewater source is used to augment existing water supplies, additional requirements are established to guarantee that the quality of the produced water is not affected by the degree of water reclamation. As such, there are many challenges associated with IPR, including public safety (i.e., reduction of biological and chemical pollutants) and issues associated with advanced treatment necessary to limit the impact of the water quality on the receiving waters.

Over the past decade, there has been a proliferation in the number of reports regarding micropollutants in wastewater. Two of the primary classes of micropollutants that have reached a pinnacle of public and scientific interest are pharmaceuticals and endocrine disrupting chemicals (EDCs). For instance, in 2008 the US Senate held two hearings on the topic of pharmaceuticals and EDCs in US waters. The Associated Press also completed a series of articles in 2008 that reported the occurrence of pharmaceuticals in the drinking water of more than 41 million Americans. Several reports have shown that trace levels of EDCs can impact the reproductive physiology of aquatic species exposed to wastewater outfalls. It is now clear that conventional wastewater treatment is not completely effective for the removal of micropollutants. In order for IPR to gain public acceptance, it is critical that sound science is used to define and apply the appropriate barriers against micropollutants needed for the protection of public and ecological health. Furthermore, detailed scientific analysis of the selected barriers is needed to maximize efficiency and minimize overall costs.

One of the most efficient water treatment processes for the removal of micropollutants is the application of advanced oxidation processes (AOPs). AOPs have been proven to efficiently eliminate a wide array of organic micropollutants (Huber et al., 2003; Rosenfeldt and Linden, 2004; Snyder et al., 2007; Snyder et al., 2006a); however, the degree of efficacy is highly variable, depending on water quality and the actual process applied. For instance, ozone has been shown to effectively remove a majority of representative pharmaceuticals and EDCs from water (Snyder et al., 2007). Ultraviolet light coupled with hydrogen peroxide (UV/H_2O_2) also has been shown to be largely effective for trace organic contaminant removal. In fact, UV/H_2O_2 is prescribed as a mandated barrier in California IPR with groundwater injection. Although the application of AOPs shows great promise, there are many unanswered questions regarding the relationship of water quality (specifically the concentration and reactivity of the organic matter (OM)) on process efficacy. The primary

goal of this project is to quantify the impact of water quality (specifically the role of OM) on advanced oxidation processes for the removal of micropollutants.

1.2 ADVANCED OXIDATION PROCESSES (AOPs)

The term AOPs refers to a series of advanced oxidative treatments based on the formation of strong radical oxidizers, such as the hydroxyl radical ($^{\bullet}OH$) (Acero et al., 2000; von Gunten, 2003; von Sonntag, 2007). The formation of these radicals results in improved removal of many micropollutants, as compared to other oxidants, because of their greater oxidative capacity. For example, the electrochemical oxidation potential of $^{\bullet}OH$ is significantly greater than other commonly used oxidants (see Table 1.1).

Table 1.1. Oxidizing Potential of Various Oxidants

Oxidizing Agent	Electrochemical Oxidation Potential (V)
Hydroxyl Radical ($^{\bullet}OH$)	2.80
Ozone	2.08
Hydrogen Peroxide (H_2O_2)	1.78
Chlorine	1.36
Chlorine dioxide	1.27

Once formed, $^{\bullet}OH$ can rapidly react with micropollutants, resulting in the elimination of the contaminant. The reactions between $^{\bullet}OH$ and micropollutants are classified as second-order reactions ($k_{MP\text{-}OH}$), where the overall reaction rate will be dependent on the concentration of both $^{\bullet}OH$ and the specific chemical. The general chemical reaction between micropollutants and $^{\bullet}OH$ is represented in eq. 1.1. The reaction results in the formation of products, which themselves can also be further oxidized ultimately leading to complete mineralization and formation of carbon dioxide. The reaction rate for this process is represented by eq. 1.2, where the total rate of the reaction is dependent on the reaction rate constant and the concentration of both micropollutants and $^{\bullet}OH$ ($C_{micropollutants}$ and C_{OH}). Reported reaction rate constants between $^{\bullet}OH$ and micropollutants in water are on the order of $10^{8\text{-}10}$ M^{-1} s^{-1} (Buxton et al., 1988); higher than the direct reaction rate constants for other oxidants (e.g. ozone). Table 1.2 presents example reaction rate constants values for $^{\bullet}OH$ and micropollutants.

$$\text{Micropollutant} + {}^{\bullet}OH \xrightarrow{k_{TrOC-OH}} \text{Products} \qquad (1.1)$$

$$r_{M-OH} = k_{M-OH} C_{OH} C_M \qquad (1.2)$$

Table 1.2. Reaction Rate Constants for the Reactions Between •OH With a Selected Group of Micro-Pollutants

Compound Name	$k_{P\text{-}OH}$ (M^{-1} s^{-1}) (Huber et al., 2003)
Carbamazepine	8.8×10^9
Diazepam	7.2×10^9
Diclofenac	7.5×10^9
Ibuprofen	7.4×10^9
Iopromide	3.3×10^9
Sulfamethoxazole	5.5×10^9

The formation of •OH radicals can be accomplished in different ways, depending on the specific requirements of the process and the applied AOP technology. Common types of AOPs include ozone[1], ozone with hydrogen peroxide (O_3/H_2O_2), and UV/H_2O_2. These types of AOPs differ in the general mechanisms for the formation of •OH and in the specific role of the applied reactants and conditions. In the case of UV/H_2O_2, •OH is formed by the direct photolysis of hydrogen peroxide. This process, with a quantum yield of unity, yields one •OH per molecule of H_2O_2 for one photon.

$$H_2O_2 + h\nu \rightarrow {}^{\bullet}OH$$

Although the formation of •OH via this process is efficient, the fraction of the overall photons (*hv*) needed to break down the hydrogen peroxide is reduced by the absorption of light by other water quality components, most important OM. Direct absorption of *hv* by specific organic micropollutants may result in direct removal (photolysis) depending on the specific properties of the compound. For example, absorption of *hv* results in the removal of N-nitrosodimethylamine (NDMA); (Sharpless and Linden, 2003).

The application of ozone with hydrogen peroxide also results in the formation of •OH as shown in the following (von Gunten, 2003). The application of ozone to waters with high total organic carbon (TOC) concentrations also results in the formation of •OH through a reaction with ambient OM. Direct reactions with ozone in addition result in micropollutants removal, although this process is more selective than reactions with •OH.

$$O_3 + OH^- \rightarrow {}^{\bullet}OH$$

$$H_2O_2 \rightarrow HO_2^-$$

$$O_3 + HO_2^- \rightarrow \rightarrow {}^{\bullet}OH$$

[1] The application of ozone to waters with high TOC is generally considered to be an AOP.

1.3 THE IMPACT OF WATER QUALITY COMPONENTS ON •OH AVAILABILITY

One of the major issues associated with the application of AOPs is the role of the water quality on the process, specifically the potential scavenging of the available •OH and subsequent reduction in the efficiency of micropollutant removal. This overall scavenging rate (SR) of the water can be estimated using eq. 1.3, which accounts for the contribution of all the species that react with •OH (not including the contribution of micropollutants), including alkalinity, nitrite, and effluent organic matter (EfOM). Knowledge of the concentration of these species, together with the corresponding reaction rate constants allow for the estimation of the overall SR and subsequent estimation of the efficacy toward micropollutant oxidation. Figure 1.1 shows calculated scavenging rates for three wastewaters showing the contributions of nitrite and EfOM that dominate in terms of overall scavenging.

$$SR \approx k_{HCO_3^- - \bullet OH}[HCO_3^-] + k_{CO_3^{2-} - \bullet OH}[CO_3^{2-}] + k_{NO_2^- - \bullet OH}[NO_2^-] + k_{EfOM - \bullet OH}[EfOM] \qquad (1.3)$$

Although the contributions of nitrite, carbonate, and bicarbonate to eq. 1.3 can be easily measured by quantifying the concentrations of these compounds, the role of the EfOM is more difficult to assess. The overall concentration of EfOM is reported in terms of the TOC. From a simple mass balance perspective, EfOM is comprised of recalcitrant drinking water and natural organic matter (NOM), in addition to other components added during anthropogenic use (i.e., synthetic organic compounds) and by-products from the biological wastewater treatment (Shon et al., 2006). As opposed to other components of the water quality, there are no chemical models to describe the physicochemical properties of EfOM and usually bulk parameters are used (including absorbance and TOC). However, measurement of TOC does not offer any information with regard to chemical properties of EfOM, therefore it is difficult to accurately establish its role on the overall •OH scavenging.

Only sparse data are available with regard to the chemistry between EfOM and •OH. In order to predict the effect of EfOM on the level of •OH availability, an accurate value for its second-order reaction rate constant ($k_{EfOM\text{-}OH}$) is needed. Most of the previous work done on the chemistry between OM and •OH was based on NOM isolates. In the past, it has been assumed that the rate constant for •OH reaction with NOM isolates, $k_{NOM\text{-}OH}$, to be on average 3×10^8 $M_C^{-1}s^{-1}$ (based on 12 g of carbon per mole-M_C). In addition, a recent report determined the second-order rate between •OH and NOM using an electron pulse radiolysis technique, with an average value of 2.23×10^8 M_C^{-1} s^{-1} for Suwannee River fulvic acid and other humic acids collected at wastewater plants (Westerhoff et al., 2007). In general, the values obtained have been approximately 3×10^8 M_C^{-1} s^{-1}. However, the use of kinetic parameters obtained from NOM isolates for wastewater applications (with EfOM) may result in erroneous estimations of scavenging capacity because of the reactivity of other components. In addition, the reactivity of EfOM toward •OH needs to be evaluated at different sites in order to evaluate its variability in overall scavenging. Last, the overall efficiency of AOPs for micropollutant removal needs to be evaluated as a function of different sources of EfOM.

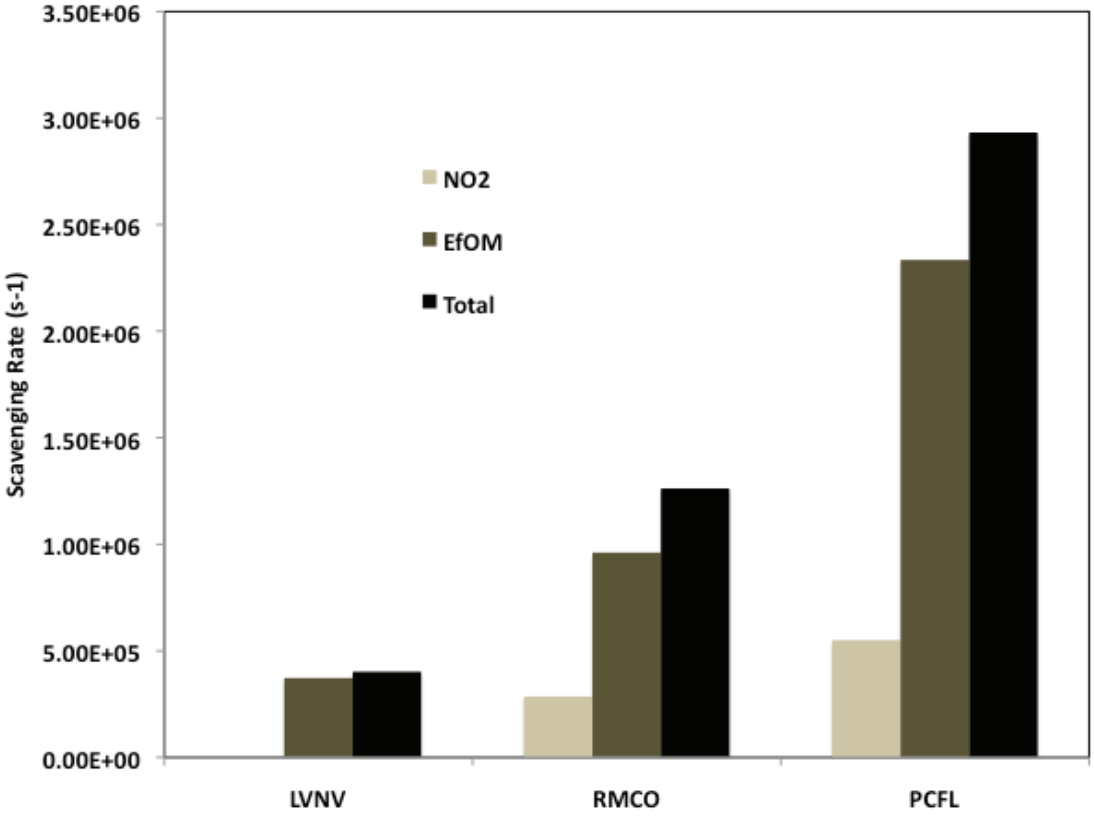

Figure 1.1. Overall scavenging rate and contributions by EfOM and nitrite for three wastewaters.

1.4 OBJECTIVES

The application of AOPs for water reuse to remove micropollutants requires a detailed understanding of how to optimize these processes. One of the main aspects that needs to be understood is the potential change in $^{\bullet}OH$ scavenging capacity of the water as a function of the type of EfOM. Furthermore, detailed information is needed on how to estimate this effect and how to change the processes accordingly.

The main objective of this project was to provide parameters for the optimization of AOPs for water reuse applications by providing guidelines based on the expected removal of micropollutants during AOP treatment as a function of the water quality (EfOM). In order to accomplish this, three specific areas were evaluated:

1. Understanding methods used to quantify $^{\bullet}OH$.
2. Performing a detailed evaluation of EfOM reactivity toward $^{\bullet}OH$.
3. Evaluation of the efficiency of AOPs (UV and ozone) for contaminant removal as a function of the water quality, specifically the EfOM reactivity.

This report is organized based on the aforementioned objectives. Chapter 2 describes the approach taken toward the experimental goals, including selection of utilities and analytical

methods. Chapter 3 describes the methodology used to quantify the •OH radical. Chapter 4 presents the results obtained during the evaluation of the scavenging capacity of EfOM from different sites, including the preliminary model developed. Chapters 5 and 6 present results on the application of ozone, ozone/H_2O_2 and UV/H_2O_2 for the removal of organic micropollutants as a function of the water quality. In addition, these two chapters offer insight into the application of AOPs at different sites. Chapter 7 provides overall project conclusions and implications.

As an additional aspect of this project, the efficiency of TiO_2 photocatalysis for the removal of micropollutants was evaluated. This information is summarized in Appendix A. The evaluations were made in drinking water.

CHAPTER 2

PROJECT APPROACH

2.1 PARTICIPATING UTILITIES

The evaluation of the reactivity between EfOM and •OH was done by measuring $k_{EfOM\text{-}OH}$ with samples collected at different sites and treatment processes. Seven wastewater treatment processes from six different utilities in different geographical regions were selected (see Table 2.1). The regions evaluated included the southeast, middle states, and the southwest. Each utility was also selected based on different treatments and water qualities.

2.2 SAMPLE COLLECTION

All bulk water samples were collected after secondary and advanced treatment but before disinfection (by either chlorine or UV). Samples were collected in 1L amber bottles, cooled overnight, and then shipped to the Southern Nevada Water Authority (SNWA) regulatory and compliance laboratory for analysis. At SNWA, samples were processed through 0.45 µm filters and stored at 4 ºC.

For the kinetic studies, eight samples were collected from the seven facilities shown in Table 2.1. One additional sample was collected at a later date at LVNV (these samples are labeled LVNV(A) and LVNV(B)). One additional sample, labeled LVNV(C) was collected at a later date to examine the effect of oxidation on the second-order reaction rates between EfOM and •OH. Samples for kinetic studies were shipped overnight to the Radiation Laboratory, University of Notre Dame, in ice-chilled coolers. These waters were then stored at ~2^{o}C until analysis. Potassium thiocyanate of the highest purity available was obtained from the Aldrich Chemical Company (St. Louis, MO) and used as received. The potassium thiocyanate was dried overnight before its use in these experiments.

For the bench-scale UV and ozone AOP tests, wastewater effluent samples were collected from three of the five wastewater treatment facilities (WWTFs) located in Las Vegas, Nevada (LVNV); the Rocky Mountain Region of Colorado (RMCO); and Pinellas County, Florida (PCFL). Samples were shipped overnight from each utility in 20-gallon plastic barrels to accommodate both bench-scale and pilot-scale experiments. Upon arrival, samples were collected for water quality analysis, specifically nitrite and TOC. The remaining sample was refrigerated at 4°C until the ozonation tests were performed the following day.

Table 2.1. Participating Utilities and Their Sample Collection and Treatments

Participating Utility	Designation	Location	Secondary Treatment	Sample Collection	Advanced Treatment
Clark County Water Reclamation District	LVNV	Las Vegas, NV	Activated sludge	Before UV disinfection	UV disinfection
Metro Wastewater Reclamation District (North Complex)	RMCO-N	Denver, CO	Activated sludge[1]	Pre-chlorine	Nitrification/limited denitrification, Cl_2
Metro Wastewater Reclamation District (South Complex)	RMCO-S	Denver, CO	Activated sludge[2]	Filtered effluent	
LA County Sanitation District	LACSD	LA, CA	Activated sludge/gravity filters	Filtered effluent	Nitrification/denitrification, Cl_2
William E Dunn Water Reclamation Facility	PCFL	Pinellas County, FL	Activated sludge	Filtered effluent	Denitrification, Cl_2
Cave Creek Water Reclamation Plant	WRP	Phoenix, AZ	Activated sludge	Tertiary effluent	UV, Cl_2
23rd Avenue Wastewater Treatment Plant	WWTP	Phoenix, AZ	Activated sludge	Pre-chlorine	Cl_2

Note. [1]Air-fed activated sludge. [2]Pure oxygen-fed system.

2.3 ANALYTICAL METHODS

2.3.1 Bulk Water EfOM Parameters

Bulk parameters, including TOC, UV absorbance, alkalinity, total organic nitrogen, and ammonia were quantified using standard methods (APHA, 1998). These analyses were conducted at the labs at the Southern Nevada Water Authority.

2.3.2 EfOM Characterization

Polarity characterization was done using the Polarity Rapid Assessment Method (PRAM). The experimental conditions of this method have been detailed previously (Rosario-Ortiz et al., 2007a; 2007b). In brief, solid phase extraction (SPE) cartridges (Alltech Associates, Deerfield, IL) were cleaned by passing through 3–5 mL of Milli-Q water. After cleaning, samples were loaded onto these cartridges. Flow (1.2 mL/min) was controlled with a syringe pump (KD Scientific, Holliston, MA) and maximum breakthrough was measured by ultraviolet absorbance (UVA) at 254 nm (Lambda 45, Perkin Elmer, Boston, MA). The retention coefficient (RC) was defined as one minus the maximum breakthrough level achieved (eq. 2.1) and describes the capacity of each SPE cartridge for specific components of the EfOM:

$$RC = 1 - \frac{C_{\max}}{C_0} \tag{2.1}$$

In this expression, C_o and C_{max} refer to the initial sample concentration and maximum breakthrough concentration (between 4–8 min) as measured by UVA.

EfOM size characterization was performed using SEC. An Agilent 1100 LC system (Palo Alto, CA) with a Toyopearl HW-50 S 250 x 20 mm column (Grom Chromatography, Rottenburg, Germany) was used. The injection volume was 1.8 mL. A diode array from Agilent was used as detector (Model 1100 Palo Alto, CA), monitoring at 254 nm. The mobile phase consisted of a phosphate buffer (0.028 M) adjusted to pH 6.8 ± 0.1. The flow rate was held at 1.0 mL/min. Polyethylene glycols (PEG; Fluka, Milwaukee, WI) were used for calibration and to estimate the weight average molecular weight (MW_W), as shown in eq. 2.2. MW_W values are presented in Daltons (Da).

$$M_w = \frac{\sum_{i=1}^{N} h_i M_i}{\sum_{i=1}^{N} h_i} \tag{2-2}$$

The fluorescence excitation-emission matrix (EEM) was recorded using a PTI fluorometer (Birmingham, NJ). Fluorescence EEM parameters were as follows: excitation from 220–460 nm in 5-nm steps, emission from 280–580 nm at 4 nm intervals, 2 nm bandwidth, and 0.1 sec integration time. The intensity of all EEM spectra was normalized on a daily basis by dividing by the intensity of the Raman water line using 350 nm excitation and 397 nm emission wavelengths. First- and second-order inner filtering effects were corrected following procedures from MacDonald et al. (1997). Data processing was done using Matlab (Version 7.4.0.287, R2007a, Natick, MA). Fluorescence index (FI) was obtained by calculating the

ratio of the emission at 450 nm by the emission at 500 nm after excitation at 370 nm (McKnight et al., 2001).

2.3.3 Kinetic Measurements

The linear accelerator electron pulse radiolysis facility at the Radiation Laboratory, University of Notre Dame, was used for the determination of $k_{EfOM\text{-}OH}$ rate constant values in this study. This irradiation and transient absorption detection system has been described in detail elsewhere (Whitham et al., 1995). Experiments were performed on individual bulk waters that had been sparged with high purity N_2O (~20 min/500 mL) to completely remove dissolved oxygen.

The radiolysis of water, or dilute aqueous solutions (solute concentrations less than 0.1 M), produces free radicals according to the following stoichiometry (Buxton et al., 1988):

$$H_2O \text{ --}\backslash\backslash\backslash\backslash\backslash\rightarrow [0.28]\bullet OH + [0.06]\bullet H + [0.27]e^-_{aq} + [0.05]H_2 + [0.07]H_2O_2 + [0.27]H^+$$

where the numbers in brackets are the yields in units of μmol/J for each species production. The total radical concentrations typically generated during the pulse experiments were ~2–4 μM per pulse.

Before each experiment, the water sample was saturated with N_2O to quantitatively convert the hydrated electrons, e_{aq}^- and hydrogen atoms, $H^\bullet$, to $^\bullet OH$ radicals, (Buxton et al., 1988):

$$e_{aq}^- + N_2O + H_2O \rightarrow N_2 + OH^- + {}^\bullet OH \qquad k_e = 9.1 \times 10^9\ M^{-1}\ s^{-1}$$

$$^\bullet H + N_2O \rightarrow {}^\bullet OH + N_2 \qquad k_H = 2.1 \times 10^6\ M^{-1}\ s^{-1}$$

The high reactivity of the produced $^\bullet OH$ means that it rapidly reacts with all components of the water matrix present, including EfOM, alkalinity, inorganics, and other organic compounds such as micropollutants of concern (present at ng/L levels). However, consideration of the relative concentrations of all the components and their reactivity toward $^\bullet OH$ for this matrix reveals that only EfOM and alkalinity reaction were significant for the waters studied.

Initial experiments showed no significant transient absorption from the EfOM over the wavelength range 250–800 nm upon its reaction with $^\bullet OH$. Therefore, the $^\bullet OH$ reaction rate constants were obtained for all these wastewaters using thiocyanate competition kinetics. The $^\bullet OH$ rate constants measurements were based on the competing reactions (Buxton et al., 1988):

$$^\bullet OH + SCN^- (+ SCN^-) \rightarrow (SCN)_2^{-\bullet} \qquad k_{SCN\text{-}} = 1.05 \times 10^{10}\ M^{-1}\ s^{-1}$$

$$^\bullet OH + EfOM \rightarrow \text{products} \qquad k_{EfOM\text{-}OH}$$

$$^\bullet OH + HCO_3^- \rightarrow H_2O + CO_3^{-\bullet} \qquad k_{HCO3\text{-}} = 8.5 \times 10^6\ M^{-1}\ s^{-1}$$

$^{\bullet}OH + CO_3^{2-} \rightarrow OH^- + CO_3^{-\bullet}$ $k_{CO32-} = 3.9 \times 10^8\ M^{-1}\ s^{-1}$

The concentration of added SCN^- was varied between ~30–150 μM by injecting known volumes of a 10 mm stock KSCN solution, and the absorbance of the $(SCN)_2^{-\bullet}$ transient at 475 nm was measured. By rearranging the standard competition kinetics equation (Buxton et al., 1988);

$$\frac{Abs^{o}_{SCN^-}}{Abs_{SCN^-}} = 1 + \frac{k_X[X]}{k_{SCN^-}[SCN^-]} \tag{2.3}$$

the following expression is obtained:

$$\frac{1}{Abs_{SCN^-}} = \frac{1}{Abs^{o}_{SCN^-}} + \left(\frac{k_X}{k_{SCN^-}} * \frac{[X]}{Abs^{o}{}_{SCN^-}}\right)\left(\frac{1}{[SCN^-]}\right) \tag{2.4}$$

where we sum the EfOM and carbonate reactions together (with the total concentration of these two species designated as [X]). Plotting the inverse of the maximum $(SCN)_2^{-\bullet}$ transient absorption (designated as $1/Abs_{SCN^-}$) against the inverse of the added thiocyanate concentration ($1/[SCN^-]$) yields a straight line with the value of the slope equal to $k_x[X]/(k_{SCN^-}*Abs^{o}_{SCN^-})$ and intercept equal to $1/Abs^{o}_{SCN^-}$. To obtain absolute $Abs^{o}_{SCN^-}$ absorbance values, corrections needed to be made for the $(SCN)_2^{-\bullet}$ formation equilibrium at these low SCN^- concentrations:

$SCN^{\bullet} + SCN^- = (SCN)_2^{-\bullet}$ $K = 2.0 \times 10^5$

and also for the significant decay of the $(SCN)_2^{-\bullet}$ radical on the timescales of study. Figure 2.1a shows the decay kinetics for $(SCN)_2^{-\bullet}$ for N_2O-saturated PCFL water at pH 7.79 and 22.9°C. Solid lines correspond to fitted second-order decays for the 29.1 (∇), 51.4 (Δ), 77.5 (O) and 131.1 μM (□) added SCN^-.

Figure 2.1b presents typical transformed plots for PCFL (□), RMCO-S (Δ) and LVNV (A) (O) waters. Error bars correspond to one standard deviation, from values obtained in (a). From the ratio of the determined slope to intercept parameters, the value of $k_x[X]/k_{SCN^-}$ is derived. Because the value of k_{SCN^-} is known ($1.05 \times 10^{10}\ M^{-1}\ s^{-1}$ (Buxton et al., 1988)), the pseudo-first-order rate constant $k_x[X]$ is derived $(8.56 \pm 0.26) \times 10^5$, $(4.85 \pm 0.16) \times 10^5$, and $(2.72 \pm 0.15) \times 10^5\ s^{-1}$, respectively). However, this rate constant includes contribution from the alkalinity (i.e., carbonate ($k_{CO32-}[CO_3^{2-}]$) and bicarbonate ($k_{HCO3-}[HCO_3^-]$)), which will also react rapidly with $^{\bullet}OH$ (Buxton et al., 1988). Using known values for the alkalinity and pH of the solutions, the contribution of carbonate and bicarbonate can be factored out of the rate constants values giving $k_{EfOM\text{-}OH}$[EfOM]. Additional division by the molar concentration of EfOM yields $k_{EfOM\text{-}OH}$ in units of $M_C^{-1}\ s^{-1}$.

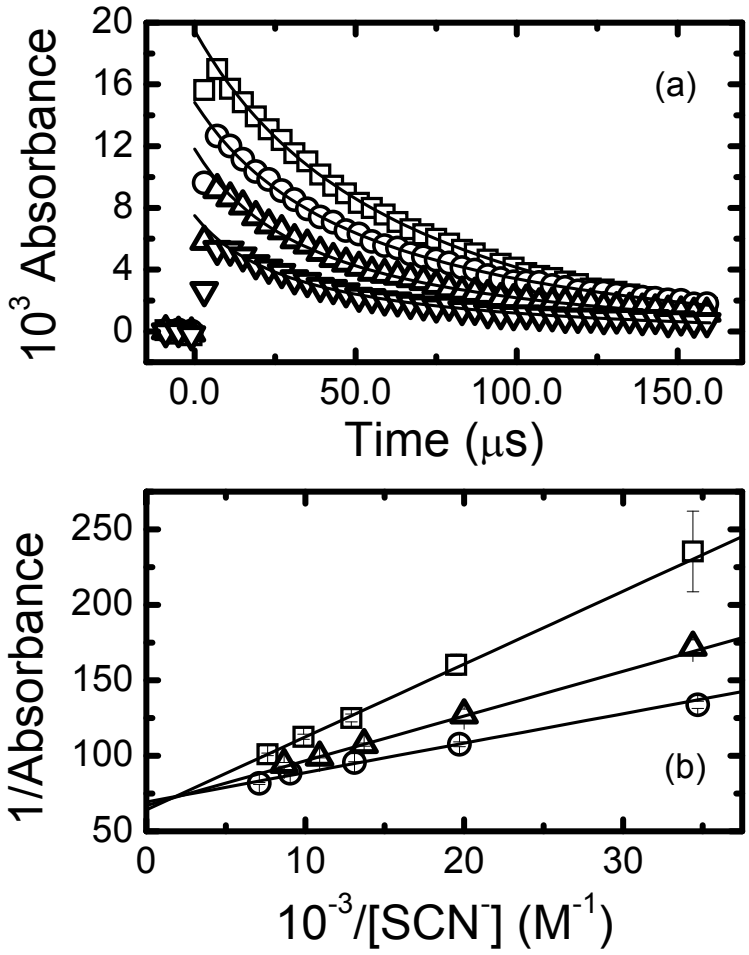

Figure 2.1. Decay kinetics for $(SCN)_2^-$ for PCFL and transformed kinetics plot for the determination of $k_{OH\text{-}EfOM}$ for PCFL, RMCO, and LVNV(A).

2.3.4 Statistical Analysis

Statgraphics (Version 15.2.05, Herndon, VA) and Microsoft Office Excel were used to evaluate the kinetic data, identify associations with bulk EfOM parameters, and create an empirical correlation model. The multivariable function from Statgraphics was used to initially evaluate the importance of each term describing the variability in rate constants. For the quantitative correlation of the measured rate constants, the in-built multilinear regression function within Excel was used to identify values for individual components and their errors.

2.3.5 Analysis of Micropollutants

Two methodologies were used for analysis of micropollutants, depending on the scale of the experiment. For the bench-scale UV/H_2O_2 experiments, a direct SPE method was used (Trenholm et al., 2009). Each sample was collected in a 40-mL vial and preserved with 0.1% sodium azide. Samples were kept at 4°C until extraction, within 14 days of collection. Prior to extraction, a 10-mL aliquot of each sample was measured out and spiked with a stock solution of isotopically labeled standard. From this sample, 1.5-mL fractions were used in 2-mL autosampler vials. This allowed enough prepared sample for duplicate analysis, matrix spikes, and dilutions when necessary.

Extraction and analysis was done using an on-line solid-phase extraction and liquid chromatography with tandem mass spectrometry (SPE-LC-MS/MS) using a Symbiosis (Spark Holland) automated solid-phase extractor and a 4000 QTRAP (Applied Biosystems) mass spectrometer (Trenholm et al., 2009). Oasis HLB cartridges were used for SPE. Separation was performed on a C18 column (Phenomenex) and with a mobile phase consisting of 5 mM ammonium acetate in DI water: methanol gradient. All samples were analyzed using positive electrospray ionization (ESI) and tandem mass spectrometry, or multiple reaction monitoring (MRM). Two MS/MS transitions were used for each compound for quantitation and confirmation. Quantification was performed using isotope dilution. Initial reporting limits are listed in Table 2.2.

Table 2.2. Compound List and Initial Reporting Limits for Bench-Scale UV/H_2O_2 Experiments

Compound	Initial Reporting Limits (ng/L)
Atenolol	10
Atrazine	25
Carbamazepine	10
Dilantin	10
Meprobamate	10
Primidone	10
TCEP	400
TCPP	400
Trimethoprim	10

For ozone and pilot-scale UV/H_2O_2 studies, a modified version of the method originally reported by Vanderford and Snyder (2006a) was used. The mass spectrometer settings were adjusted to reflect the MRM transitions of the new analyte list, and isotopically labeled internal standards, where applicable (Table 2.3). The method detection limit (MDL) and method reporting limit (MRL) values for the analytes are reported in Table 2.3. The MDL values were determined by extracting eight deionized water samples containing analytes at levels near their expected detection limits and labeled internal standards at 10, 100, or 200 ng/L. The standard deviation of the eight measurements for each analyte was multiplied by the appropriate Student T value for n-1 degrees of freedom. The MRL was set to be a minimum of three times larger than the MDL and higher where applicable because of background levels.

For micropollutant steroid analysis, 500 mL of sample was spiked with isotopically labeled standards and then extracted by SPE. Final extracts were concentrated to 500 µL. Steroids were analyzed by LC-MS/MS using electrospray ionization (ESI) in both negative and positive modes. All analytes were monitored using MRM with two transitions for each compound, one for quantitation and the other for confirmation. MDLs were determined by extracting 12 deionized water samples fortified with the analytes at levels near their expected detection limits and labeled internal standards at 10 ng/L. The standard deviation of the 12 measurements for each analyte was multiplied by the appropriate Student T value for n-1 degrees of freedom. The MRL was set above the MDL.

Table 2.3. Method Reporting Limit (MRL) and Method Detection Limit (MDL) for Ozone and Pilot-Scale UV/H_2O_2 Experiments

Analyte	CAS #	Precursor Ion (m/z)	Product Ion (m/z)	MDL (ng/L)	MRL (ng/L)
Tris(2-chloroethyl) phosphate (TCEP)	115-96-8	285	99	0.89	10
TCEP-d12		297	102		
Tris(1-chloro-2-propyl) phosphate (TCPP)	13674-84-5	327	99	33	100
N,N-diethyl-3-methylbenzamide (DEET)	134-62-3	192	91	0.14	1.0
DEET-d6		198	119		
Benzophenone	119-61-9	183	105	9.2	50
Benzophenone-d10		193	110		
Iopromide	73334-07-3	792	573	0.47	1.0
Caffeine	58-08-2	195	138	0.22	5.0
Caffeine-d9		204	144		
Primidone	125-33-7	219	162	0.16	0.5
Primidone-d5		224	167		
Octylphenol	27193-28-8	205	134	3.3	25
Butylated hydroxyanisole (BHA)	25013-16-5	179	164	0.13	1.0
Musk ketone	81-14-1	293	251	7.2	25
Ibuprofen	15687-27-1	205	161	0.20	1.0
Ibuprofen-d3		208	163		
Estrone	53-16-7	269	145	0.11	0.2
β-Estradiol	57-91-0	271	145	0.35	0.5
Ethynylestradiol	57-63-6	295	145	0.42	1.0
Testosterone	58-22-0	289	109	0.25	0.5
Progesterone	57-83-0	315	109	0.18	0.5

2.4 OZONE AND OZONE AOP TESTING

2.4.1 Bench-Scale Ozone System

Bench-scale tests were performed using a batch reactor measuring O_3 decomposition and $^{\bullet}OH$ exposure (Figure 2.2). A sample of Nanopure™ water was placed inside a water-jacketed flask and cooled to 2°C. Once cooled, 11% gaseous O_3 was diffused into the water using an oxygen-fed generator (model CFS-1A, Ozonia North America Inc., Elmwood Park, NJ). O_3 stock solution concentrations and dissolved residuals were measured according to Standard Methods 4500-O_3 (APHA, 1998; Bader and Hoigne, 1982). Ozone dosages were administered by injecting an aliquot of the stock solution into a 1-L amber glass container with a repeating pipette dispenser containing the sample.

Figure 2.2. Equipment used to generate O_3 stock solution in batch mode.

2.4.2 Bench-Top Pilot Plant

A 1 L/min bench-top pilot plant (BTPP) made from inert materials including glass, stainless steel, and fluorocarbon polymers was used to conduct the testing (Figure 2.3). A peristaltic pump was used to transport the wastewater from a 208-L stainless steel drum into the contactor. During O_3/H_2O_2 experiments, H_2O_2 (3% stock, Fisher Scientific, Pittsburgh, PA) was injected into the wastewater flow stream followed by static mixing prior to entering the contactor. The O_3 contactor consisted of 12 glass chambers each providing 2 min of contact time, for a total of 24 min. Ozone feed gas was produced from oxygen gas using a laboratory-scale generator (model LAB2B, Ozonia North America Inc., Elmwood Park, NJ). O_3 was added in the first contactor chamber with counter-current flow through a glass-fitted diffuser

with bubble size of 0.1 μm. A mass-flow controller (model AFC2600D, Aalborg Instruments and Controls, Inc., Orangeburg, NY) and a feed gas concentration analyzer (model H1-S, IN USA Inc., Needham, MA) were used to calculate and control the O_3 dosage. Because of the column height of 0.83 m and diameter of 0.055 m, the transfer efficiency varied between 40% to 70% depending on the desired dose and corresponding gas flow rate. The off-gas was collected from the top of each cell into a central manifold and destroyed by manganese dioxide catalyst.

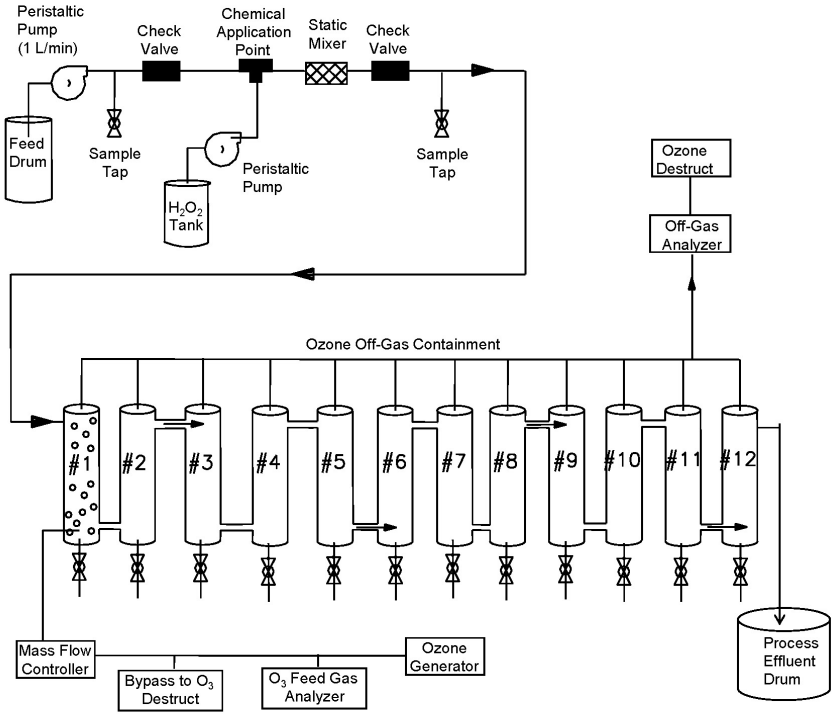

Figure 2.3. Schematic of Bench-Top Pilot Plant (BTPP) for ozone experiments.

2.5 UV/H_2O_2 TESTING

2.5.1 Bench-Scale UV/H_2O_2

A custom-made low-pressure (LP) collimated beam system was used for all bench-scale experiments (Figure 2.4). The system included two G15T8 germicidal lamps (General Electric, Fairfield, CT), housed inside a wooden box. The intensity was measured using a radiometer from International Light (Peabody, MA), Model 1700 (probe model SEL 240). The unweighted doses were calculated from the product of the fluence rate and exposure time (Bolton and Linden, 2003). Three UV fluences were tested: 300, 500, and 700 mJ/cm^2. Five H_2O_2 doses were also tested: 0, 2, 5, 10, 15, and 20 mg/L. The H_2O_2 concentrations were measured using the I_3 method (Klassen et al., 1994).

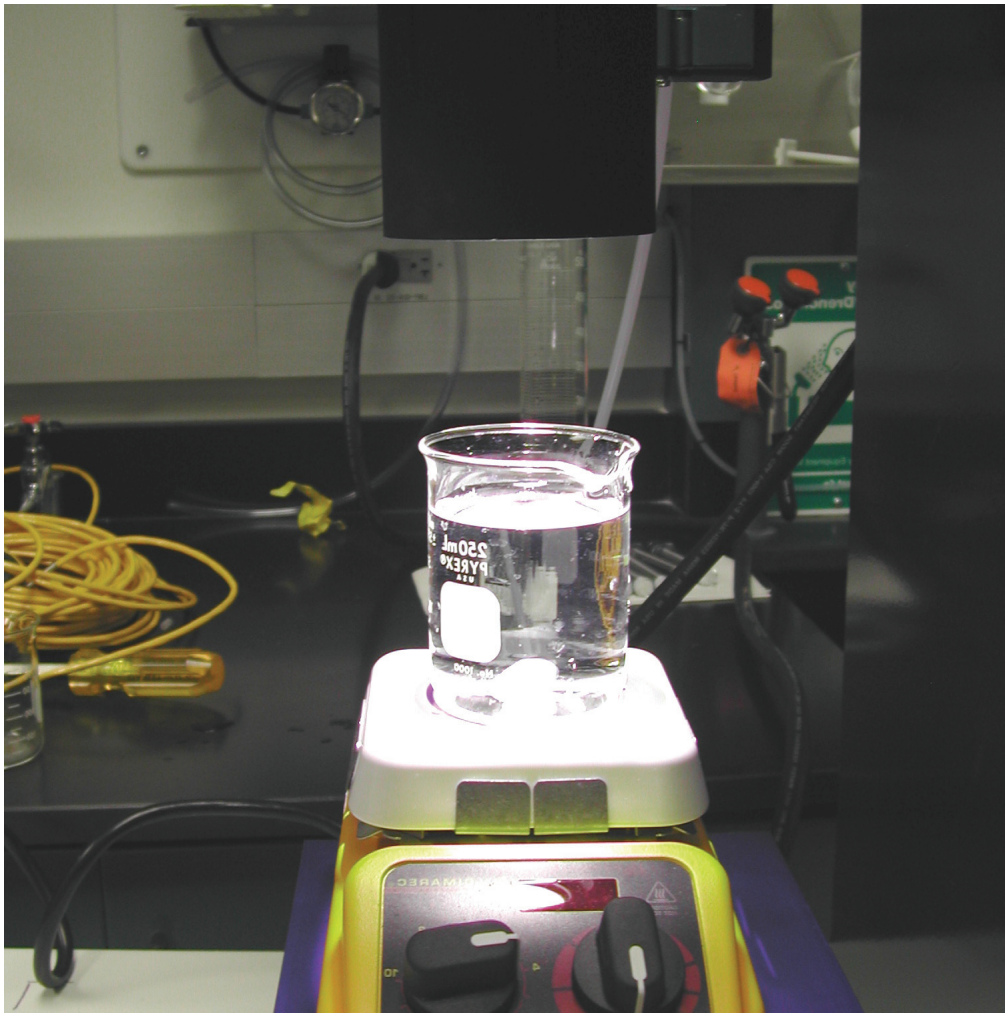

Figure 2.4. Bench-scale UV/H_2O_2 setup.

2.5.2 UV/H_2O_2 Pilot-Scale

A pilot-scale UV/H_2O_2 reactor from Trojan was tested at LVNV (Figure 2.5). The reactor was a 30AL50 (total volume 90 gal), low pressure, high output TrojanUVPhox with 30 (257 watt) lamps. Three flows were tested (60, 80, and 118 gallons per minute [gpm]) and five H_2O_2 doses were added. The flows were selected based on predicted 1-log removals for NDMA and 17α-Ethynylestradiol (EE2; approximately 80 gpm) and also included lower and higher flows to test the overall performance of the system. The concentration of peroxide was targeted to be between 2 and 25 mg/L. A 35% H_2O_2 stock solution was used. The H_2O_2 was added via a peristaltic pump approximately 15 feet from the reactor. The H_2O_2 flow was added to the center of the flow running through a 4-inch diameter pipe before a flow meter to allow for proper mixing. The estimated retention times in the reactor were between 0.8 and 1.5 min depending on flow. The H_2O_2 concentrations were measured immediately after addition using the I_3 method (Klassen et al., 1994).

Figure 2.5. UV/H_2O_2 pilot reactor.

2.6 QUALITY ASSURANCE AND QUALITY CONTROL

2.6.1 Sample Collection and Preservation

All sampling collection, preparation, extraction, and analysis were performed using nitrile gloves to prevent accidental contamination of samples with target analytes.

All samples were collected in glass, amber-colored bottles complete with Teflon-lined caps to ensure sample integrity. In addition, a concerted effort was made to keep bottle headspace to a minimum. Samples were extracted within 14 days of initial sampling. All samples were kept refrigerated at ≤ 4°C from the time of collection until sample extraction had taken place. In addition to standard samples, quality control samples were also taken. This included at least one blank (trip and/or equipment) and one duplicate for each sampling event. Matrix spike samples were also collected at one sampling location for each sample matrix during each sampling event.

2.6.2 Sample Preparation

All sample preparations were performed in distinct batches. A batch was defined as the total number of samples that could be extracted together, including all quality control tests. This usually consisted of six samples per batch (four tests and two quality controls). Sample extractions did not exceed four batches per day to ensure that appropriate time and care were taken with all sample preparation. Each preparation batch was accompanied by one reagent water blank and one reagent water spike.

2.6.3 Micropollutants Quantification

Prior to each analysis, MDL and reporting limits were generated for each analyte. The MDL is the concentration of an analyte that can be measured and reported with 99% confidence that it is greater than zero. Unlike the instrument detection limit (IDL), it measures the entire process of analysis, including extraction/preparation and instrumental detection. It is defined as the amount determined by multiplying the standard deviation of multiple replicate analyses by the appropriate T-statistic. The concentration of the analyte used to determine the MDL should be approximately the value of the expected MDL. The reporting limit is generally defined as no less than 3 to 5 times the calculated MDL, with a signal-to-noise ratio ≥ 10 for all analyte peaks. The reporting limits can increase/decrease depending on additional factors such as blank contamination, calibration, and analyst confidence.

2.6.4 Initial Calibration

To calibrate an analytical instrument, the relationship between the response of the instrument and the amount of an analyte introduced must be determined. Two types of calibration procedures were used: isotope dilution internal calibration and external calibration for analytes when there were no isotopically labeled standards available. Both calibration procedures used linear regression with $1/x^2$ weighting. All analyte calibration curves had a minimum of five points, the lowest standard of which was at, or below, the reporting limit. Calibration curves were required to have regression coefficients of at least 0.99. Sample concentrations that were outside the calibration range were diluted and reanalyzed.

2.6.5 Instrumental QC

All sample batches were bracketed by both blanks and calibration verification samples (CVS). CVS's were prepared at concentrations that fell in the middle of the calibration curve.

For the isotope dilution internal calibration methodology, every sample analyzed had isotopically labeled versions of each analyte added at the beginning of sample preparation to give a final amount equal to that in the initial calibration standard. Isotope standard raw area counts were monitored to allow for any deterioration of system performance.

2.6.6 Rate Constant Measurements

The individual wastewater samples were shipped overnight in 1.0 L amber glass bottles to the Radiation Laboratory, University of Notre Dame using ice-chilled coolers. These bottles were then placed in a refrigerator (~2–3^{o}C) until used (typically within 48 hrs). Experiments on samples that were deliberately kept for longer periods (up to 3 weeks) showed no change in the measured reaction kinetics (show values).

To determine an individual wastewater $k_{EfOM\text{-}OH}$ rate constant value, 500 mL of the wastewater was initially placed in a glass volumetric vessel and sparged with N_2O(g) for at least 20 min. Extended gas sparging did not change the kinetics obtained. Once gas saturation had been achieved, this solution was flowed through a quartz irradiation flow cell placed in front of the accelerator, using an all-glass tubing system to ensure no air ingress occurred. Solution flow was achieved by using a peristaltic pump to create a vacuum on the waste side of the piping. The solution flow was sufficient that each irradiation pulse (0.4 Hz) occurred on a completely fresh sample.

Individual aliquots (50–150 uL) of a 10 mM KSCN solution were then sequentially added to give 5 separate thiocyanate concentrations in the N_2O-saturated water within the range 30–150 μM. For each SCN^- concentration, 3 to 4 separate kinetic decay traces (see Figure 2.1) were obtained by averaging 15 individual pulses. By computer fitting these kinetic decay traces to integrated second-order decay kinetics, individual initial absorbance intensities were determined. Blank, high-purity (Milli-Q >18.2 MΩ) water samples that were treated in this same manner gave higher initial absorbance values for the same SCN^- concentrations, as expected.

The analysis of these averaged individual kinetic curves showed that the extrapolated initial absorbances were precise to within 2 to 3%. Transforming these initial absorbances as described earlier gives the straight lines seen in Figure 2.1, with R^2 values greater than 0.99. The ratio of the slope to the intercept of these transformed lines gave the $k_x[X]/k_{SCN^-}$ ratio. From the known k_{SCN^-} value, water alkalinity and EfOM concentration, the desired second-order reaction rate constants, $k_{EfOM\text{-}OH,}$ could be calculated.

This measurement methodology was benchmarked using a standard 7.0 mg/L Suwannee River fulvic acid solution made in Milli-Q water without carbonate present. This hydroxyl radical reaction rate constant was determined to be (1.61 ± 0.06) x 10^8 M_C^{-1} s^{-1} (Rosario-Ortiz et al., 2008), which is in excellent agreement with the previously reported value of (1.60 ± 0.24) x 10^8 M_C^{-1} s^{-1} that had been determined both directly and by another competition kinetics method. Moreover, repeat experiments on the same wastewater batch using this approach gave the same second-order $k_{EfOM\text{-}OH}$ values within experimental error.

CHAPTER 3

QUANTIFICATION OF •OH DURING ADVANCED OXIDATION PROCESSES

3.1 INTRODUCTION

Chemical isolation and quantification of •OH during AOPs using common analytical instrumentation is nearly impossible. The lifetime of •OH in typical wastewaters is less than a few microseconds. Therefore, during water treatment, typical concentrations of •OH are in the order of 0.001 ng/L, much lower than for other water quality components. However, quantification of •OH is needed in order to maintain a certain level of effectiveness during the application of these processes and to study in detail the overall process. In this section, the different methods commonly used to quantify •OH are described. The methods presented were used throughout this project.

3.2 APPLICATION OF pCBA FOR THE QUANTIFICATION OF •OH

Direct quantification of •OH during treatment processes is extremely difficult; instead, •OH is indirectly estimated through the use of probe compounds, such as para-chlorobenzoic acid (pCBA, see Figure 3.1; Acero and Von Gunten, 2001; Elovitz and von Gunten, 1999; Pi et al., 2005; Rosenfeldt and Linden, 2007; Wert et al., 2007). The application of a probe compound must meet certain requirements, including easy quantification, known chemical kinetics, and selectivity toward •OH. This probe meets all of the requirements, especially for small-scale experiments. pCBA reacts relatively fast with •OH but is stable to ozone degradation. The kinetic information for pCBA is shown in the following.

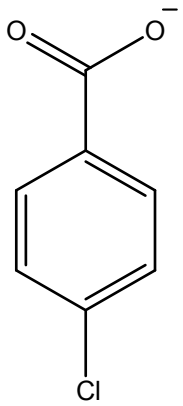

Figure 3.1. Chemical structure of de-protonated pCBA.

In the case of •OH quantification during ozone processes, pCBA rapidly reacts with •OH, whereas its reaction with ozone is much slower:

$$pCBA + OH \xrightarrow{k_{pCBA-OH} = 5.0x10^9\ M^{-1}s^{-1}} P_1 \quad (3.1)$$

$$pCBA + O_3 \xrightarrow{k<0.50 M^{-1}s^{-1}} P_2 \quad (3.2)$$

Experimentally, pCBA is spiked into solution and its decay that is due to the selective reaction with •OH is monitored. Evaluation of its decay allows the estimation of the •OH exposure, which is necessary in order to judge the efficiency of the process. The loss of pCBA during this application is directly related to the concentration or exposure of •OH as shown in eq. 3.3 and 3.4.

$$\frac{-d[pCBA]}{dt} = k_{OH-pCBA}[pCBA][^{\bullet}OH] \quad (3.3)$$

Integration of eq. 3.3 results in the following expression, which takes into consideration the overall •OH exposure:

$$\ln\left(\frac{[pCBA]}{[pCBA]_0}\right) = -k_{OH-pCBA}\int [^{\bullet}OH]dt \quad (3.4)$$

For ozone applications, the introduction of the term R_{CT}, as defined below, allowed the •OH exposure to be substituted for the ozone exposure, which analytically is easier to quantify.

$$R_{CT} = \frac{\int [OH]dt}{\int [O_3]dt} \quad (3.5)$$

Substituting eq. 3-5 into eq. 3-4 results in

$$\ln\left(\frac{[pCBA]}{[pCBA]_0}\right) = -k_{OH-pCBA}R_{CT}\int [O_3]dt \quad (3.6)$$

Therefore plotting the natural log of the ratio $[pCBA]/[pCBA]_o$ versus the ozone exposure gives a straight line whose slope is equal to the product of the R_{CT} and the rate constant, which is known. Figure 3.2 presents an example of the application of this procedure for the characterization of an ozonation process.

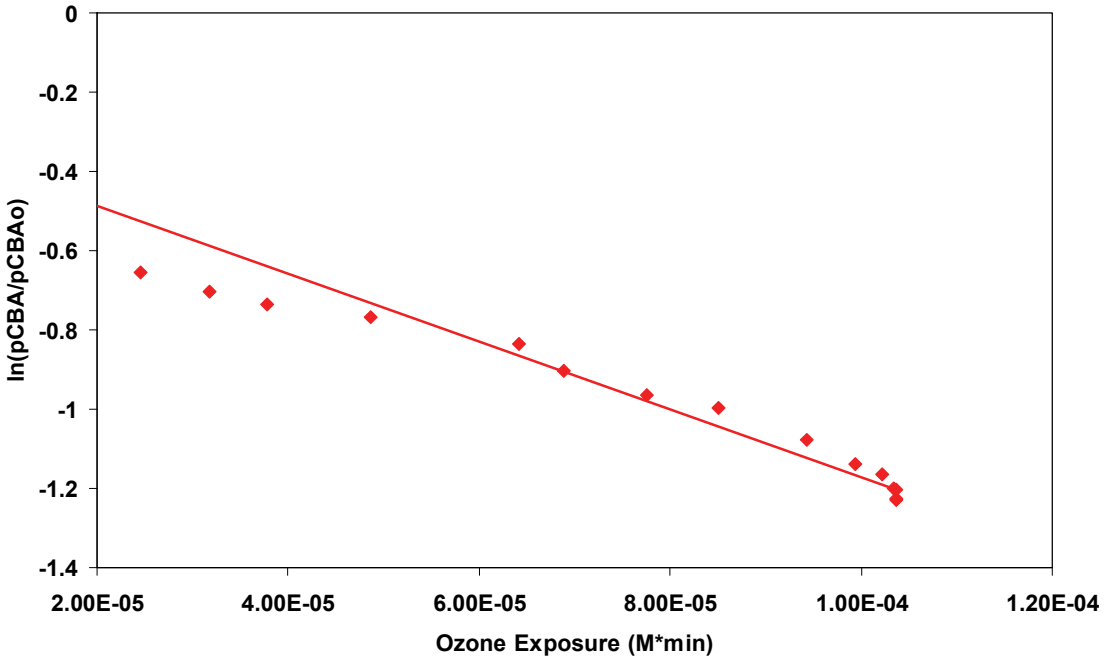

Figure 3.2. Determination of R_{CT} during the application of ozone.

For the second-order decomposition of ozone, the R_{CT} value has been shown to be constant (Elovitz and von Gunten, 1999), resulting in the determination of the $^{\bullet}OH$ at any given time, assuming the ozone exposure is known. The R_{CT} method has been extensively applied to the analysis of ozone dynamics at bench-scale, as it requires addition of pCBA.

In cases where the ozone residual is zero (as it is in the case for the application of ozone to wastewaters when the applied dose is below the ozone demand), use of pCBA yields the overall $^{\bullet}OH$ exposure, rather than the actual concentration of $^{\bullet}OH$ at any stage as for R_{CT}.

For the application of UV/H_2O_2, the introduction of the $R_{OH,UV}$ concept (see eq. 3.7) also allows quantification of $^{\bullet}OH$ exposure (Rosenfeldt and Linden, 2007). The $R_{OH,UV}$ concept is based on the decay of pCBA as a function of applied H_2O_2 and UV fluence. Application of this concept introduces fluence-based reaction rate constants, k^D, which describes the decay of a chemical in fluence-based units instead of typical time-based kinetics. The reaction rate constants are transformed from time-based to fluence-based by dividing by the UV average fluence rate, E, with units of mW cm^{-2}. The final UV fluence during UV application, H (mJ/cm^2) is obtained by multiplying E by the exposure time.

Experimentally, the decay of pCBA is initially followed as a function of UV fluence with no added H_2O_2. A plot of the natural log of the inverse of the normalized pCBA concentration versus UV fluence results in a straight line, where the slope of line yields k^D_d, which represents the fluence-based reaction rate constant for the photolytic decay of pCBA. Addition of variable concentrations of H_2O_2 and following a similar analysis yields k^D_T which represents the total fluence-based rate of pCBA decay, which includes both photolysis and $^{\bullet}OH$ decay of pCBA. Figure 3.3 presents the decay of pCBA as a function of fluence and

H_2O_2. With these two values and the known reaction rate constant between pCBA and •OH, the $R_{OH,UV}$ is calculated. Once the $R_{OH,UV}$ is obtained, multiplication by H yields the •OH exposure.

$$R_{OH,UV} = \frac{\int_0^t [^\bullet OH]dt}{H} = \frac{k_T^D - k_d^D}{k_{pCBA-OH}} \tag{3.7}$$

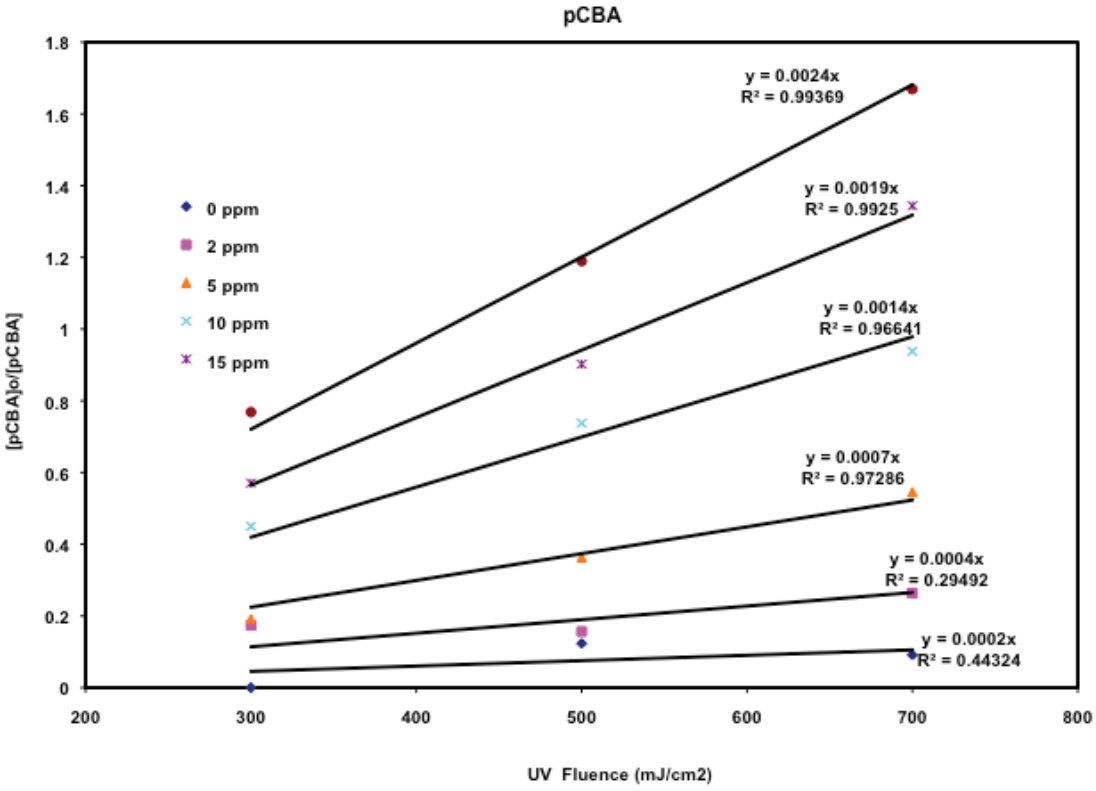

Figure 3.3. Decay of pCBA during UV/H_2O_2 for the calculation of $R_{OH,UV}$.

3.2.1 Quantification of pCBA

The quantification of pCBA using liquid chromatography with UV detection (LC-UV) has been reported previously (Acero and Von Gunten, 2001; Elovitz and von Gunten, 1999; Park et al., 2004; Wert et al., 2007). Typical reporting limits (RLs) using this method are approximately 4 µg/L. However, concerns with the sensitivity of this method have shown the need for lower detection limits. Because the probe is being used to estimate •OH concentration while inherently being an •OH scavenger itself, its concentration must be minimized to prevent it from artificially increasing the •OH demand of the system. In addition, under AOP conditions, such as those found during ozonation of waters containing high levels of TOC, the concentration of pCBA quickly decreases below the RL even with a relatively high initial concentration.

Recently, a sensitive and selective method for the detection of pCBA was developed using liquid chromatography-tandem mass spectrometry (LC-MS/MS; Vanderford et al., 2007). The RL was determined to be 100 ng/L, a 40-fold decrease from the LC-UV RL. The method was applied to wastewater and found to be comparable to LC-UV detection at high pCBA concentrations and sensitive enough at low pCBA concentrations to avoid the sensitivity concerns associated with LC-UV detection.

3.3 QUANTIFICATION OF •OH DURING FULL-SCALE APPLICATIONS

The application of pCBA for the quantification of •OH is limited to bench-scale experiments because of the impracticality of spiking pCBA in a pilot- or full-scale plant. For the latter, the determination of •OH exposure could be performed utilizing organic micropollutants already present in the water. As discussed previously, the requirements for an ideal •OH probe could be met by multiple organic compounds, provided they have rapid •OH reaction rate constants and only limited reactivity to ozone and UV light.

There are a series of micropollutants that are good candidates for being replacement pCBA probes. Relatively recalcitrant compounds, such as TCEP and meprobamate, which have been shown to be unreactive toward UV and ozone, may be used. The decay of these micropollutants is represented by:

$$\frac{-d[P]}{dt} = k_{OH-P}[P][^{\bullet}OH] \tag{3.8}$$

$$\ln\left(\frac{[P]}{[P]_0}\right) = -k_{OH-P}\int [^{\bullet}OH]dt \tag{3.9}$$

Table 3.1 presents the reaction rate constants measured using the SCN^- competition kinetics method for several micropollutants utilizing the procedure described in Chapter 2. By following the decay of these compounds, additional information could be obtained about the formation and exposure of •OH. Throughout this report, most of the •OH was done using pCBA. The decay of these additional micropollutants was used as a confirmation of •OH exposures measured with pCBA.

Table 3.1. Measured Second-Order Reaction Rate Constants for Three Micro-Pollutants With •OH ($k_{P\text{-}OH}$)

Compound	$k_{P\text{-}OH}$ (M^{-1} s^{-1})
TCEP	$(4.31 \pm 0.12) \times 10^8$
Iopromide	$(5.09 \pm 0.33) \times 10^9$
Meprobamate	$(9.55 \pm 0.37) \times 10^9$

CHAPTER 4

QUANTIFICATION OF $k_{EFOM\text{-}OH}$ FOR THE APPROXIMATION OF THE OVERALL SCAVENGING CAPACITY

4.1 INTRODUCTION

The real-world application of AOPs is hindered by the overall $^{\bullet}OH$ scavenging capacity of the water. This scavenging capacity raises costs by reducing the effectiveness of an AOP toward contaminant removal and is directly related to the second-order reaction rate constants between $^{\bullet}OH$ and a specific chemical. Among the most important $^{\bullet}OH$ scavengers (in terms of reactivity and relative concentration) are alkalinity, nitrite, and EfOM. As opposed to the alkalinity and nitrite, for which the chemistry has been well defined and the concentrations are measured using standard methods, the reactivity of the EfOM has been studied less and its overall structure may vary between sites.

4.2 OBJECTIVE

This part of the study evaluated the overall influence of EfOM toward the $^{\bullet}OH$ scavenging. This was accomplished by measuring the second-order reaction rate constant between EfOM and $^{\bullet}OH$ ($k_{EfOM\text{-}OH}$) from different sites. In addition, a model was developed that could be used to predict this value for different EfOM from different sites based on its specific properties.

4.3 QUANTIFICATION OF $k_{EFOM\text{-}OH}$

A total of eight samples were collected at different utilities, as described in Chapter 2. The determination of the $k_{EfOM\text{-}OH}$ values was done following the procedure described in Section 2.3.3. Water quality parameters for the eight samples used in this study are presented in Table 4.1. The TOC of the samples varied between 6.3 and 20 mg/L. The specific UV absorbance (SUVA) of the samples varied between 0.99 and 2.3 L/mg_C m, all indicative of low aromatic content in these waters (Weishaar et al., 2003).

Table 4.1. Water Quality Parameters for the Samples Collected

Sample Description	Location	TOC (mgC/L)	UVA (254 nm) (1/cm)	SUVA (L/mgC m)	UVT (254 nm) (%)
PCFL	Florida	8.5	0.199	2.3	63
LACSD	California	6.3	0.108	1.7	78
LVNV (A)	Nevada	6.6	0.115	1.8	77
LVNV (B)	Nevada	6.4	0.111	1.7	77
RMCO-N	Colorado	11	0.172	1.6	67
RMCO-S	Colorado	20	0.197	1.0	64
WWTP	Arizona	8.7	0.155	1.8	70
WRP	Arizona	7.1	0.131	1.9	74

The individual $k_{EfOM\text{-}OH}$ for the eight samples of this study are summarized in Table 4.2 and shown in Figure 4.1. The values ranged from 0.27 x 10^9 M_C^{-1} s^{-1} observed for the samples collected at RMCO-S to 1.21 x 10^9 M_C^{-1} s^{-1} observed for one of the samples collected at LVNV (B). The average value observed was 0.87 (± 0.36) x 10^9 M_C^{-1} s^{-1} and, in general, these values show a factor of 3–5 variation, with most of the rate constants considerably faster than previously determined for NOM isolates (Larson and Zeep, 1988; Westerhoff et al., 2007). The difference between the rate constants measured in this study and previously reported values for isolates could be attributed to the fact that the EfOM used in this study was not fractionated; therefore, it would be expected to be structurally different and more complex than specific isolates.

Table 4.2. Summary of Water Quality Parameters Used for Hydroxyl Radical Reaction Rate Constant Determinations

Location	Alkalinity mg/L	Solution pH	Measured 10^{-5} $k_x[X]$ s^{-1}	Calculated 10^4 $k_{carb.}$ s^{-1}	[DOC] µM	10^9 $k_{EfOM\text{-}OH}$ M_C^{-1} s^{-1}
PCFL	224	7.79	8.57±0.26	4.23	708	1.15±0.03
LACSD	178	7.97	6.10±0.56	5.50	525	1.06±0.10
LVNV (A)	133	7.99	2.72±0.15	2.74	550	0.45±0.03
LVNV (B)	131	7.99	6.70±0.93	2.74	533	1.21±0.17
RMCO-N	98.2	7.34	9.52±0.94	2.36	917	1.02±0.10
RMCO-S	222	7.15	4.85±0.16	3.37	1667	0.27±0.01
WWTP	161	7.37	8.03±0.40	2.64	725	1.07±0.05
WRP	206	7.70	4.38±0.13	3.76	592	0.68±0.02

k_x[X] is the measured total reaction rate constant for the N_2O-saturated wastewater, k_{carb} is the calculated component of hydroxyl radical reaction rate constant with carbonate and bicarbonate as derived from the alkalinity and known rate constants.

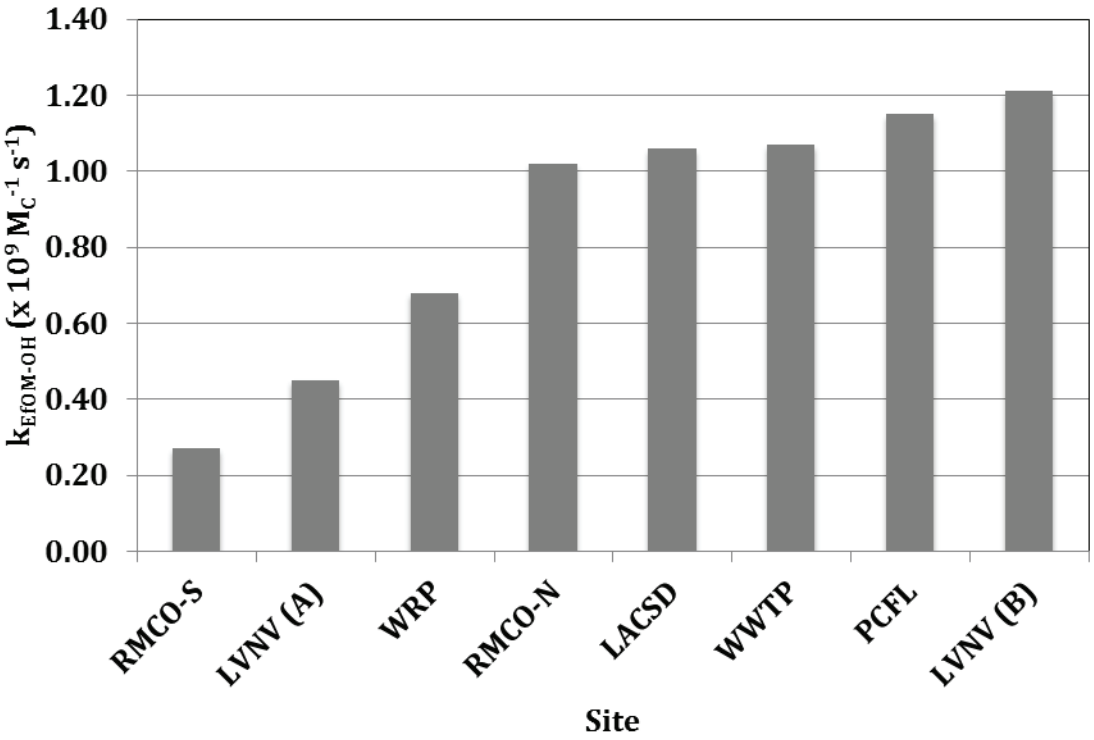

Figure 4.1. Second-order reaction rate constants between EfOM and $^{\bullet}OH$($k_{EfOM-OH}$).

4.4 DEVELOPMENT OF A MODEL DESCRIBING THE SCAVENGING CAPACITY ASSOCIATED WITH EfOM

As shown in Table 4.2, the rate constants (and therefore the overall scavenging) between $^{\bullet}OH$ and EfOM varied between sampling sites. Because of the complexity of the measurements and potential variations both geographically and temporarily, the development of a predictive model that could be used to estimate the rates based on easily measurable parameters would be extremely helpful both to design engineers and operators of AOP systems. In order to do this, a comprehensive EfOM characterization was done on these water samples, with emphasis on the characterization under ambient conditions, therefore limiting potential changes and homogenization of the EfOM.

4.4.1 EfOM Characterization

EfOM characterization was done using polarity, fluorescence, absorbance, and SEC techniques. Figure 4.2. presents the SEC chromatograms for the collected samples. The first peak, at retention times between 22 and 30 min., has been assigned to the high molecular components of NOM (Lee et al., 2004), including polysaccharides (Sachse et al., 2001). The second region, with elution times between 35 and 55 min., was attributed to humic substances, including building blocks and other components such as low molecular weight acids (Lee et al., 2004). The third region, between 60 and 70 min. corresponds to the low molecular weight acids and amphiphiles (Sachse et al., 2005). All the samples had peaks at

25 min., outside the exclusion limit. With the exception of the PCFL sample, all others had similar peak distributions. The PCFL sample had a larger peak at 38 min., indicating higher molecular weight material with respect to the other samples. The number average and weight average (molecular weight) and polydispersity (d) are presented in Table 4.3. The obtained values were within 980 and 1500 Da. Polydispersity is defined as the ratio of the weight average molecular weight (M_W) and the number average molecular weight (M_N) and reflects the differences in both calculation as a function of the wide variety of the molecular weight of the components of the EfOM. As the components of the EfOM become more diverse, in terms of apparent molecular weight, the value of the polydispersity will increase.

Table 4.3. Data Used for the Development of a Model Describing the Relation Between $k_{EfOM\text{-}OH}$ and EfOM Properties

Sample	M_w[1] (Da)	d[2]	Fluorescence Index[3]	C18 RC [4]	NH2 RC [5]	SUVA 254 [6] (L/mgC m)
PCFL	1484	1.64	1.28	0.24	0.58	2.3
LACSD	982	1.50	1.56	0.28	0.40	1.7
LVNV (A)	1050	1.38	1.56	0.26	0.31	1.8
LVNV (B)	1078	1.53	1.64	0.28	0.36	1.7
RMCO-N	999	1.57	1.48	0.25	0.39	1.6
RMCO-S	935	1.49	1.52	0.28	0.46	1.0
WWTP	1172	1.58	1.53	0.26	0.35	1.8
WRP	1181	1.53	1.46	0.27	0.32	1.9

[1] Weight average apparent molecular weight.

[2] Dispersity.

[3] Ratio of the fluorescence at 370 nm excitation and 450/500 nm emission.

[4] Retention coefficient for C18. Measure of hydrophobicity.

[5] Retention coefficient for NH2. Measure of hydrophilicity/anionic character.

[6] Specific UV absorbance. Measure of aromaticity.

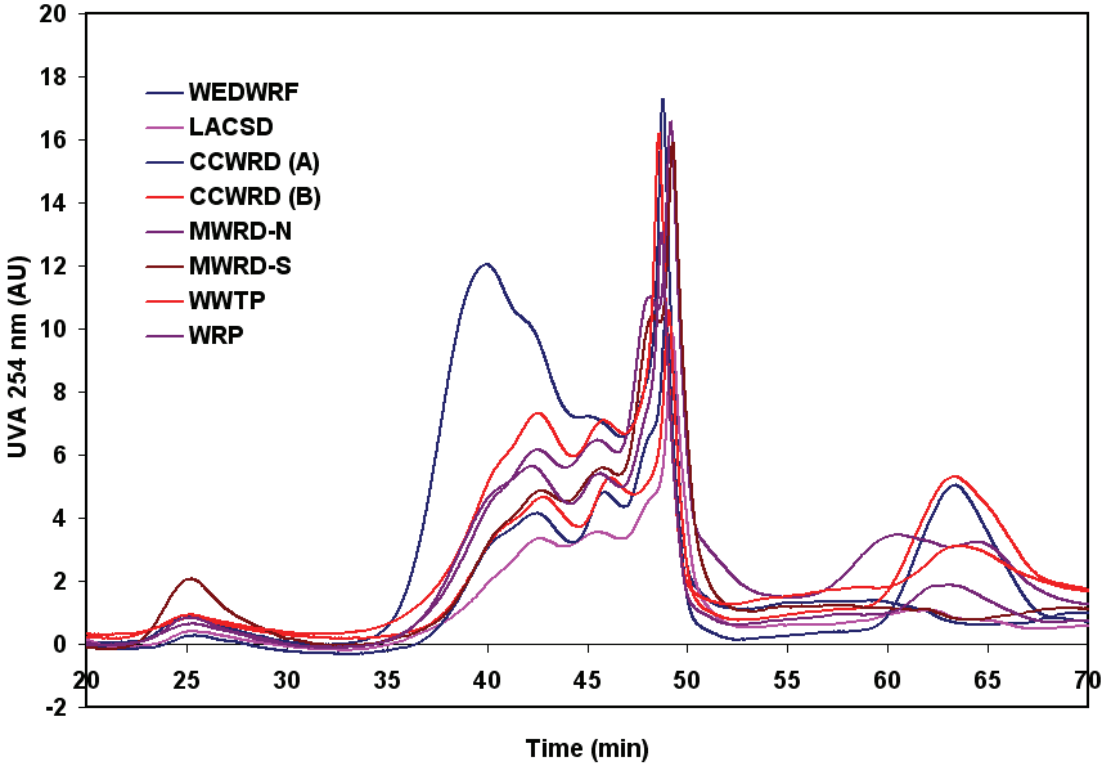

Figure 4.2. Size exclusion chromatogram for the samples studied.

Figure 4.2 represents using ultraviolet absorbance (UVA) at 254 nm. Conditions: pH 6.8; 0.028 M phosphate buffer; flow = 1 mL/min; Toyopearl HW-50 S 250 x 20 mm column.

Figure 4.3 shows the results from the polarity characterization. The analysis of PRAM data has been described earlier (Rosario-Ortiz et al., 2007a; 2007b). Each SPE sorbent has an RC associated with it, which indicates the fraction of EfOM with a similar polarity. For example, retention onto C18 has been correlated to hydrophobic surface area (Rosario-Ortiz et al., 2007b). As a result, the values for the C18 RCs are correlated to the hydrophobicity of the EfOM.

Analysis of Figure 4.3 reveals that the EfOM is characterized by C18 RCs between 0.23–0.28, which indicates 23–28% non-polar character (Rosario-Ortiz et al., 2007b). This decreases to 0.13–0.17 for C8 and 0.01–0.06 for C2. The differences are due to the capacity of each sorbent to adsorb hydrophobic compounds. The amine (NH2) RCs were between 0.31 and 0.57 and generally lower than those observed for the strong anion exchanger (SAX; Rosario-Ortiz et al., 2007a). The NH2 and SAX both adsorb negatively charged moieties. The SAX RCs varied between 0.59–0.85, with a larger standard deviation compared to the non-polar characterization (0.09 versus 0.02) indicating that the overall proportion of anionic moieties was more variable than that of hydrophobic moieties.

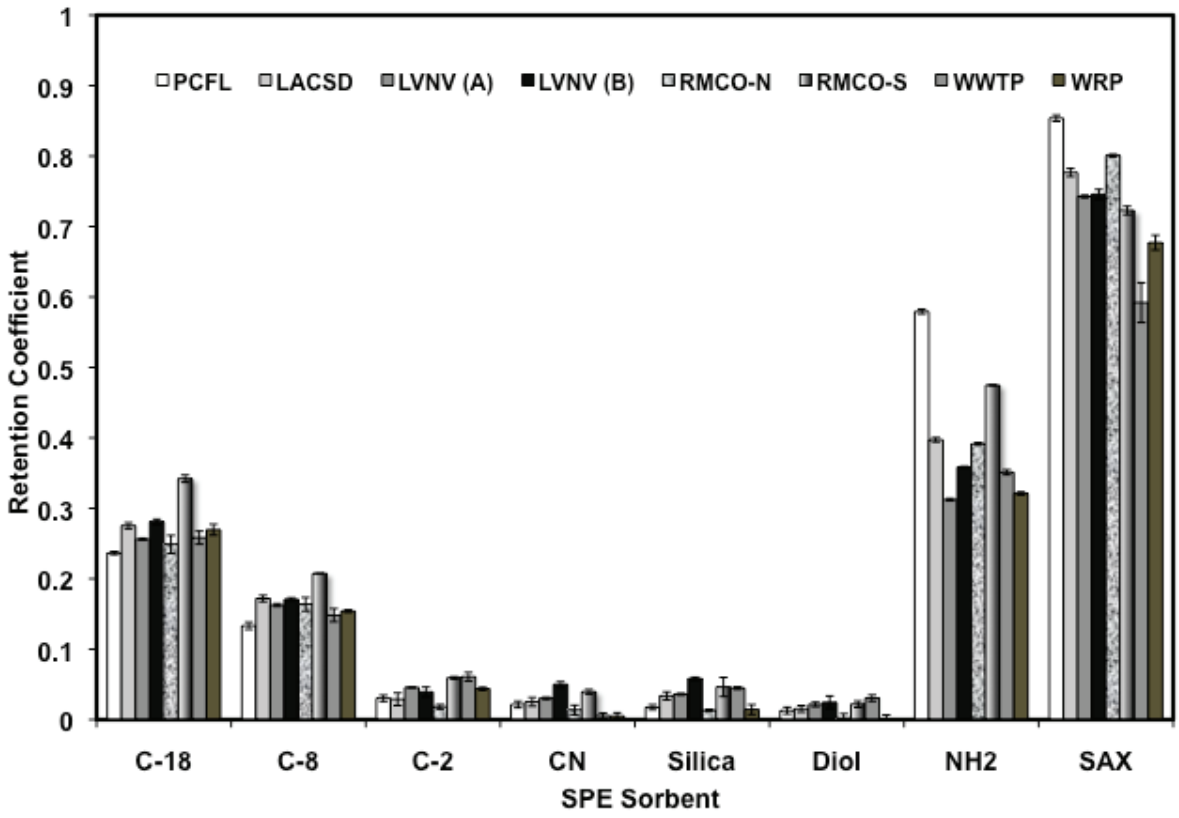

Figure 4.3. Polarity results for the characterization of the samples.

Figure 4.4 presents the UV-Vis spectra for all of the samples. Table 4.3 presents the FI for the samples. This index, defined as the ratio of the fluorescence intensity at 450 and 500 nm with an excitation wavelength of 370 nm, has been used to characterize the origin of the EfOM, differentiating between aquatic and terrestrial origin (McKnight et al., 2001). These index values were between 1.28–1.64.

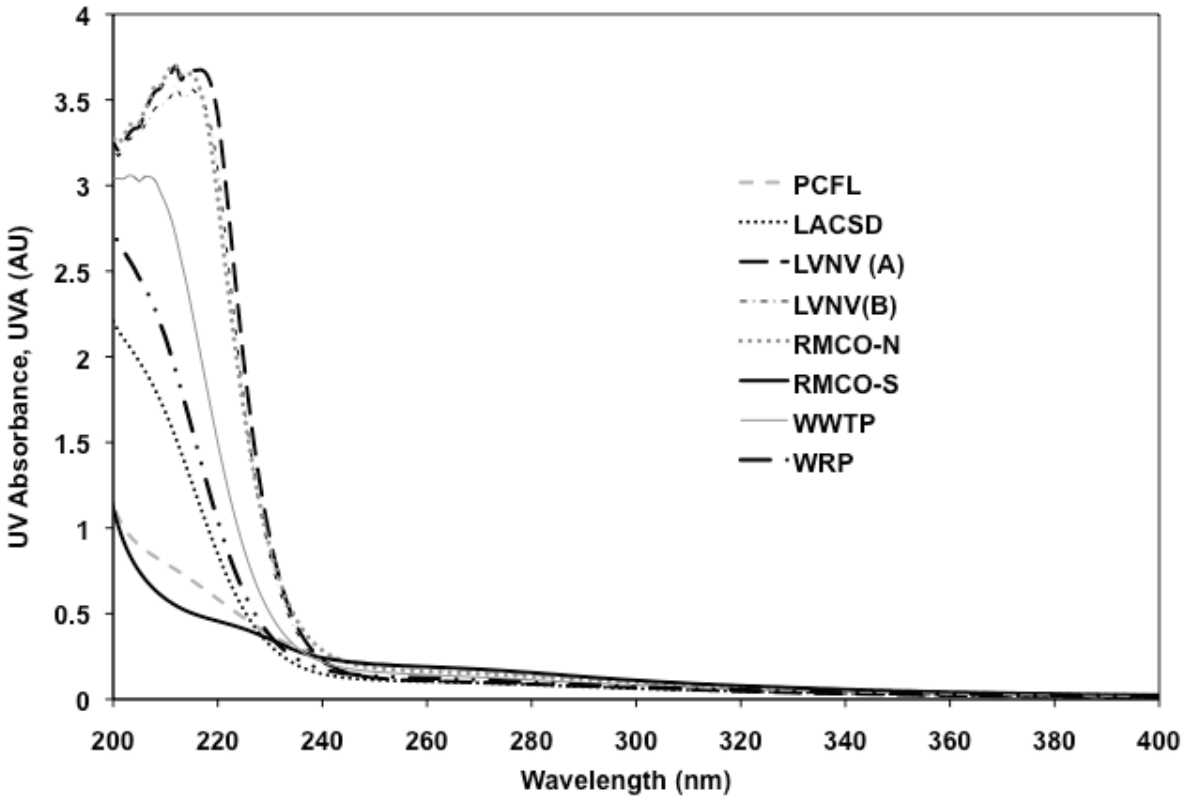

Figure 4.4. UV-Vis spectra for all the collected raw wastewater samples.

4.4.2 Computer Modeling

In order to ultimately allow prediction of $k_{EfOM\text{-}OH}$, multivariable linear regression was used to create an empirical model to describe the observed variability in the reaction rate constants based on EfOM properties (Eq. 4-1). This model could be used as a first approximation to the reactivity of EfOM at different sites. Table 4.2 presents the properties selected for the model, which include SUVA 254, RC-NH2, RC-C18, MW_W, d, and the fluorescence index. Inclusion of other parameters did not increase the goodness-of-fit, and removal of any of the these six parameters resulted in significantly lesser agreement. Using these six parameters a multilinear regression analysis resulted in the following expression for the prediction of rate constants, derived using the in-built function in Excel ($R^2 > 0.99$):

$$10^9 k_{OH-EfOM} = 1.13 \times SUVA + 1.22 \times RCNH2 + 2.31 \times FI - 1.82 \times RCC18 - 0.0018 \times MW_W + 4.12 \times d - 8.90 \qquad (4-1)$$

Figure 4.5 presents the measured and calculated rates and the fit obtained using this equation. The numerical values have errors less than 10%. Sensitivity analysis also revealed that the most important predictors were FI and d. Recent data suggest that there is a clean difference in reactivity between the low and high molecular weight fraction of the EfOM, which would explain the role of d on the prediction of reactivity. The role of FI needs to be assessed in a more mechanistic approach.

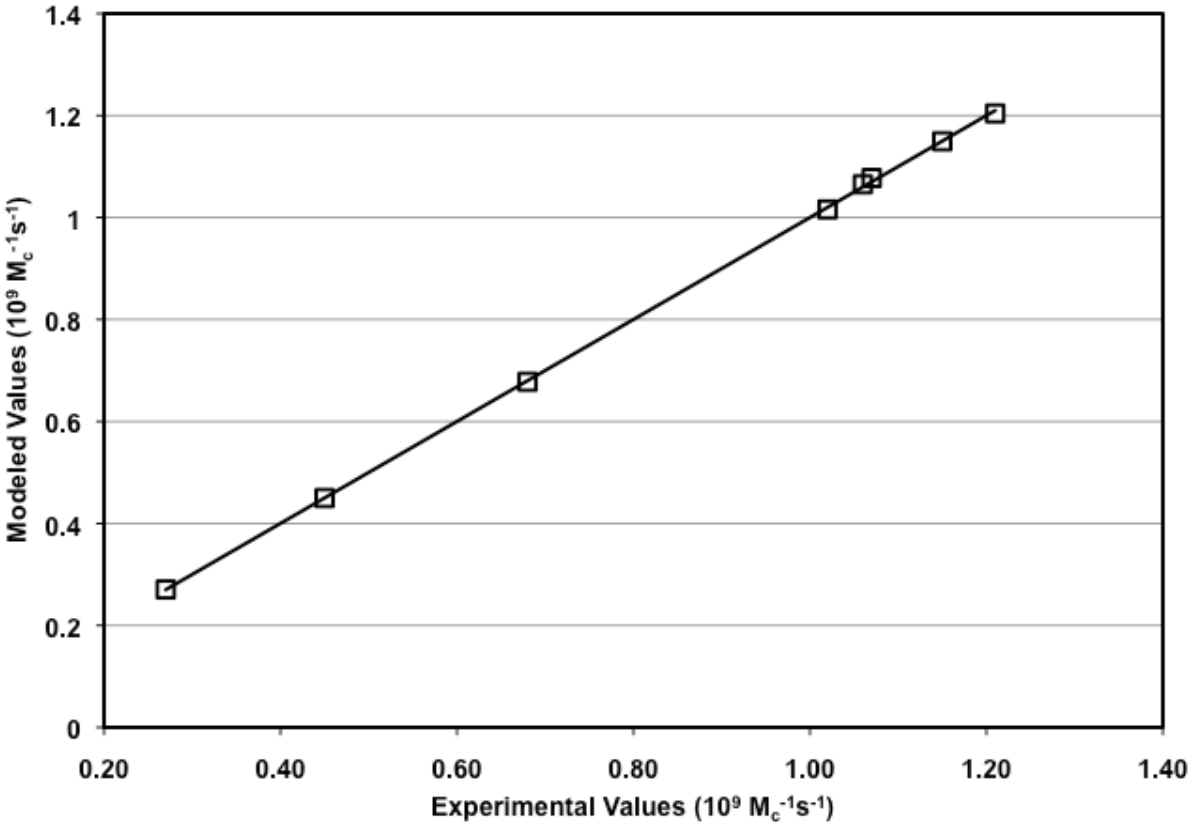

Figure 4.5. Experimental and modeled (based on eq. 4.1) second-order reaction rate constants between EfOM and $^{\bullet}$OH ($r^2 > 0.999$).

4.5 EFFECT OF OXIDATION ON $k_{EFOM\text{-}OH}$

In the previous section, the second-order reaction rate constants between $^{\bullet}$OH and EfOM were measured and an empirical model was developed that could allow utilities to estimate the EfOM scavenging capacity at different sites. However, these values are for the initial state of the EfOM. During advanced oxidation, the EfOM may also be oxidized, and these changes could result in changes in the reactivity of the EfOM. In this section, we tested this by pre-oxidizing the EfOM and evaluating the effect on the $k_{EfOM\text{-}OH}$.

4.5.1 EfOM Oxidation

Five ozone dosages were applied to a sample collected at the LVNV (Table 4.4). Ozone dosages of 0.9 and 2.0 mg/L were below the instantaneous ozone demand (IOD), thus no dissolved ozone residual was present. The IOD is the initial phase of ozonation occurring during mass transfer of ozone into solution (Buffle et al., 2006c). These two dosages below the IOD were applied to oxidize a portion of the fast-reacting EfOM. The other two ozone dosages were above the IOD. The dissolved ozone residual decay curves are shown in Figure 4.6. The dosages of 3.3 and 6.0 mg/L are within the range that a wastewater plant would use

for disinfection and micropollutant oxidation. The ozone dose of 11.6 mg/L was used to oxidize a vast amount of the EfOM, changing the character of the EfOM the most.

Ozone results showed a reduction in UVA at 254nm as the dose increased, as expected (Table 4.4). The corresponding SUVA values decreased, indicating a reduction in the aromatic carbon present. Bromate formation was also monitored and is shown in Table 4.4. At the dosages below the IOD, bromate formation was either less than or around the detection limit. As the IOD was exceeded, bromate formation reached 54 µg/L at a dose of 11.6 mg/L.

Table 4.4. Water Quality Changes After Ozonation of LVNV (C) Effluent

Ozone Dose (mg/L)	TOC (mg/L)	UVA (254 nm) (cm^{-1})	SUVA ($L\ m^{-1}\ mg^{-1}$)	Fluorescence Index	Bromate ($\mu g\ L^{-1}$)
0.0	6.7	0.114	1.70	1.63	<1.0
0.9	6.5	0.099	1.52	1.58	<1.0
2.0	6.5	0.081	1.25	1.43	1.5
3.3	6.4	0.064	1.00	1.38	5.6
6.0	6.2	0.053	0.86	1.35	17
11.6	6.0	0.043	0.72	1.34	54

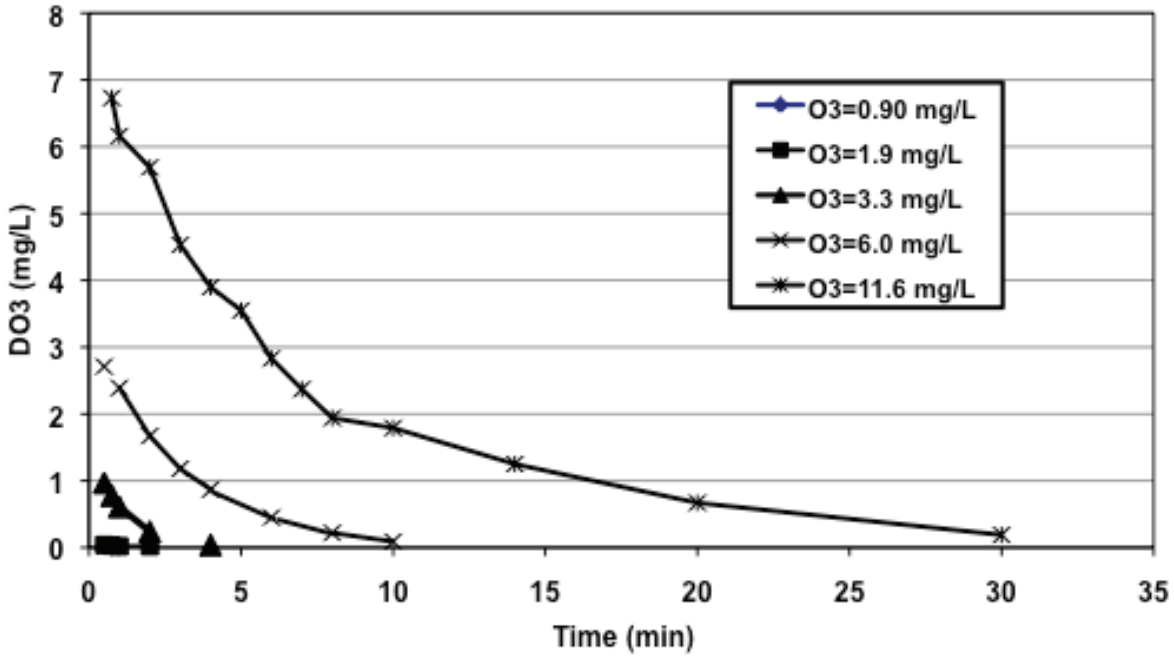

Figure 4.6. Dissolved ozone residual decay profile in tertiary effluent.

4.5.2 Effect of Oxidation on the EfOM

The changes in EfOM physicochemical properties were examined using SEC, polarity and fluorescence spectroscopy. The SEC UVA chromatogram is shown in Figure 4.7. Exposure to ozone clearly had an effect on the apparent molecular weight distribution, with an overall shift observed from high to low molecular weight after ozonation. This change has also been reported by numerous authors (Becker and O'Melia, 1996; Hesse et al., 1999; Vuorio et al., 1998). The overall proportion of aromatic EfOM changes from higher molecular weight to lower molecular weight. Recent models suggest that these mechanisms include reaction of ozone within the hydrophobic core, resulting in the production of smaller molecular weight fragments (aldehydes, carboxylic acids, etc.; Jansen et al., 2006).

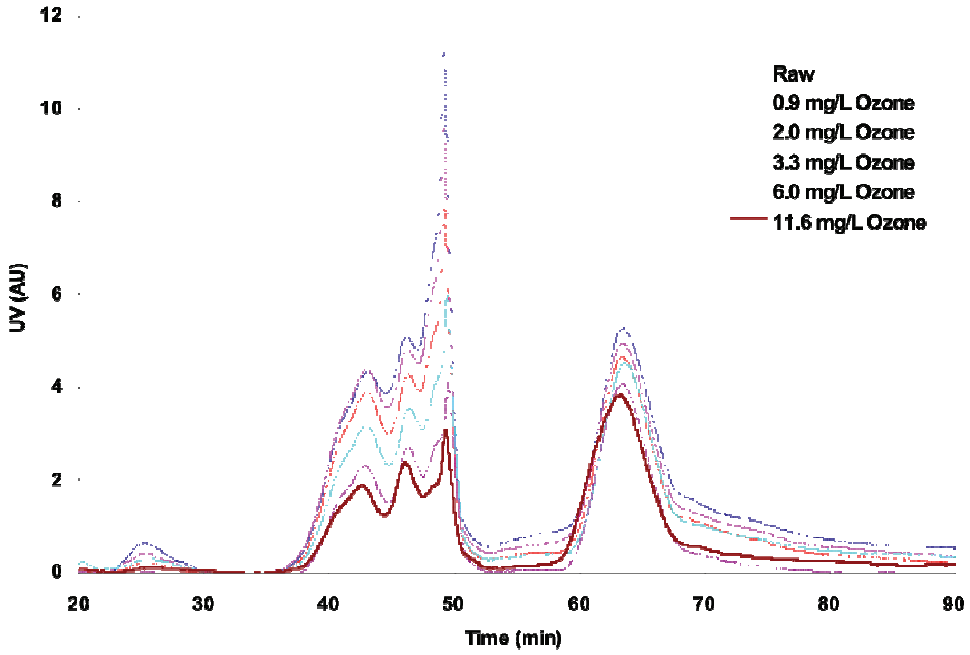

Figure 4.7. SEC chromatograms with UVA detection.

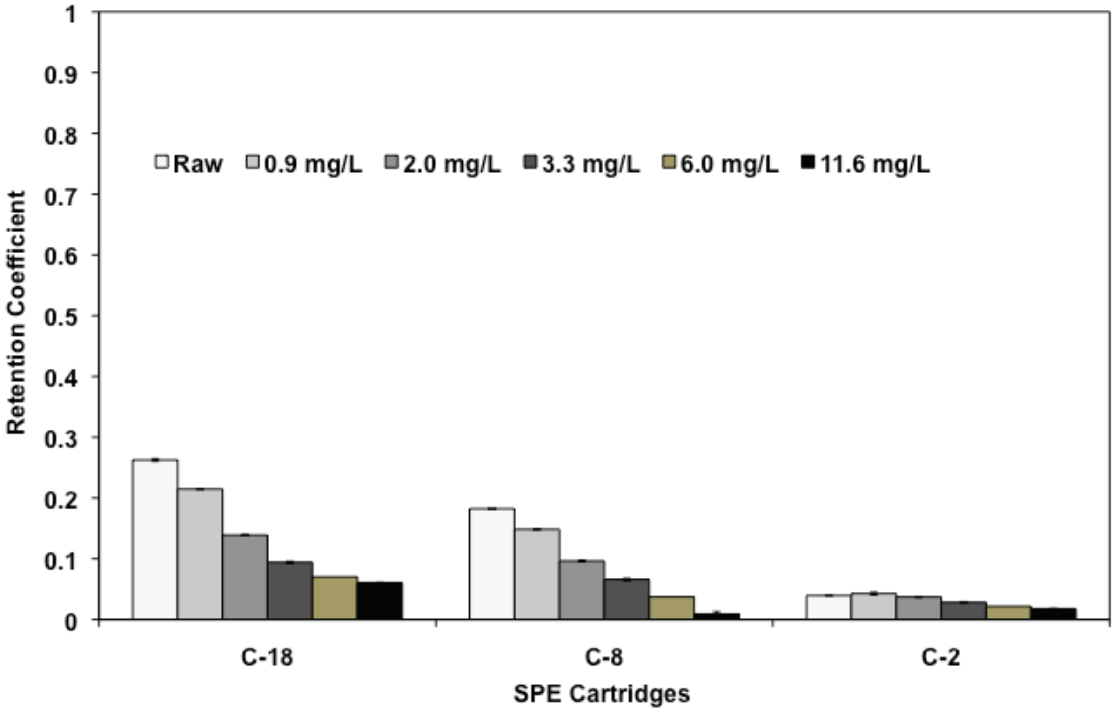

Figure 4.8. Polarity results for the characterization of the samples.

Analysis of Figure 4.8 reveals that ozonation also resulted in a decrease of hydrophobic EfOM as shown by the reduction in the RC for C18 and C8. The fluorescence index data are shown in Table 4.4. As the ozonation dose increased, the index value decreased, indicating a change in the properties of EfOM.

4.5.3 Effect of Oxidation on $k_{EfOM\text{-}OH}$

The measured values for the rate constants for ozonated waters are shown in Table 4.5 and Figure 4.9. The rate constant for the raw water was $(4.38 \pm 0.06) \times 10^8$ M_C^{-1} s^{-1}. Two previous determinations of this rate constant, 4.50 and 12.1 x 10^8 M_C^{-1} s^{-1}, have been reported (Rosario-Ortiz et al., 2008). In this study, these differences were attributed to variations in the properties of the EfOM between samples.

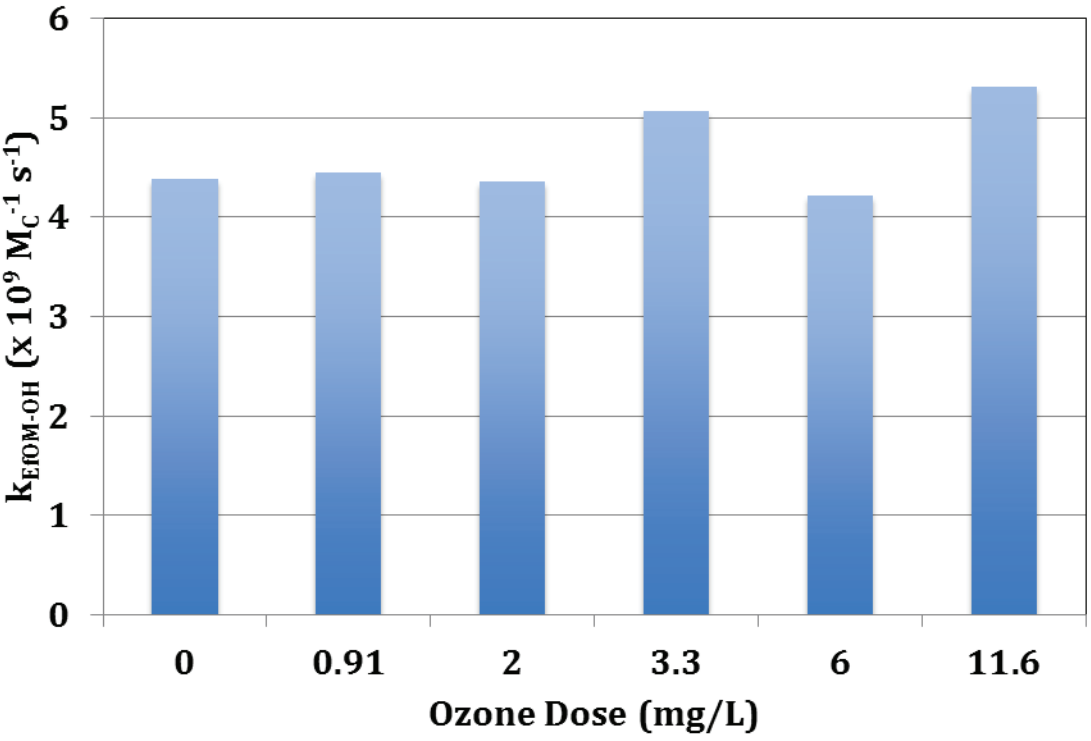

Figure 4.9. Effect of ozone oxidation on $k_{EfOM-OH}$

Table 4.5. Summary of Wastewater Parameters Used for Hydroxyl Radical Rate Constant Determinations

Ozone (mg/L)	Alkalinity (mg/L)	Solution pH	TOC (mg/L)	Calc. 10^5 k_x[X] s^{-1}	Calc. 10^4 k_{carb}, s^{-1}	Calc. 10^8 $k_{EfOM-OH}$ M_C^{-1} s^{-1}
0.0	120	7.55	6.7	2.66	2.09	4.38 ± 0.06
0.91	118	7.50	6.4	2.57	2.02	4.45 ± 0.05
2.0	114	7.50	6.3	2.29	1.95	4.36 ± 0.04
3.3	113	7.48	6.1	2.76	1.92	5.06 ± 0.26
6.0	105	7.50	5.6	2.15	1.80	4.22 ± 0.13
11.6	98	7.50	5.0	2.38	1.68	5.31 ± 0.25

After oxidation using ozone, the values for the reaction rate constant between •OH and EfOM remained effectively the same, with an average value of (4.63 ± 0.45) x 10^8 M_C^{-1} s^{-1}. Even though oxidation dramatically changed the physicochemical properties of the EfOM, these changes did not result in significant change to the EfOM-•OH reaction rate constants. The reaction mechanism of •OH includes H -atom abstraction, radical addition and direct oxidation (Buxton et al., 1988). As a result, the number of available sites for reaction is far more numerous. Oxidation by ozone would have a limited effect on the overall rate because

there will always be excess active sites present. Therefore, no change in the EfOM-•OH rate constant would be expected unless the rate of mineralization increases, and the number of active sites is considerably reduced, which is not expected during typical AOP conditions.

4.6 IMPLICATIONS

The ability to estimate the value of $k_{EfOM\text{-}\bullet OH}$ and any possible variations in it using simple parameters would allow design engineers and modelers to predict the overall scavenging of the •OH and the effectiveness of an AOP to remove specific micropollutants. This would allow better estimation of the concentration and exposure of •OH during large-scale application processes.

Amongst all the AOPs currently used, UV-AOP is preferred for reuse applications. In this application, •OH is formed by photolysis of hydrogen peroxide. During the course of the irradiation, the •OH concentration reaches a steady state value, as defined by Eq. 4.2 (Rosenfeldt and Linden, 2007).

$$[^{\bullet}OH]_{ss} = \frac{E_0 \varepsilon_{H_2O_2}[H_2O_2]\phi_{OH}}{U_{254}\left(k_{EfOM-{}^{\bullet}OH}[EfOM] + k_{CO_3^{-2}-{}^{\bullet}OH}\left[CO_3^{-2}\right] + k_{HCO_3^{-}-{}^{\bullet}OH}\left[HCO_3^{-}\right] + k_{H_2O_2-{}^{\bullet}OH}\left[H_2O_2\right]\right)} \quad (4.2)$$

The numerator described the rate of formation of •OH based on the photolysis of hydrogen peroxide (E_0 is the fluence in units of mW/cm^2; ε is the molar absorptivity coefficient in units of M^{-1} cm^{-1}; and Φ_{OH} is the quantum yield for the formation of •OH in units of mole Einstein^{-1}). The denominator represents the overall contribution of different •OH scavengers, including organic micropollutants, carbonate, peroxide, and EfOM. U_{254} is the energy per mole of photons. In order to accurately predict the •OH concentration, detailed information on each rate is needed.

Figure 4.10 shows the normalized steady state •OH concentrations predicted for a reuse system using eq. 4.1 with different reaction rate constants between EfOM and •OH. Values were normalized to maximum calculated $[^{\bullet}OH]_{ss}$ obtained with k_{OH} = 1.39 x 10^8 M$_c^{-1}$ s^{-1} and are presented in this way to show the effect of the faster rates on the estimated •OH concentrations. Reported rates ($k_{EfOM\text{-}OH}$; from this study) and literature values from Westerhoff et al. (2007). The model assumed [H_2O_2] = 0.15 mM; [CO_3^{2-}] = 0.02 mM; [HCO_3^-] = 2.05 mM; [EfOM] = 0.58 mM (as C). Second-order rate constants: $k_{CO3\text{-}OH}$ = 3.9 x 10^8 M^{-1} s^{-1}; $k_{HCO3\text{-}OH}$ = 8.5 x 10^6 M^{-1} s^{-1}; $k_{H2O2\text{-}OH}$ = 2.7 x 10^7 M^{-1}s^{-1}. Taking the average rate constants from Westerhoff et al. (2007), and the average values from this work, a 25% reduction in estimated •OH concentration is predicted. When taking the slowest value from Westerhoff et al. (2007) and the fastest rate constant here, a 72% decrease is calculated. These results indicate that detailed information on the reactivity between bulk EfOM and •OH is needed, as use of other reported values may cause significant differences in the available concentration of •OH. Results from Chapters 5 and 6 illustrate the effect of variable EfOM reactivity on micropollutants removal.

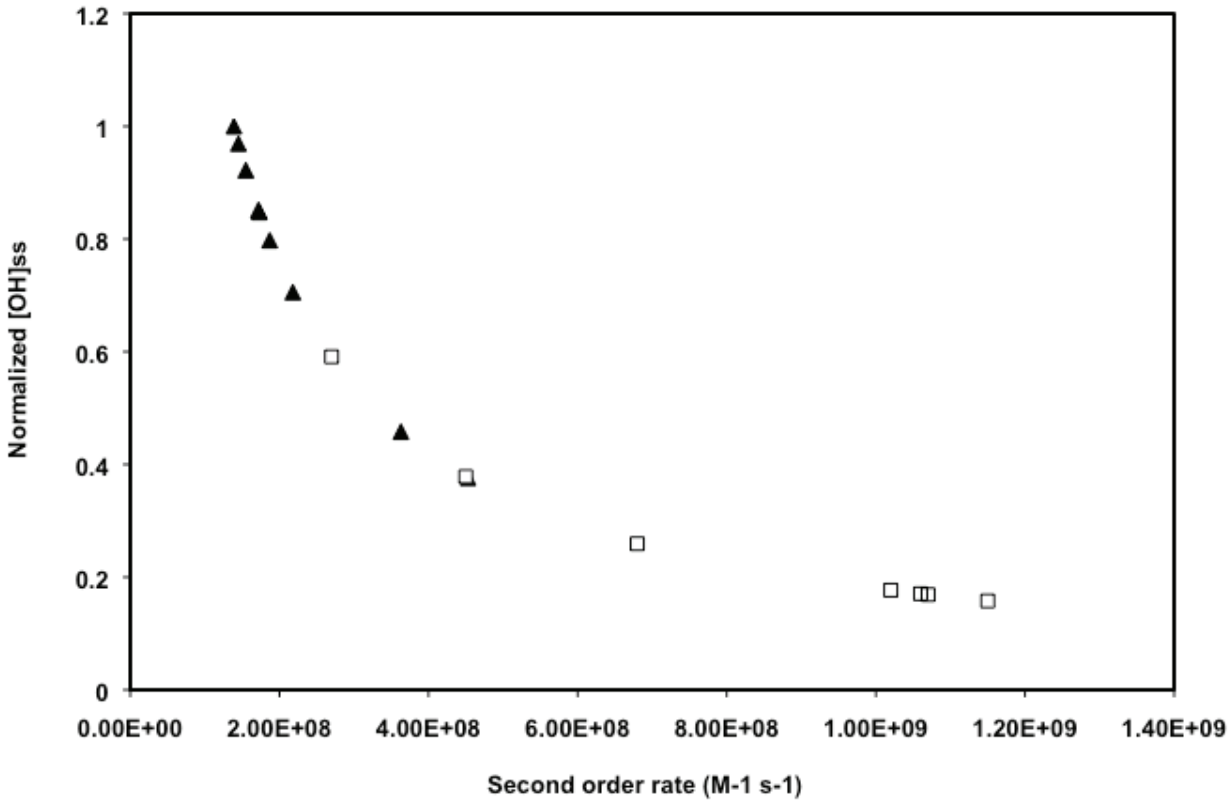

Figure 4.10. Normalized predicted ˙OH steady state concentrations.

CHAPTER 5

APPLICATION OF UV/H_2O_2 FOR MICROPOLLUTANTS REMOVAL AND THE EFFECT OF THE WATER QUALITY

5.1 INTRODUCTION

The use of UV and UV with hydrogen peroxide (UV/H_2O_2) for contaminant removal has gained attention because of the increased interest in removing organic micropollutants (i.e., NDMA) and meeting disinfection goals, while minimizing byproduct formation (Benitez et al., 2002; Hengesbach et al., 1993; Lopez et al., 2002; 2003; Meulemans, 1987; Rosenfeldt and Linden, 2004; Rosenfeldt et al., 2005; Sharpless and Linden, 2003; von Sonntag and Schuchmann, 1992). Application of UV has been shown to be effective at disinfecting, although application of UV photolysis alone does not result in considerable reduction in the concentrations of organic micropollutants. The addition of hydrogen peroxide increases the production of $^{\bullet}OH$, which also increases contaminant oxidation.

One of the most important factors associated with the application of UV/H_2O_2 is the overall efficiency of $^{\bullet}OH$ formation and its overall exposure and the influence of the water quality (i.e., EfOM). The amount and type of EfOM will influence UV exposure by absorbing some fraction of the radiation, thereby limiting the photolysis of H_2O_2 and subsequent production of $^{\bullet}OH$. In addition, scavenging by various water quality components limits the availability of $^{\bullet}OH$ for contaminant removal. As shown in Chapter 4, the $^{\bullet}OH$ scavenging effect of the EfOM will be dependent on the specific physicochemical properties of the EfOM.

In order to evaluate the efficiency of UV/H_2O_2 for the removal of micropollutants, two sets of experiments were conducted. In the first set, three samples were collected from different wastewater and reuse plants across the United States. These samples were treated using a bench-scale, low-pressure UV system. Samples were exposed to different UV fluences and H_2O_2 concentrations. The $^{\bullet}OH$ exposures and scavenging capacities were quantified for each water in order to evaluate the effect of water quality on $^{\bullet}OH$ production. This was followed by the quantification of overall removal of pharmaceuticals. For the second set of experiments, a site with low EfOM scavenging was selected for pilot-scale UV/H_2O_2 experiments to evaluate the removal of micropollutants.

5.2 MATERIALS AND METHODS

5.2.1 Bench-Scale UV/H_2O_2

The bench-scale system is described in Chapter 2. Samples were collected at three wastewater treatment plants (LVNV, RMCO and PCFL). Samples were collected in 20-gal drums and shipped overnight to SNWA. Water quality was obtained following standard methods (APHA, 1998) by the SNWA laboratory. EfOM characterization was done using polarity, SEC, and fluorescence (McKnight et al., 2001; Rosario-Ortiz et al., 2007a; 2007b).

5.2.2 Pilot-Scale UV/H_2O_2

The pilot system, described in Chapter 2, was installed at the LVNV site.

5.3 RESULTS

5.3.1 Bench-Scale UV/H_2O_2

5.3.1.1 Water Quality

The water quality is presented in Table 5.1. The TOC of the samples varied from 6.6 to 10.3 mg/L and the UV transmittance (UVT) ranged from 55 to 72%. These values represent amounts in typical wastewater and water reuse facilities. The low UVT values resulted in longer exposures in order to reach the predetermined UV doses and represent the low end of UVT values used during UV treatment. The alkalinity and nitrite concentrations, which will influence the effectiveness of the treatment for pharmaceutical removal, also varied. The SUVA values were between 2.5 and 1.7, indicating low aromatic character, expected for wastewater effluents. The initial concentrations of the organic micropollutants studied are shown in Table 5.2. The concentration of micropollutants such as meprobamate and atenolol varied between waters.

Table 5.1. Water Quality Parameters for the Samples Studied During Bench-Scale UV/H_2O_2

Site	TOC (mg/L)	UV 254 (1/cm)	UVT	SUVA (m^{-1} mg^{-1} L)	pH	Alkalinity (mg/L)	Ammonia (mg/L)	Nitrite (mg/L)	Nitrate (mg/L)
LVNV	6.6	0.14	0.72	2.1	8.2	128	<0.2	<0.05	14.8
RMCO	10.3	0.17	0.67	1.7	7.1	101	1.28	0.40	13.8
PCFL	10.3	0.26	0.55	2.5	7.6	269	6.98	0.77	9.38

Table 5.2. Initial Concentration of Micro-Pollutants (ng/L)

	LVNV	RMCO	PCFL
Meprobamate	1000	510	720
Dilantin	160	260	210
Carbamezapine	210	460	320
Primidone	190	200	240
Atenolol	1400	2600	320
Trimethoprim	120	760	38

Table 5.3 presents the results for the characterization of the EfOM for each water sample. The PRAM results indicate that the nonpolar character for the entire sample, at ambient pH and ionic strength, was between 20 and 30%. These results are comparable to other samples also evaluated at ambient conditions (Rosario-Ortiz et al., 2007a). The results for -NH2, which represents the anionic or charged portion of the EfOM, were between 27 and 58%. The EfOM from the LVNV sample had the lowest proportion of anionic character. The molecular weight of the samples was between 1054 and 1506 Da. The highest molecular weight was observed for the EfOM on the PCFL site. The properties described here have been shown to influence $k_{\text{EfOM-OH}}$, as described in the following and in Chapter 4.

Table 5.3. EfOM Properties

Site	SUVA[1] (m-1 mg-1 L)	RC NH2[2]	FI[3]	RC C18[4]	Mw[5] (Da)	d[6]
LVNV	1.8	0.27	1.6	0.24	1141	1.46
RMCO	1.7	0.39	1.6	0.30	1054	1.52
PCFL	2.6	0.58	1.4	0.20	1506	1.90

Note. [1]Specific UV absorbance. Measure of aromaticity. [2]Retention coefficient for NH2. Measure of hydrophilicity/anionic character (Rosario-Ortiz et al., 2007b). [3]Ratio of the fluorescence at 370 nm excitation and 450/500 nm emission (McKnight et al., 2001). [4]Retention coefficient for C18. Measure of hydrophobicity (Rosario-Ortiz et al., 2007b). [5]Weight average apparent molecular weight. [6]Dispersity.

5.3.1.2 Scavenging Capacities

The overall $^{\bullet}$OH scavenging rates for each water was estimated using eq. 5.1, which includes the contribution of the major species in terms of overall concentration and reactivity (the scavenging of H_2O_2 at the conditions studied here was insignificant). The values for the reaction rate constants with $^{\bullet}$OH are: $k_{CO3\text{-}OH}$ is 3.9×10^8 M^{-1} s^{-1}; $k_{HCO3\text{-}OH}$ is 8.5×10^6 M^{-1} s^{-1}; $k_{NO2\text{-}OH}$ is 1.0×10^{10} M^{-1} s^{-1} (Buxton et al., 1988), and their concentrations are easily measured following standard procedures (APHA, 1998). (The contribution of peroxide is insignificant at <20 mg/L)

$$SR \approx k_{HCO_3^- - {}^{\bullet}OH}[HCO_3^-] + k_{CO_3^{2-} - {}^{\bullet}OH}[CO_3^{2-}] + k_{NO_2^- - {}^{\bullet}OH}[NO_2^-] + k_{EfOM - {}^{\bullet}OH}[EfOM] \qquad (5.1)$$

The value of $k_{EfOM\text{-}OH}$ was estimated using the model described in Chapter 4, which is based on measurable properties of the EfOM. Table 5.4 presents the measured properties and estimated second-order reaction rate constants between EfOM and •OH for the three waters tested. These values refer to the initial expected reactivity between EfOM and •OH, although it has been shown that the initial values are expected to remain constant during the course of the oxidation (see Chapter 4).

Table 5.4. Second-Order Reaction Rate Constant Between EfOM and •OH for Each Water and Estimated Overall Scavenging Capacity

Site	Rates [1] (10^9 M_C^{-1} s^{-1})	Estimated Scavenging Rate [2] (10^5 s^{-1})
LVNV	0.68	4.02
RMCO	1.12	12.6
PCFL	2.72	23.9

[1]Using equation # 1 from Chapter 4.

[2]$k_{EfOM\text{-}OH}$[EfOM] + $k_{HCO3\text{-}OH}$ [HCO3-] + $k_{CO3\text{-}OH}$[CO32-] + $k_{NO2\text{-}OH}$[NO2-]

Using this information, an estimate of the scavenging capacity of the waters was obtained. Table 5.4 presents the obtained values, which ranged from 4.02 x 10^5 s^{-1} for LVNV to 239 x 10^5 s^{-1} for PCFL. The high SF for PCFL indicates that, when comparing to the other two waters, the removal by •OH oxidation will be less (see the following).

5.3.1.3 Effect of Water Quality on •OH Exposure

Initially, the effectiveness of UV/H_2O_2 for contaminant oxidation was assessed by evaluating the specific •OH exposure for each sample under different conditions. The •OH exposure was evaluated utilizing pCBA measurements. Figure 5.1 presents the observed decay in pCBA for each of the conditions studied. Because the experimental conditions were the same for all three waters, the fraction of •OH available for pCBA decomposition will be dependent on the overall scavenging of the water matrix. The •OH exposure for the LVNV sample was higher than for the other two, as evidenced by the greater decrease in pCBA. For a fluence of 300 mJ/cm^2 and 20 mg/L of H_2O_2, there was a 70% decrease in the concentration of pCBA. Under these conditions, only 54% and 44% were observed for the other two samples (RMCO and PCFL, respectively). At 500 mJ/cm^2 and 20 mg/L of H_2O_2, the percent decrease in the concentration of pCBA was 85% for LVNV, whereas for the other two samples it was 65% and 45%. A dose of 700 mJ/cm^2 with 20 mg/L of H_2O_2 resulted in 92% removal of pCBA for the LVNV water and 80% for RMCO.

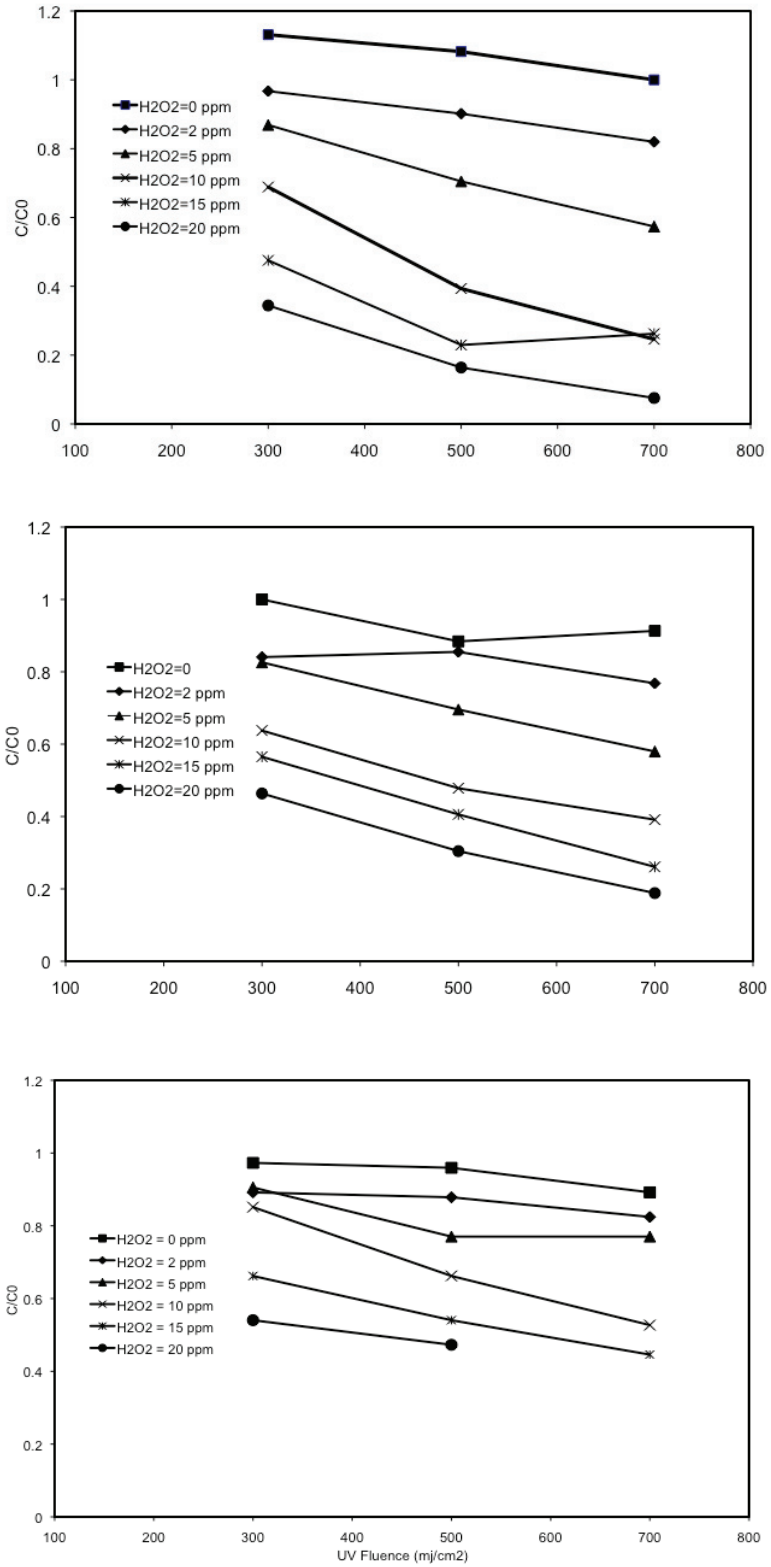

LVNV (top), RMCO (middle) and PCFL (bottom)

Figure 5.1. pCBA decay for the studied samples.

The overall exposure to •OH was quantified using the method described by Rosenfeldt and Linden (2007), which is based on the monitoring of the decay of a probe compound, pCBA. Table 5.5 presents the calculated $R_{OH,UV}$ obtained for all the conditions tested. The $R_{OH,UV}$ values were between 4.0 x 10^{-14} and 7.4 x10^{-13} M s cm^2 mJ^{-1} for the conditions tested. The higher values were obtained for LVNV at high H_2O_2 values. The lowest value was for PCFL.

Table 5.5. Calculated $R_{OH,UV}$ Values for the Various Tests (units M s cm^2 mJ^{-1})

	H_2O_2 (mg/L)				
Sites	**2**	**5**	**10**	**15**	**20**
LVNV	6.1 x 10^{-14}	1.6 x 10^{-13}	4.0 x 10^{-13}	4.8 x 10^{-13}	7.4 x 10^{-13}
RMCO	4.0 x 10^{-14}	1.0 x 10^{-13}	2.4 x 10^{-13}	3.4 x 10^{-13}	4.4 x 10^{-13}
PCFL	4.0 x 10^{-14}	6.0 x 10^{-14}	1.4 x 10^{-13}	2.2 x 10^{-13}	n/a

From the calculated $R_{OH,UV}$, the •OH exposure can be calculated by multiplying this value by the overall fluence rate for each condition (only the data for 10 mg/L H_2O_2 are shown for clarity). Table 5.6 presents the •OH exposures. The exposures ranged from 2.8 x 10^{-10} to 4.2 x 10^{-11} M s. The highest exposures values corresponded to the 700 mJ/cm^2 for LVNV, and lowest for the PCFL water.

Table 5.6. OH Exposure Conditions [H_2O_2] = 10 mg/L (units M s)

	UV Fluence		
Site	**300**	**500**	**700**
LVNV	1.2 x 10^{-10}	2 x10^{-10}	2.8 x 10^{-10}
RMCO	7.2 x 10^{-11}	1.2x 10^{-10}	1.7 x10^{-10}
PCFL	4.2x 10^{-11}	7.11x10^{-11}	9.8 x10^{-11}

5.3.1.4 The Effect of Water Quality on Contaminant Removal at Bench-Scale

The two mechanisms for the removal of micropollutants using UV/H_2O_2 are direct photolysis and reactions with $^{\bullet}OH$ radicals. Direct photolysis will be important if the compound of interest absorbs UV at 254 nm and adsorption of this photon results in the fragmentation of the molecule (i.e., a high quantum yield). In the case of molecules that do not absorb light at this wavelength, direct reaction with $^{\bullet}OH$ will be the main removal mechanism. For this pathway, the reactivity of the EfOM would be important.

Figures 5.2 through 5.4 present the observed removal of selected organic micropollutants for each of the waters tested at 300, 500 and 700 mJ/cm^2. Overall, the removal of micropollutants was better for LVNV (top), followed by RMCO and PCFL. For example, at 300 mJ/cm^2 and 20 mg/L of H_2O_2, five compounds (dilantin, carbamezapine, primidone, atenolol and trimethoprim) were removed by greater than 50% for LVNV, whereas no significant removal (less than 50%) was observed for any of the compounds at the other two sites. When 10 mg/L of H_2O_2 were added, only 3 compounds were removed by greater than 90% in LVNV. With UV fluence of 500 mJ/cm^2 and 20 mg/L of H_2O_2, six compounds were removed by greater than 50%, including the five mentioned earlier along with meprobamate. Five compounds (dilantin, carbamezapine, primidone, atenolol, and trimethoprim) were removed at greater than 50% for RMCO and only one (dilantin) for PCFL. For LVNV, five compounds were removed by greater than 90% with 500 mJ/cm^2 20 mg/L of H_2O_2. For the LVNV site, greater than 50% removal of some compounds was observed with a H_2O_2 dose of 10 mg/L, once again indicating that the efficiency of UV/H_2O_2 at this location would be better than for the other two locations.

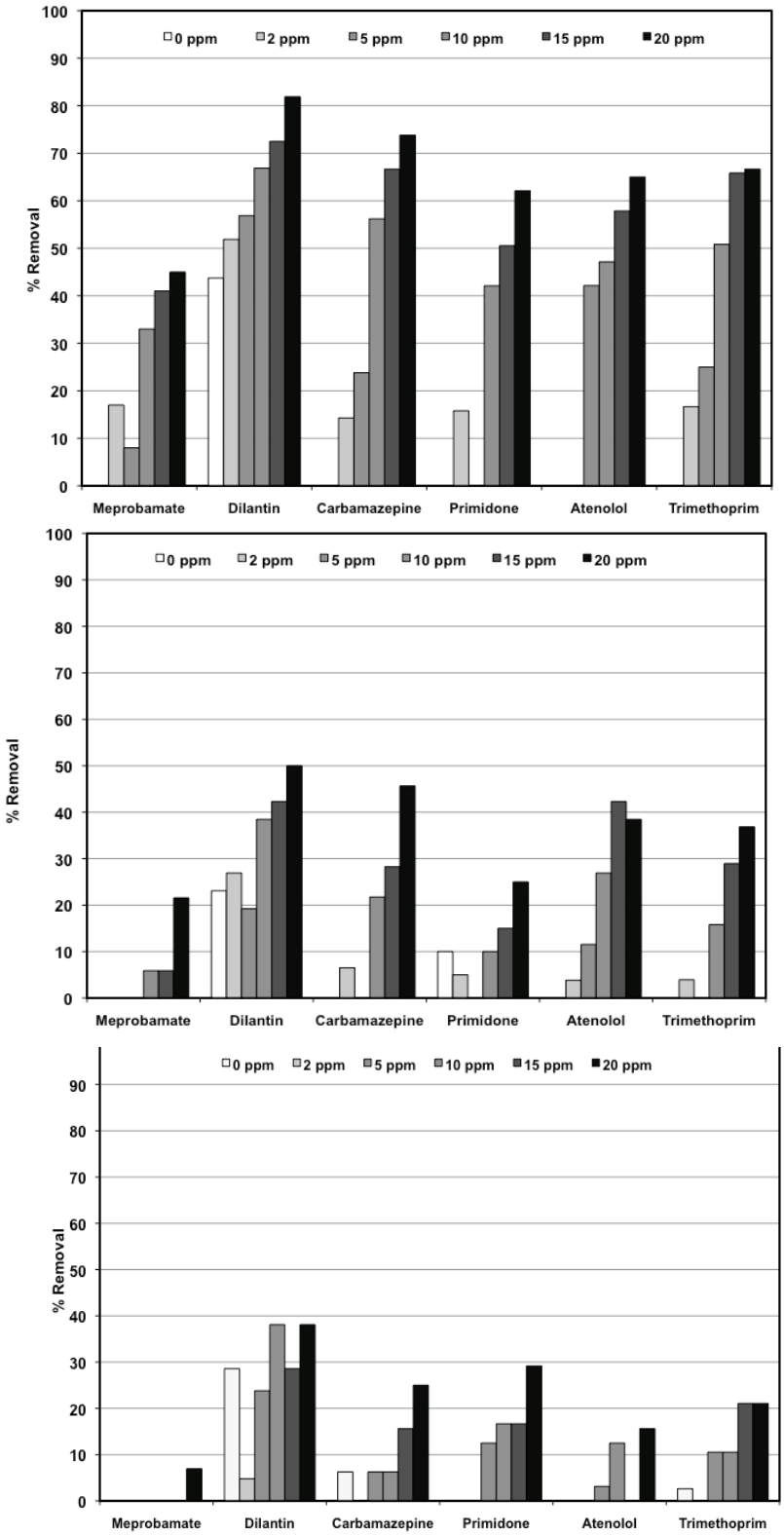

Figure 5.2. Percentage removal of pharmaceuticals, condition: 300 mJ/cm^2. LVNV (top), RMCO (middle), and PCFL (bottom).

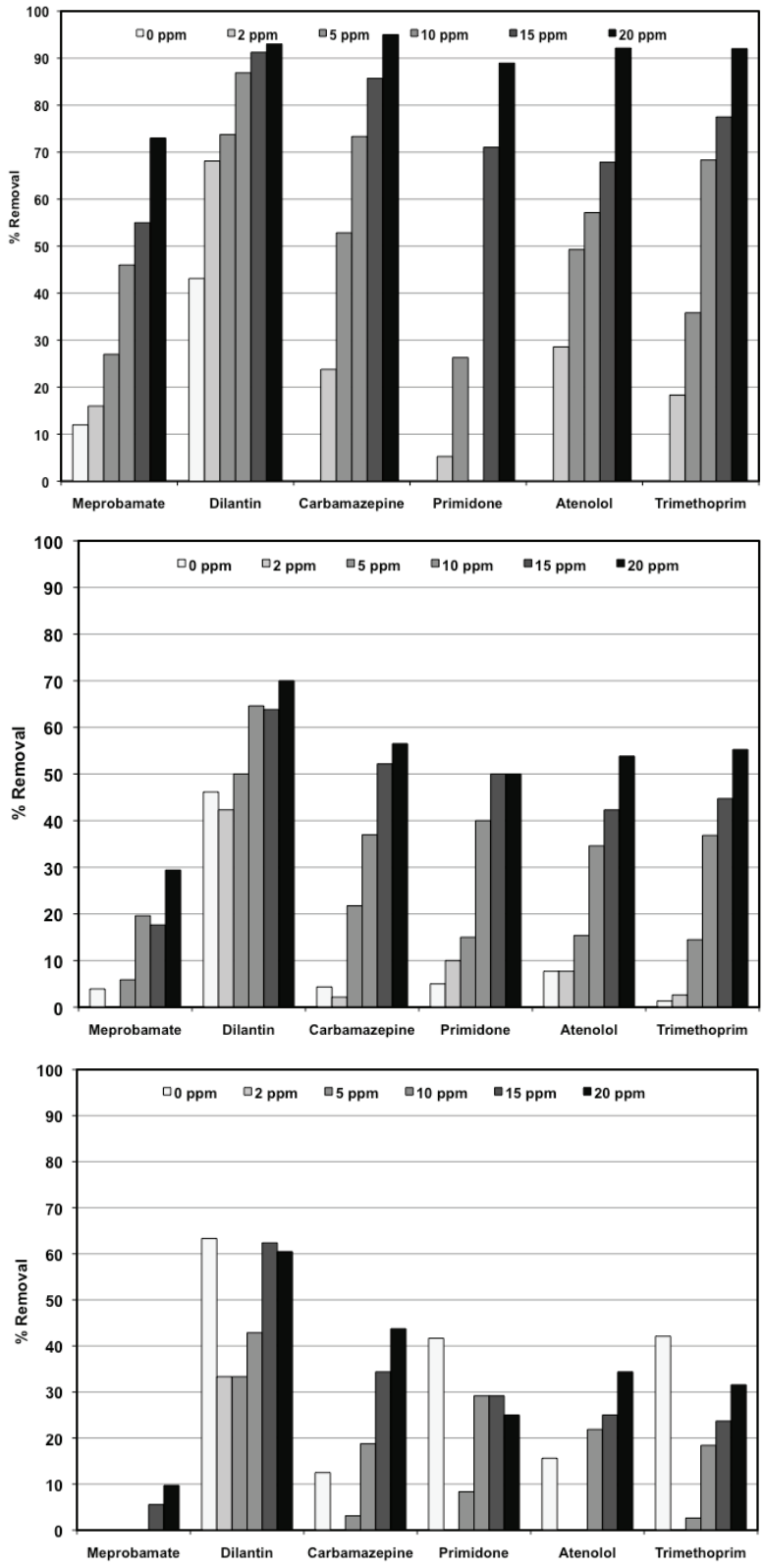

Figure 5.3. Percentage removal of pharmaceuticals, condition: 500 mJ/cm^2. LVNV (top), RMCO (middle,) and PCFL (bottom).

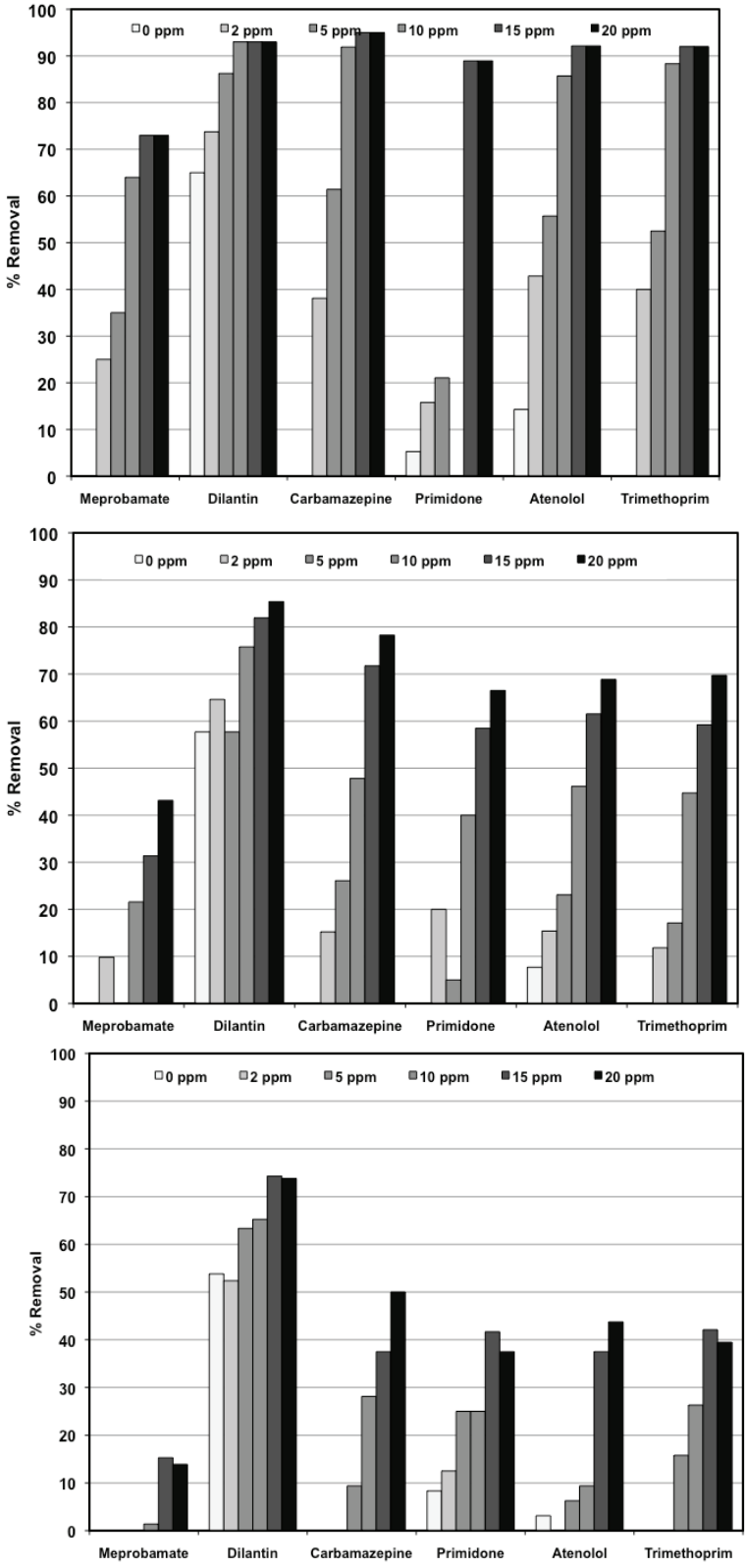

Figure 5.4. Percentage removal of pharmaceuticals, condition: 700 mJ/cm^2. LVNV (top), RMCO (middle), and PCFL (bottom).

In the case of 700 mJ/cm^2 and 20 mg/L of H_2O_2, all six compounds described previously were greater than 80% removed in LVNV. Five compounds were removed by greater than 50% at Denver. For PCFL, only dilantin was removed by greater than 50%. For LVNV, 10 mg/L of H_2O_2 was enough to remove five of the compounds by greater than 60%. The removal of dilantin was also a function of direct photolysis, as the removals were up to 60% for the 700 mJ/cm^2.

Based on the results presented previously ($^{\bullet}$OH exposures), it was expected that contaminant exposure would be better for LVNV and worse for PCFL based on their water qualities. Figure 5.5 presents a direct comparison between the removal of micropollutants for each water at one of the conditions tested (500 mJ/cm^2 and 10 mg/L of H_2O_2). This figure clearly shows how the differences in water quality affected the overall removal. Figure 5.6 presents the percentage removal of meprobamate in addition to the overall scavenging rates presented previously. The removal of meprobamate is presented at two conditions; 5 and 10 mg/L of H_2O_2, with a fluence of 500 mJ/cm^2 (lower H_2O_2 doses are not shown as limited removal is observed under 5 mg/L of H_2O_2). As the $^{\bullet}$OH scavenging by water quality components increases, the removal decreases. These data suggest that detailed characterization of the EfOM is needed in order to assess the overall effectiveness of an AOP for contaminant removal at a specific location.

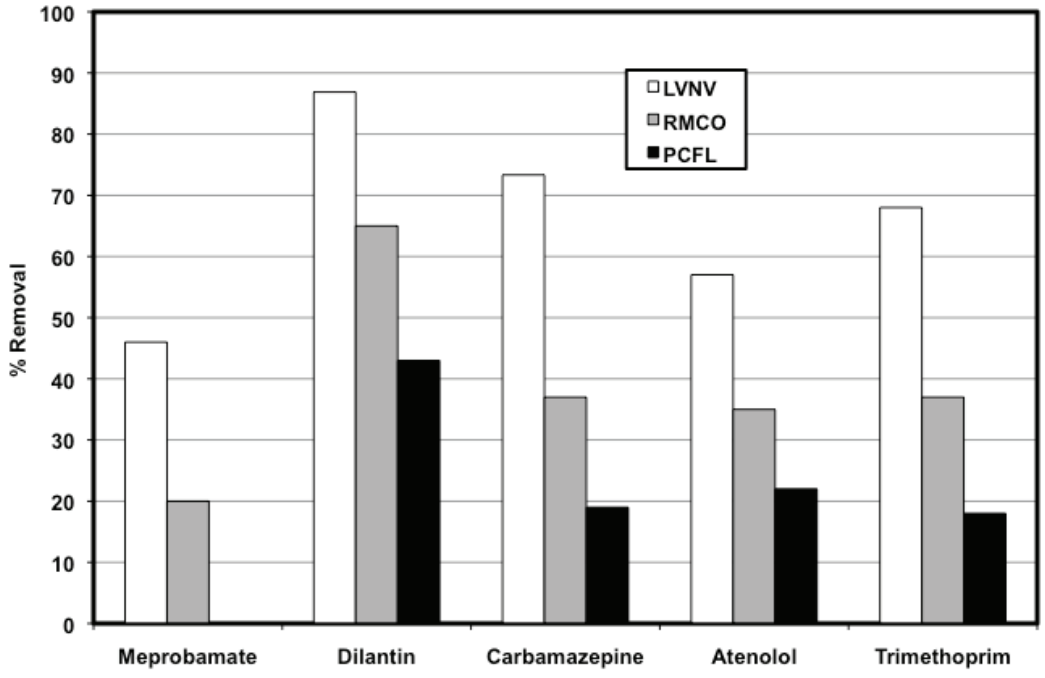

Figure 5.5. Percentage removal of micropollutants at 500 mJ/cm^2 and 10 mg/L of H_2O_2.

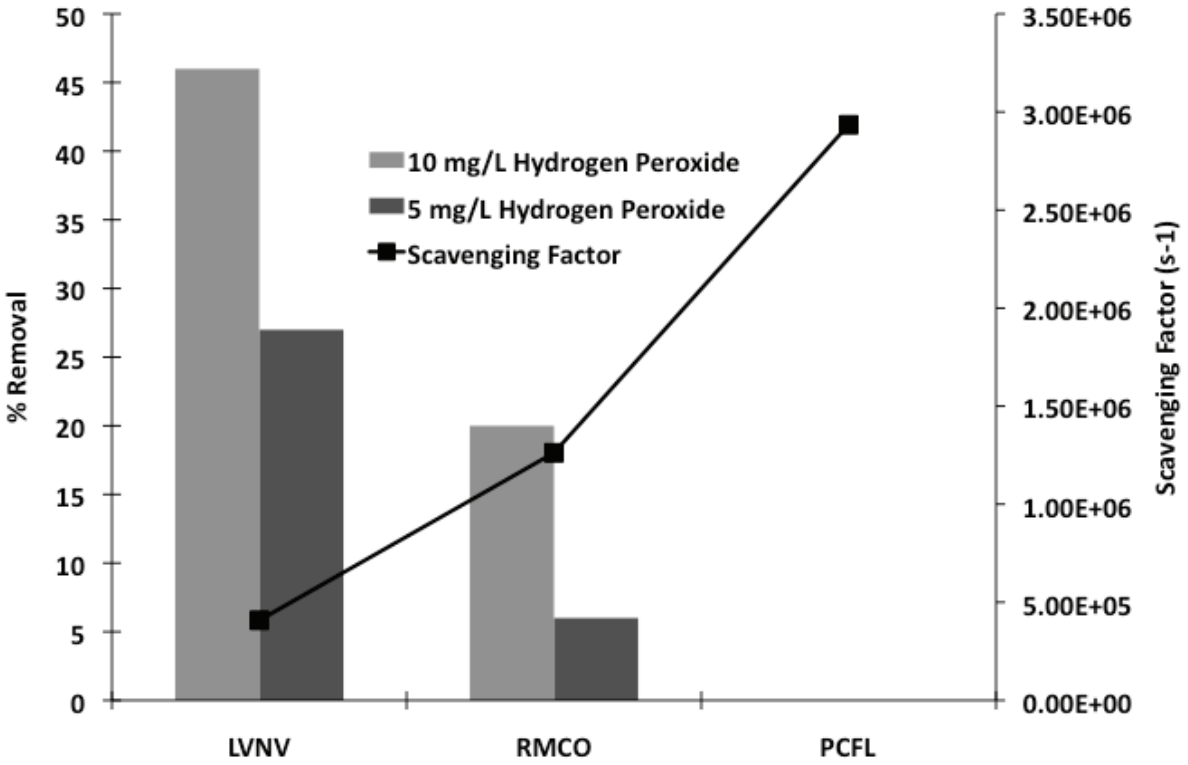

Figure 5.6. Percentage removal of meprobamate at two doses of H_2O_2 (5 and 10 mg/L) and a fluence of 500 mJ/cm2 and scavenging factors for the three wastewaters tested.

5.3.2 Pilot-Scale UV/H_2O_2

Based on the bench-scale studies, an additional test using a pilot-scale UV reactor was planned at LVNV. This site was chosen primarily because of its geographical location but also because of the fact that the EfOM scavenging capacity was the lowest determined for all samples, indicating that the application of a UV/H_2O_2 reactor would be efficient at removing a wide range of organic micropollutants. Table 5.7 presents the initial concentrations of organic micropollutants studied. These concentrations were monitored throughout the day that the experiments were performed and no significant changes were observed.

Table 5.7. Initial Concentration of Compounds

Compound	Concentration (ng/L)
Sulfamethoxazole	1200
Atenolol	590
Trimethoprim	16
Iopromide	66
Fluoxetine	30
Meprobamate	290
Dilantin	190
Carbamazepine	210
Diazepam	4
Atorvastatin	13
Primidone	170
TCPP	1300
DEET	250
TCEP	550
Gemfibrozil	2
Diclofenac	66
Naproxen	16
Triclosan	21
BHA	2.6
Musk Ketone	39

For these tests, a larger subset of 20 organic micropollutants was studied, which included fire retardants, X-ray contrast media and diverse pharmaceuticals. Some of the compounds tested have been shown to be recalcitrant to oxidative treatment (Snyder et al., 2007). For these tests, three flows were tested (60, 80, and 118 gpm) with different concentrations of added H_2O_2. There was no estimation of UV fluences. The concentration of H_2O_2 was reduced by up to 20%.

At the lowest flow (60 gpm; see Table 5.8), which corresponds with the highest overall UV fluence, greater than 90% removal of more than 6 compounds was observed with the lowest concentration of added H_2O_2 (1.82 mg/L). When this dose was increased to 13 mg/L, 14 compounds were more than 90% removed. Removal of iopromide was greater than 62% for all of the conditions tested, whereas TCEP removal was 40% at the highest H_2O_2 dose.

At a flow of 80 gpm (Table 5.9), a total of 5 compounds were removed by more than 90% with the lowest H_2O_2 dose (1.74 mg/L). At the highest dose (17 mg/L), 13 compounds were removed by more than 90%. With the highest flow used during testing (118 gpm; see Table 5.10), which corresponds to the lowest experimental UV fluence, only 3 compounds were removed by greater than 90% with the lowest H_2O_2 dose (2.50 mg/L). At the highest peroxide dose, 11 compounds were more than 90% removed.

Overall, the experimental results indicate that UV/ H_2O_2 would be effective at removing a wide variety of micropollutants at this location. It is expected that the overall efficiency would be less as the EfOM scavenging capacity increases.

Table 5.8. Percentage Removal of Micro-Pollutants (Flow = 60 gpm; 2.14 kWh/kgal)

		H_2O_2 (mg/L)				
Compound	**Initial Concentration**	**1.82**	**3.26**	**6.50**	**9.80**	**13.00**
Sulfamethoxazole	1200	97	97	>99	>99	>99
Atenolol	590	59	80	93	>99	>99
Trimethoprim	16	61	79	>96	>96	>96
Iopromide	66	>62	>62	>62	>62	>62
Fluoxetine	30	97	97	>98	>98	>98
Meprobamate	290	24	41	71	90	96
Dilantin	190	94	96	>99	>99	>99
Carbamazepine	210	69	84	97	>99	>99
Diazepam	4	61	76	>93	>93	>93
Atorvastatin	13	90	96	>96	>96	>96
Primidone	170	58	76	93	>99	>99
TCPP	1300	0	23	23	48	54
DEET	250	60	76	93	98	>99
TCEP	550	11	13	20	31	40
Gemfibrozil	2	55	71	>88	>88	>88
Diclofenac	66	92	96	>99	>99	>99
Naproxen	16	88	93	>97	>97	>97
Triclosan	21	>95	>95	>95	>95	>95
BHA	2.6	>61	>61	>61	>61	>61
Musk Ketone	39	>35	>35	>35	>35	>35

Table 5.9. Percentage Removal of Micro-Pollutants (Flow = 80 gpm; 1.60 kWh/kgal)

		H_2O_2 (mg/L)			
Compound	**Initial Concentration**	**1.74**	**4.00**	**8.60**	**17.00**
Sulfamethoxazole	1200	95	96	98	>99
Atenolol	590	53	76	89	98
Trimethoprim	16	40	65	89	>96
Iopromide	66	>62	>62	>62	>62
Fluoxetine	30	93	96	>98	>98
Meprobamate	290	24	45	71	89
Dilantin	190	91	94	98	>99
Carbamazepine	210	60	81	96	>99
Diazepam	4	49	71	90	>94
Atorvastatin	13	75	95	>96	>96
Primidone	170	52	70	89	97
TCPP	1300	0	15	23	37
DEET	250	0	68	90	98
TCEP	550	16	20	29	31
Gemfibrozil	2	20	65	>88	>88
Diclofenac	66	92	96	>99	>99
Naproxen	16	69	84	>97	>97
Triclosan	21	>95	>95	>95	>95
BHA	2.6	>61	>61	>61	>61
Musk Ketone	39	>35	>35	>35	>35

Table 5.10. Percentage Removal of Micro-Pollutants (Flow = 118 gpm; 1.09 kWh/kgal)

		H_2O_2 (mg/L)				
Compound	**Initial Concentration**	**2.50**	**6.30**	**12.00**	**19.00**	**25.50**
Sulfamethoxazole	1200	90	93	94	96	97
Atenolol	590	44	68	83	84	89
Trimethoprim	16	6	48	73	83	88
Iopromide	66	>62	>62	>62	>62	>62
Fluoxetine	30	85	90	95	>98	>98
Meprobamate	290	24	41	59	66	69
Dilantin	190	81	85	94	97	97
Carbamazepine	210	48	72	87	94	96
Diazepam	4	32	66	81	91	93
Atorvastatin	13	64	86	94	>96	>96
Primidone	170	42	63	78	86	91
TCPP	1300	8	23	29	24	32
DEET	250	44	67	78	88	90
TCEP	550	22	24	24	31	33
Gemfibrozil	2	7	45	71	>88	>88
Diclofenac	66	92	97	>99	>99	>99
Naproxen	16	48	72	89	95	95
Triclosan	21	90	93	95	>95	>95
BHA	2.6	>61	>61	>61	>61	>61
Musk Ketone	39	>35	>35	>35	>35	>35

The overall removal was used to calculate the electrical energy per order ($_{EEO}$) for the conditions tested. The $_{EEO}$ (in units of kW-h/1,00 g) values were calculated using eq. 5.2, as described by Bolton et al., 2001 (P is the rated power for the reactor, F is the flow, and c_i and c_f are the initial and final concentrations).

$$E_{EO} = \frac{P}{F \log\left(\frac{c_i}{c_f}\right)} \tag{5.2}$$

The rated power for the reactor was estimated at 8.26 kW. Tables 5.11 through 5.13 present the E_{EO} values.

Table 5.11. $_{EEO}$ (kW-h/kgal) for UV/H_2O_2 Pilot Study at Flow = 60 gpm

Compound	**Concentration of H_2O_2 (mg/L)**				
	1.8	**3.3**	**6.5**	**9.8**	**13.0**
Sulfamethoxazole	1.58	1.51	1.17	0.92	0.73
Atenolol	5.88	3.32	1.98	1.13	0.86
Trimethoprim	5.67	3.41	1.67	n/a	n/a
Iopromide	n/a	n/a	n/a	n/a	n/a
Fluoxetine	1.52	1.45	n/a	n/a	n/a
Meprobamate	19.14	9.90	4.31	2.33	1.66
Dilantin	1.91	1.63	1.06	n/a	n/a
Carbamazepine	4.57	2.86	1.46	0.90	n/a
Diazepam	5.62	3.72	n/a	n/a	n/a
Atorvastatin	2.30	1.66	n/a	n/a	n/a
Primidone	6.06	3.65	1.99	1.20	1.00
TCPP	n/a	20.16	20.16	8.16	6.84
DEET	5.77	3.75	1.97	1.27	1.02
TCEP	45.78	38.85	23.70	14.30	10.35
Gemfibrozil	6.56	4.23	n/a	n/a	n/a
Diclofenac	2.13	1.60	1.13	n/a	n/a
Naproxen	2.54	1.98	n/a	n/a	n/a
Triclosan	n/a	n/a	n/a	n/a	n/a
BHA	n/a	n/a	n/a	n/a	n/a
Musk Ketone	n/a	n/a	n/a	n/a	n/a
Ibuprofen	n/a	n/a	n/a	n/a	n/a

Table 5.12. $_{EEO}$ (kW-h/kgal) for UV/H_2O_2 Pilot Study at Flow = 80 gpm

Compound	Concentration of H_2O_2 (mg/L)			
	1.7	**4.0**	**8.6**	**17.0**
Sulfamethoxazole	1.77	1.62	1.34	1.04
Atenolol	7.10	3.68	2.35	1.36
Trimethoprim	10.35	5.04	2.36	n/a
Iopromide	n/a	n/a	n/a	n/a
Fluoxetine	1.95	1.60	n/a	n/a
Meprobamate	19.14	8.89	4.23	2.43
Dilantin	2.24	1.91	1.31	1.04
Carbamazepine	5.77	3.14	1.67	1.12
Diazepam	7.90	4.30	2.27	n/a
Atorvastatin	3.77	1.78	n/a	n/a
Primidone	7.25	4.39	2.36	1.44
TCPP	n/a	31.66	20.16	11.48
DEET	n/a	4.59	2.30	1.41
TCEP	29.59	23.70	15.38	14.30
Gemfibrozil	23.70	5.08	n/a	n/a
Diclofenac	2.07	1.67	n/a	n/a
Naproxen	4.55	2.85	n/a	n/a
Triclosan	n/a	n/a	n/a	n/a
BHA	n/a	n/a	n/a	n/a
Musk Ketone	n/a	n/a	n/a	n/a
Ibuprofen	n/a	n/a	n/a	n/a

Table 5.13. $_{EEO}$ (kW-h/kgal) for UV/H_2O_2 Pilot Study at Flow = 118 gpm

Compound	Concentration of H_2O_2 (mg/L)				
	2.5	**6.30**	**12.0**	**19.0**	**25.5**
Sulfamethoxazole	2.30	1.96	1.85	1.59	1.50
Atenolol	9.10	4.67	2.98	2.88	2.43
Trimethoprim	81.94	8.06	4.02	2.97	2.48
Iopromide	n/a	n/a	n/a	n/a	n/a
Fluoxetine	2.75	2.33	1.77	1.35	1.39
Meprobamate	19.14	9.90	5.99	4.87	4.48
Dilantin	3.18	2.76	1.86	1.52	1.45
Carbamazepine	8.18	4.11	2.58	1.90	1.69
Diazepam	13.87	4.92	3.19	2.20	2.00
Atorvastatin	5.20	2.67	1.90	n/a	n/a
Primidone	9.60	5.33	3.53	2.64	2.24
TCPP	66.07	20.16	15.30	19.41	13.96
DEET	9.12	4.80	3.49	2.45	2.26
TCEP	21.49	19.61	19.61	14.30	13.34
Gemfibrozil	76.65	8.76	4.31	n/a	n/a
Diclofenac	2.08	1.49	1.25	n/a	n/a
Naproxen	8.21	4.17	2.42	1.75	1.74
Triclosan	2.25	1.95	1.79	n/a	n/a
BHA	n/a	n/a	n/a	n/a	n/a
Musk Ketone	n/a	n/a	n/a	n/a	n/a
Ibuprofen	n/a	n/a	n/a	n/a	n/a

5.4 IMPLICATIONS

The results reported here indicate that the overall effectiveness of UV/H_2O_2 for contaminant removal will vary greatly among sites, as a function of the water quality, including EfOM. EfOM interferes not only with the overall UV exposure required to achieve a specific dose (as a function of the UVT), but also in the overall fraction of $^{\bullet}OH$ available for contaminant removal. Of the three waters tested during the bench-scale section, LVNV proved to be the best suited for UV/H_2O_2, not only because of the higher UVT, which will result in less power needed to achieve a specific UV dose, but also because of specific properties that rendered the EfOM less reactive toward $^{\bullet}OH$. These characteristics resulted in an increased effectiveness toward contaminant destruction both at bench- and pilot-scale. The other two waters proved to be more difficult to treat, based on both higher UVT and EfOM $^{\bullet}OH$ scavenging.

The results from this study indicate that UV/H_2O_2 may be effective for contaminant removal for wastewaters, depending on the water quality. Low nitrite and alkalinity, together with low EfOM reactivity will result in increased removals of pharmaceuticals. In cases where the

EfOM is more reactive (i.e., PCFL), UV/ H_2O_2 may not be effective. Physical or chemical treatments may be tested as a way of decreasing the reactivity of EfOM. The reactivity of EfOM toward $^{\bullet}OH$ should be investigated as a function of properties such as molecular weight to evaluate whether physical removal of [specific fractions] could decrease scavenging. Oxidative treatments have been shown to have no effect on the reactivity of EfOM toward $^{\bullet}OH$ (Chapter 4). Effective nitrification and de-nitrification will reduce the scavenging that is due to nitrite, although the effect of EfOM, if any, should be investigated.

CHAPTER 6

APPLICATION OF OZONE FOR CONTAMINANT REMOVAL AND THE EFFECT OF THE WATER QUALITY

6.1 INTRODUCTION

Ozone (O_3) is a strong oxidizer known for its ability to provide microbial disinfection and contaminant oxidation during drinking water and wastewater applications. The use of O_3 during wastewater and water reuse applications has gained more attention in recent years for its ability to oxidize micropollutants prior to discharge into the aquatic environment (Huber et al., 2005a; Huber et al., 2005b; Snyder et al., 2006a; Zhang et al., 2008). During the O_3 process, contaminant oxidation may occur selectively by O_3 and nonselectively by $^{\bullet}OH$. In the case of AOP, O_3 reacts with hydrogen peroxide (O_3/H_2O_2) to increase the oxidation by $^{\bullet}OH$ (von Gunten, 2003; see Chapter 1).

The application of O_3 for wastewater treatment differs from that for drinking water because of the increased levels of TOC found in wastewater, commonly known as effluent organic matter (EfOM). Greater concentrations of TOC lead to greater ozone demand and faster O_3 decay rates resulting in greater amounts of ozone being applied to achieve disinfection or contaminant oxidation goals. The O_3 demand phase ($t < 30$ s) has been shown to exhibit characteristics similar to AOPs resulting in significant $^{\bullet}OH$ exposure (Buffle et al., 2006b). O_3/H_2O_2 increases the production of $^{\bullet}OH$ when the H_2O_2 dose is applied in excess and initiates the formation of $^{\bullet}OH$ in parallel to O_3-EfOM reactions (Buffle et al., 2006a). H_2O_2 may also increase $^{\bullet}OH$ exposure when the O_3 dose exceeds the O_3 demand. In this case, H_2O_2 can react with dissolved O_3 residual to form $^{\bullet}OH$. In either case, greater concentrations of EfOM increase the scavenging capacity of wastewater. The $^{\bullet}OH$ formed may be rapidly consumed by EfOM, decreasing the effectiveness of AOP treatment for trace contaminant removal as discussed in Chapters 1 and 4.

6.2 OBJECTIVE

The focus of this portion of the project was to evaluate the efficiency of O_3 for the removal of micropollutants (most important EfOM) as a function of the water quality in three tertiary wastewaters. O_3 dosages above and below demand were applied to assess the effect of EfOM on ozone demand, O_3 exposure, $^{\bullet}OH$ exposure, and contaminant removal. Second-order rate constants between EfOM and $^{\bullet}OH$ were determined previously (see Chapters 4 and 5), and this information was used to establish an approximate scavenging capacity for each wastewater (see Chapter 5). The O_3 and $^{\bullet}OH$ exposures were related to the removal of 31 micropollutants.

6.3 METHODS

In order to evaluate O_3 exposure, bench-scale testing was performed to investigate the O_3 decay rate and exposure. Duplicate bench-scale experiments were performed with pCBA to evaluate $^{\bullet}OH$ exposure. A 1 L/min pilot plant was used to study the effect of specific O_3 dosages on contaminant removal. The experimental apparatus for both of these systems were

described in Chapter 2. Specific components of the experimental approach are discussed in the following.

6.3.1 Water Samples

For a detailed description of the samples used and water quality information refer to Chapter 5 (Table 5.3).

6.3.2 Bench-Scale Ozonation

The effective applied O_3 dose will be a function of the TOC and nitrite, because both of these species contribute to O_3 decay. As a result, the O_3-to-TOC ratio (O_3:TOC) was used to determine the O_3 dosages to observe any differences in $^{\bullet}OH$ exposure that were due to different EfOM composition. Inorganic water quality constituents found in these wastewaters were also considered as they can react with O_3, (von Gunten, 2003). Once TOC and nitrite analyses were performed, the O_3 dose was determined according to Eq. 6.1.

$$O_3 \text{ Dose} = 1.1*(NO_2) + r*TOC \qquad (6.1)$$

where: O_3 Dose = transferred O_3 dose (mg/L)
NO_2 = nitrite concentration (mg/L)
r = O_3:TOC ratio = 0.2, 0.4, 0.6, 0.8, and 1.0
TOC = total organic carbon (mg/L)

Dissolved O_3 residual and pCBA samples were collected at 10-second intervals during the first minute of reaction and each minute thereafter to investigate O_3 decomposition and $^{\bullet}OH$ exposure. Dissolved O_3 residual and pCBA samples were collected until the O_3 residual decayed to less than 0.05 mg/L, or until a contact time of 15 min was achieved. O_3 exposure was calculated by integrating the dissolved residual concentration over time (CT). The O_3 demand was calculated as the difference between the O_3 dose and the measured dissolved O_3 residual after 30 seconds of reaction time. Particular interest was given to the O_3 demand phase of ozonation, as wastewater utilities may want to consider operating in this range for trace contaminant removal. From previous work using LVNV tertiary effluent, the O_3 demand was approximately 3.1 mg/L with DOC of 7.1 mg/L (an O_3:TOC ratio of 0.43; Wert et al., 2007). We performed five O_3 experiments at bench-scale using the three waters with O_3:TOC ratios of 0.2, 0.4, 0.6, 0.8, and 1.0. These ratios will provide O_3 conditions above and below the expected O_3 demand.

Five additional experiments were performed using the O_3/H_2O_2 advanced oxidation process (AOP). During O_3/H_2O_2 experiments, H_2O_2 was added 30 seconds prior to the addition of O_3 stock solution to the reaction vessel. The O_3:TOC ratios mentioned earlier were tested using H_2O_2. In these cases, H_2O_2 was added prior to ozonation at a ratio of 0.5 mg-H_2O_2/mg-O_3. The 0.5 ratio provided excess H_2O_2 in an attempt to promote or accelerate $^{\bullet}OH$ exposure.

The $^{\bullet}OH$ exposure was quantified at different dosages for all three wastewaters at bench-scale using pCBA as a probe. The $^{\bullet}OH$ exposure was obtained using eq. 6.:

$$\int_0^t [OH]dt = \frac{\ln\left(\frac{[pCBA]}{[pCBA]_0}\right)}{-k_{OH-pCBA}} \qquad (6.2)$$

6.3.3 Pilot-Scale Ozonation

Bench-top pilot plant (BTPP) experiments were performed using the three wastewaters in order to evaluate removal of organic micropollutants. In all experiments, ambient concentrations were used; therefore, there was no need to spike. The O_3 dosages were determined according to eq. 6,1 using O_3:TOC ratios of 0.2, 0.6, 1.0. Samples for contaminant analysis were collected when no O_3 residual was left.

6.4 RESULTS

6.4.1 Bench-Scale

6.4.4.1 Ozone Demand and Decay Rate at Bench-Scale

The dissolved O_3 decay is shown in Figures 6.1, 6.2, and 6.3 for LVNV, PCFL, and RMCO, respectively. First-order O_3 decay is illustrated in the inset of each figure. The rate of dissolved O_3 residual decay was different for the three waters indicating that EfOM composition directly impacts O_3 demand reactions. PCFL had the greatest O_3 demand and fastest O_3 decay rate of the three wastewaters examined. These differences can be attributed to having greater high molecular weight compounds than the other two wastewaters according to SEC results shown in the following. PCFL wastewater also had higher SUVA, which indicates there is more aromatic content present in this water, possibly resulting in more available reaction site for O_3 oxidation.

O_3 demand and CT were calculated for each of the conditions tested (see Table 6.1). Results show that the O_3 demand was different for each of the three wastewaters. The O_3 demand satisfied at O_3/TOC ratios of 0.2, 0.6, and 0.4 for LVNV, PCFL, and RMCO, respectively. O_3 CT was measurable when these O_3/TOC ratios were exceeded in each wastewater. LVNV had the lowest O_3 demand, whereas PCFL had the highest, again related to the EfOM composition of each wastewater. At an O_3/TOC ratio of 0.2, there was no measurable dissolved O_3 residual in any of the wastewaters. Measurable CT was observed in all three wastewaters at O_3/TOC ratios of 0.8 and 1.0. These O_3/TOC ratios would be applicable for microbial disinfection.

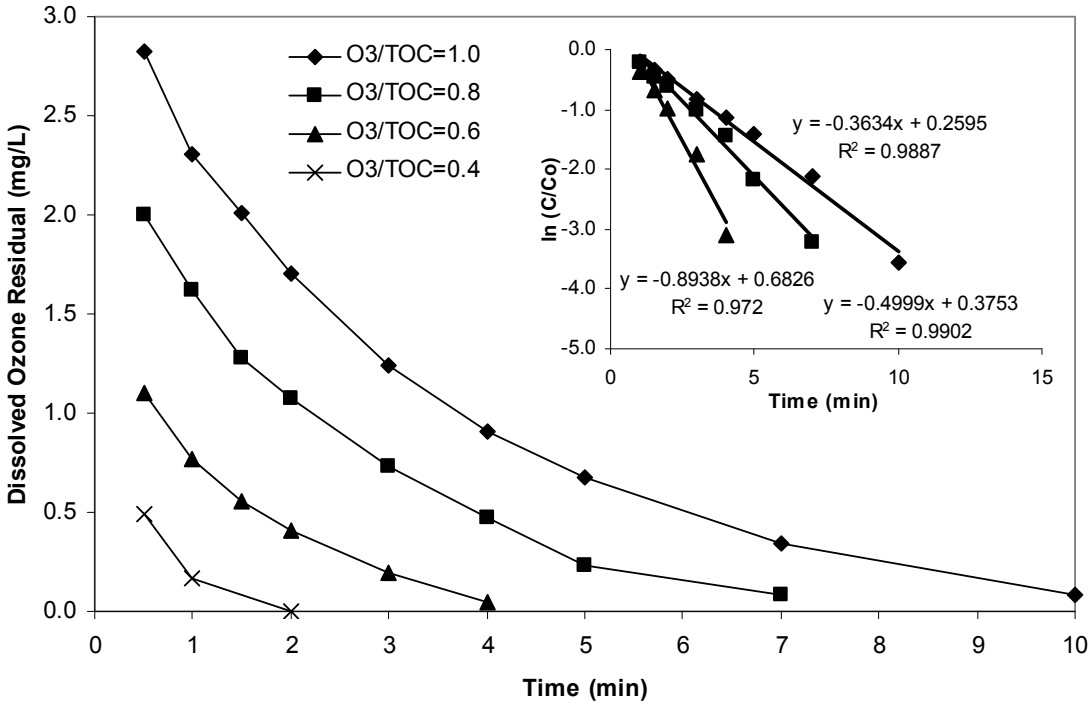

Figure 6.1. Ozone decay in LVNV effluent during bench-scale testing.

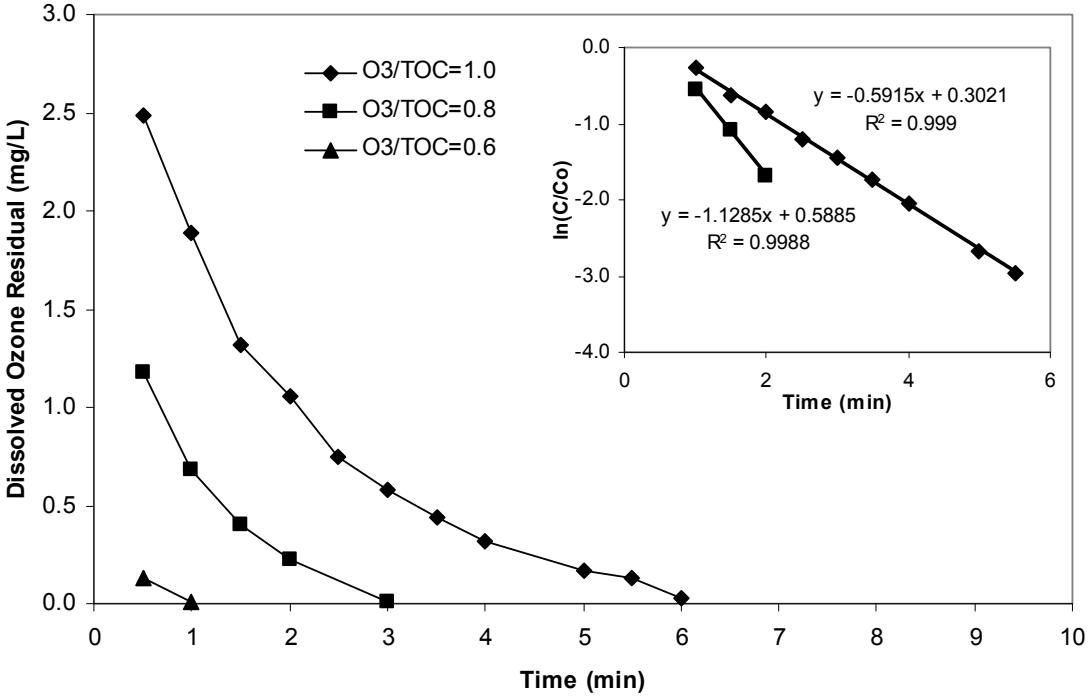

Figure 6.2. Ozone decay in PCFL effluent during bench-scale testing.

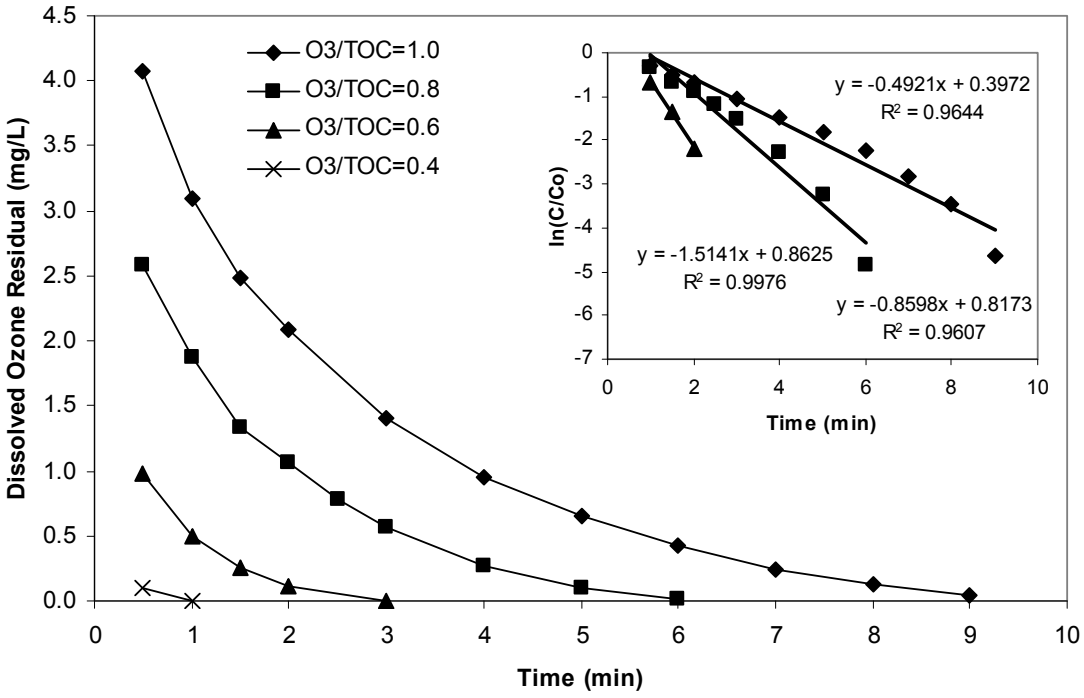

Figure 6.3. Ozone decay in RMCO effluent during bench-scale testing.

Table 6.1. Summary of Ozone Dose, O_3 Demand, and CT Determined From Bench-Scale Experiments

	LVNV			PCFL			RMCO		
O_3:TOC	O_3 Dose (mg/L)	O_3 Demand (mg/L)	CT (mg-min/L)	O_3 Dose (mg/L)	O_3 Demand (mg/L)	CT (mg-min/L)	O_3 Dose (mg/L)	O_3 Demand (mg/L)	CT (mg-min/L)
0.2	1.7	1.7	0	2.6	2.6	0	2.5	2.5	0
0.4	3.0	2.5	0.5	5.0	5.0	0	4.7	4.6	0
0.6	4.0	2.9	1.2	7.0	6.9	0	6.6	5.6	0.6
0.8	5.3	3.3	4.0	9.0	7.8	1.0	8.9	6.3	3.6
1.0	6.6	3.8	7.6	10.5	8.0	3.5	10.7	6.6	8.2

6.4.4.2 Hydroxyl Radical Exposure

The $^{\bullet}OH$ exposure was measured through the use of the probe compound pCBA. Results from bench-scale testing are shown in Figures 6.4 through 6.6 and Table 6.2 for LVNV, PCFL, and RMCO wastewater. LVNV and RMCO results showed that $^{\bullet}OH$ exposures were similar based on O_3:TOC ratio when comparing O_3/H_2O_2 to O_3 after the completion of first-order decay. H_2O_2 addition accelerated the formation of $^{\bullet}OH$ within the first 30 seconds of exposure. Therefore, H_2O_2 addition would allow a smaller contactor to be used when targeting primarily $^{\bullet}OH$ oxidation. However, there would be minimal exposure to dissolved O_3 residual that could reduce microbial disinfection. PCFL wastewater experienced 10% to 40% less $^{\bullet}OH$ exposure when using H_2O_2. In addition, PCFL wastewater had greater concentrations of alkalinity (269 mg/L) than either LVNV (128 mg/L) or RMCO (101 mg/L).

There was little pCBA degradation when using an O_3/TOC ratio of 0.2 in RMCO wastewater, and O_3/TOC ratios of 0.2 and 0.4 in PCFL wastewater. These O_3/TOC ratios resulted in O_3 dosages below the O_3 demand of each wastewater. This does not indicate that there is no $^{\bullet}OH$ exposure; rather it is rapidly consumed by EfOM and unavailable to react with pCBA. These results also indicate that there is little $^{\bullet}OH$ available for contaminant oxidation when using these ratios. In order for the O_3 demand phase to behave as an AOP, the initial demand must be slightly exceeded to result in appreciable pCBA destruction. When satisfying or exceeding the O_3 demand, around 30% to 40% of the pCBA added was destroyed during the O_3 demand phase. Trace contaminant oxidation could be expected when operating under this condition.

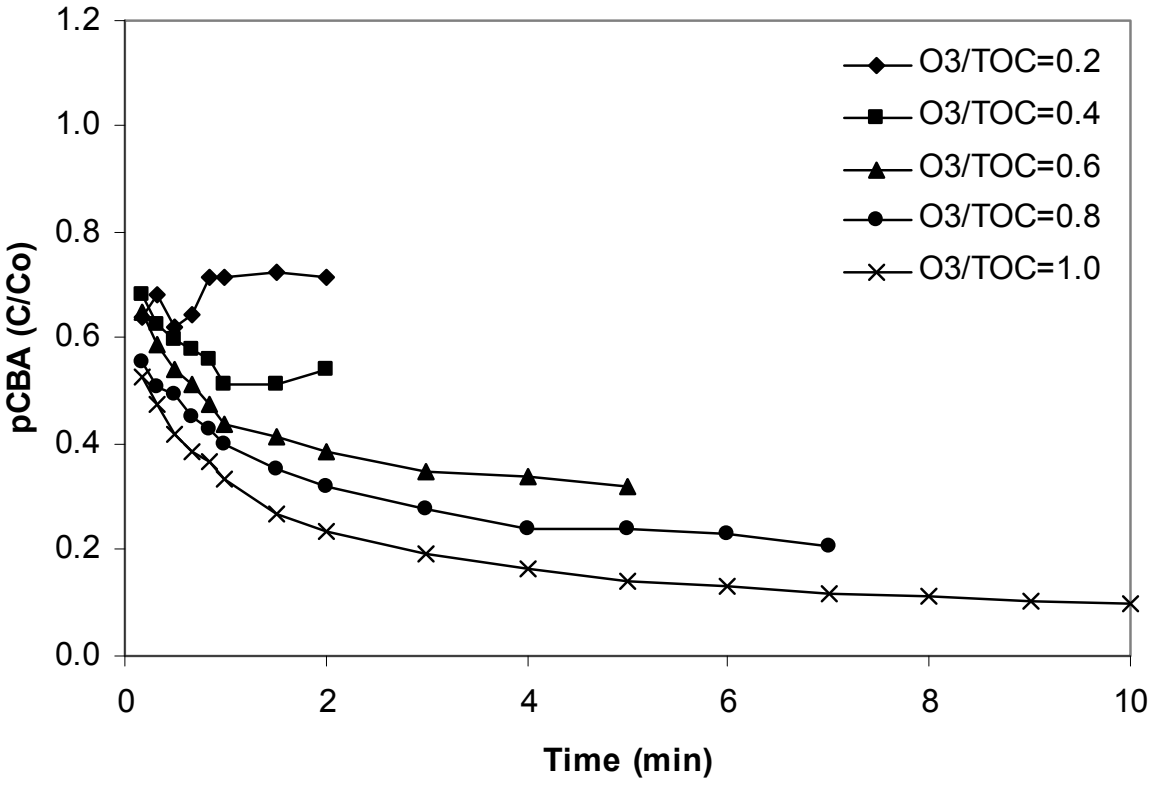

Figure 6.4. Degradation of pCBA in LVNV effluent during O_3.

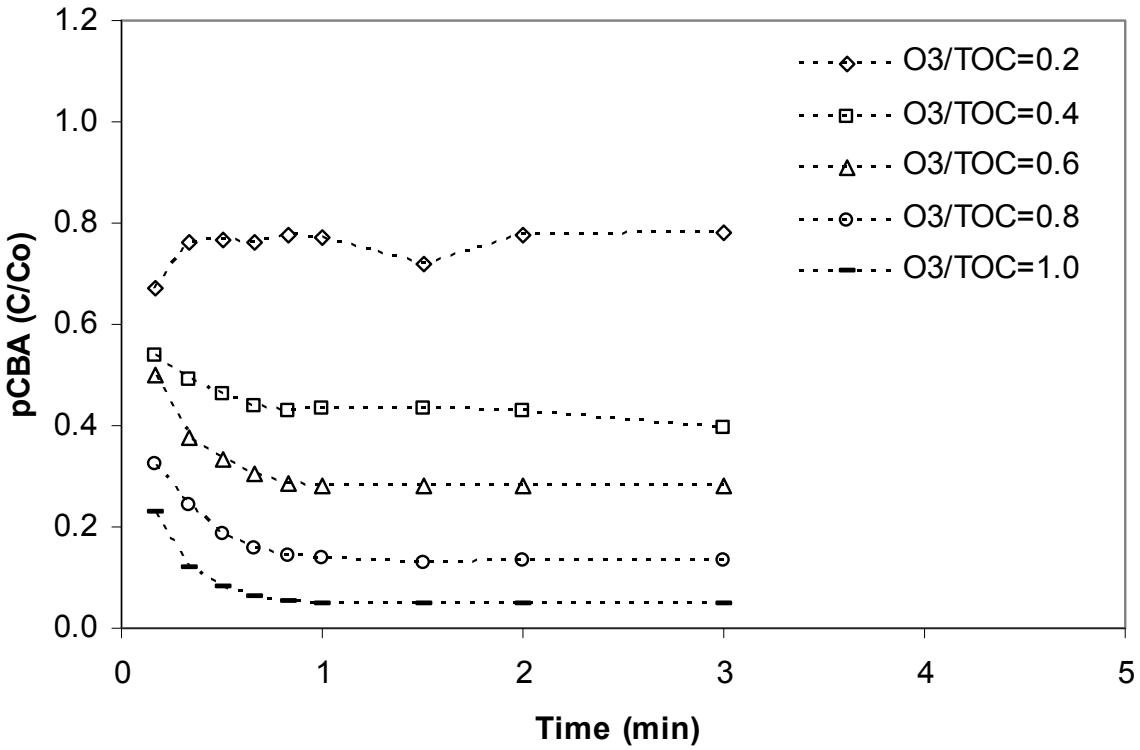

Figure 6.5. Degradation of pCBA in LVNV effluent during O_3/H_2O_2.

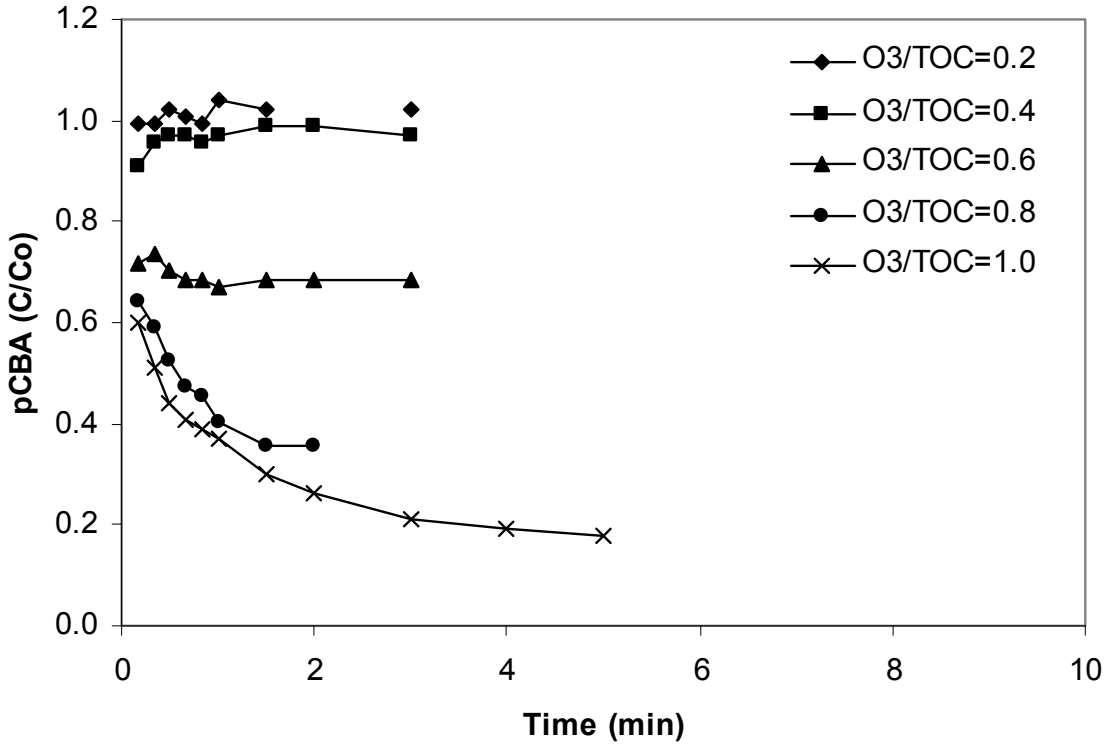

Figure 6.6. Degradation of pCBA in PCFL effluent during O_3.

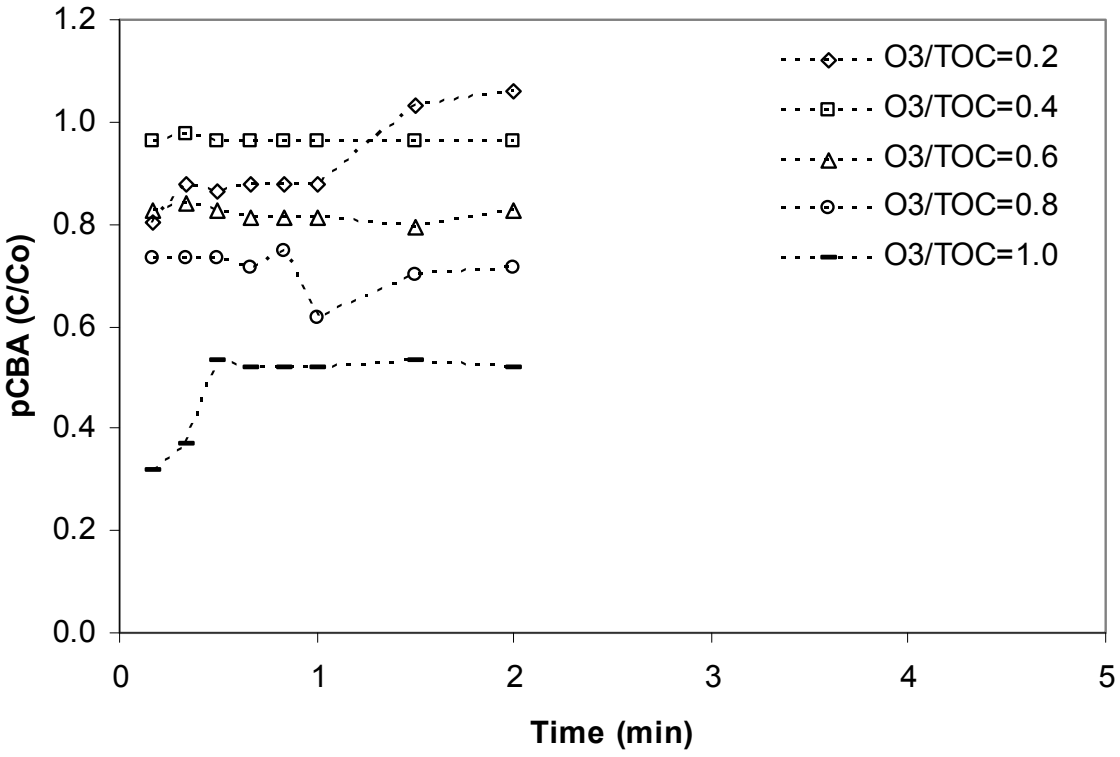

Figure 6.7. Degradation of pCBA in PCFL effluent during O_3/H_2O_2.

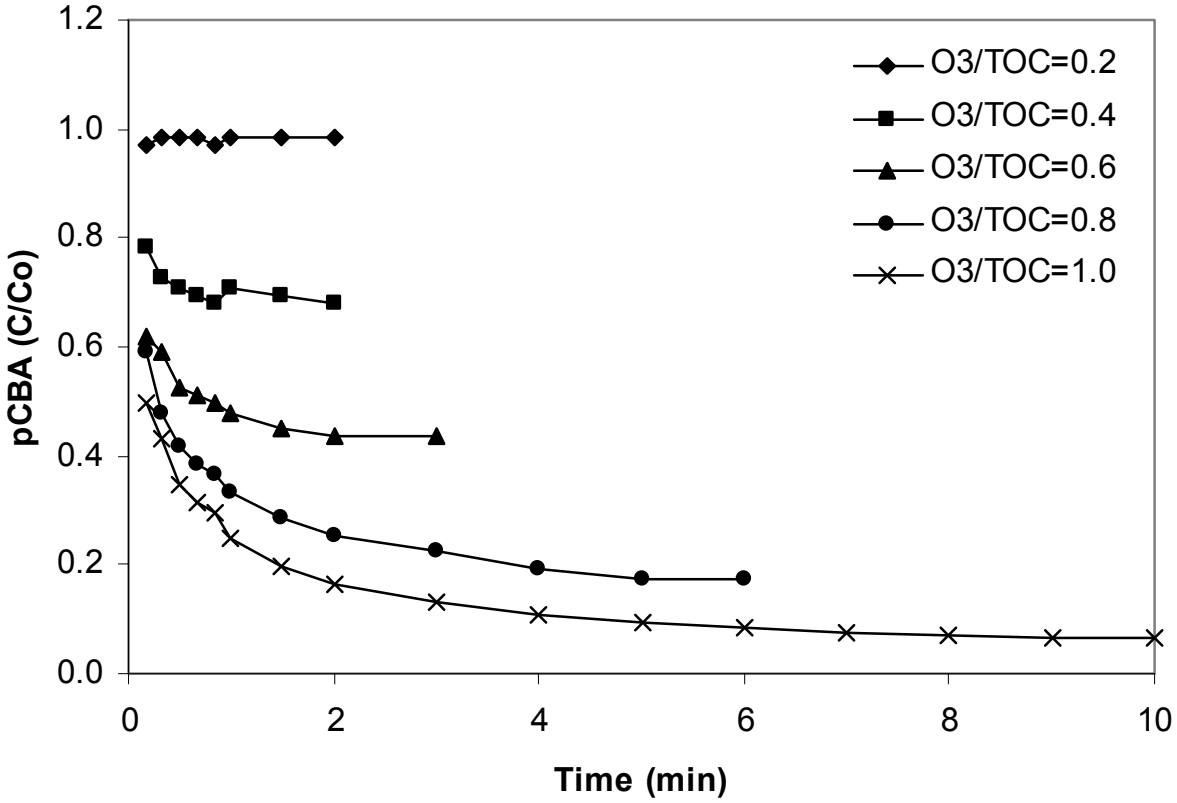

Figure 6.8. Degradation of pCBA in RMCO effluent during O_3.

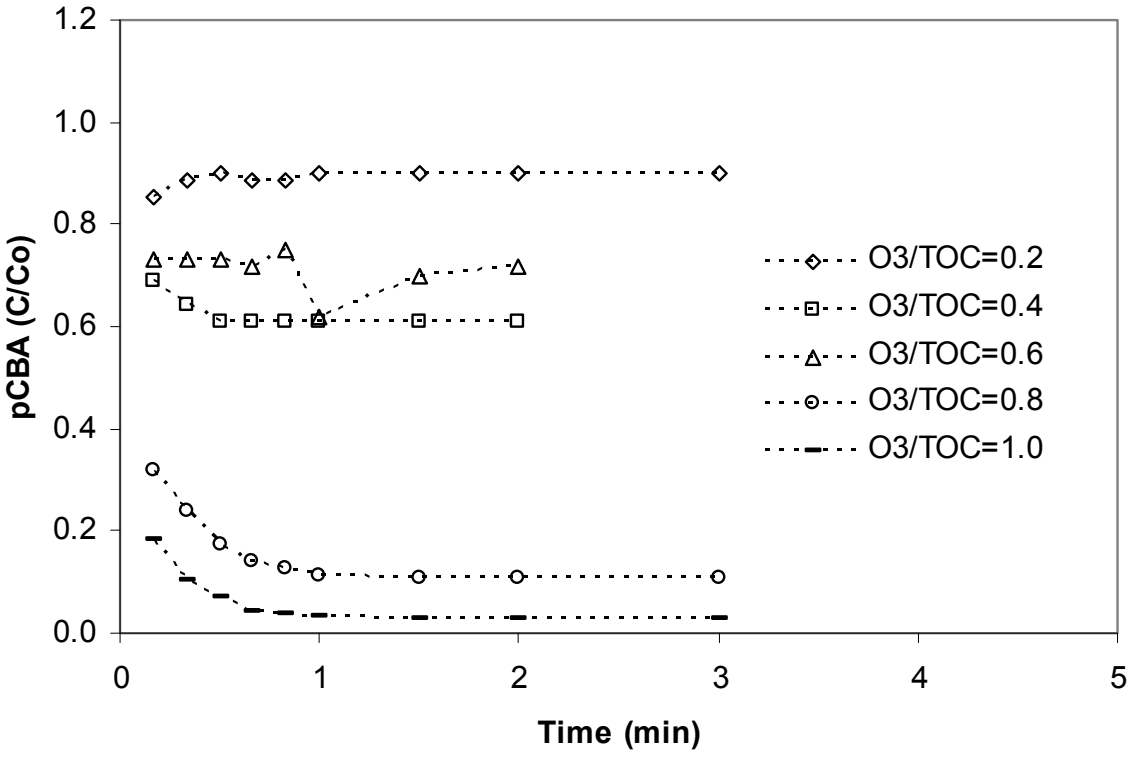

Figure 6.9. Degradation of pCBA in RMCO effluent during O_3/H_2O_2.

Table 6.2. $^{\bullet}OH$ Exposures (M s)

O_3/TOC	Ozone		
	LVNV	**PCFL**	**RMCO**
0.2	$6.57x10^{-11}$	nd	$2.01x10^{-12}$
0.4	$1.23x10^{-10}$	$2.01x10^{-12}$	$7.71x10^{-11}$
0.6	$1.94x10^{-10}$	$7.42x10^{-11}$	$1.69x10^{-10}$
0.8	$2.28x10^{-10}$	$2.10x10^{-10}$	$2.69x10^{-10}$
1.0	$2.85x10^{-10}$	$2.69x10^{-10}$	$3.67x10^{-10}$
	Ozone/Peroxide		
	LVNV	**PCFL**	**RMCO**
0.2	$5.23x10^{-11}$	0	$2.10x10^{-11}$
0.4	$1.69x10^{-10}$	$8.16x10^{-12}$	$9.89x10^{-11}$
0.6	$2.55x10^{-10}$	$3.72x10^{-11}$	$6.57x10^{-11}$
0.8	$4.08x10^{-10}$	$6.57x10^{-11}$	$4.41x10^{-10}$
1.0	$5.99x10^{-10}$	$1.30x10^{-10}$	$7.01x10^{-10}$

6.4.4.3 EfOM Changes

SEC results are shown in Figures 6.10 through 6.12 for LVNV, PCFL, and RMCO wastewaters, respectively. The region between 35 to 55 min indicates the presence of humic substances, including building blocks and other components such as low molecular weight acids (Huber, 1998; Lee et al., 2004; Rosario-Ortiz et al., 2007a; Sachse et al., 2001; Sachse et al., 2005). Significant peak intensity between 35 to 40 min indicates that within the humic substances fraction there are components with higher molecular weight. Detection at elution times between 60 to 70 min indicates the presence of low molecular weight acids and amphiphiles (Sachse et al., 2005).

Exposure to O_3 clearly had an effect on the apparent molecular weight distribution, as shown previously. The PCFL wastewater had the greatest intensity between 35 to 40 min. The SEC results coupled with the O_3 demand and decay results indicate that the presence of higher molecular compounds exerted greater O_3 demand than at either LVNV or RMCO. There were more reaction sites in the PCFL wastewater than in LVNV or RMCO wastewaters. These reactions have been shown to produce lower molecular weight fragments including aldehydes and carboxylic acids (Wert et al., 2007).

SUVA was also monitored to observe the decrease in aromatic carbon as the O_3/TOC ratio increased (Figure 6.13). Results showed that PCFL had the highest SUVA of the three waters. It also showed that minimal aromatic carbon was oxidized using O_3/TOC ratios greater than 0.6.

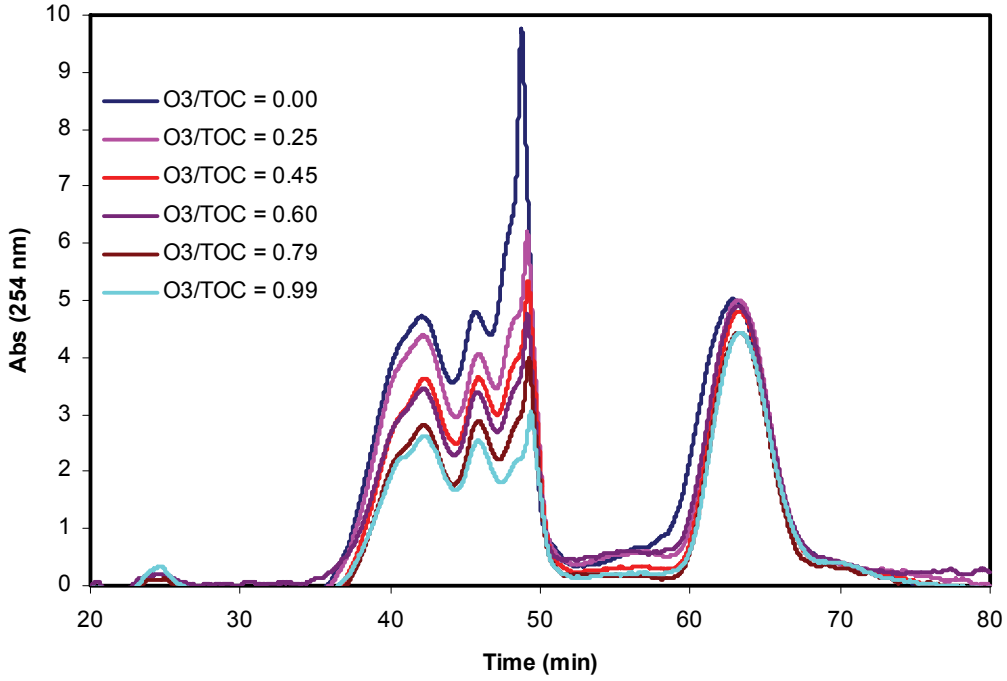

Figure 6.10. SEC results from LVNV during bench-scale experiments.

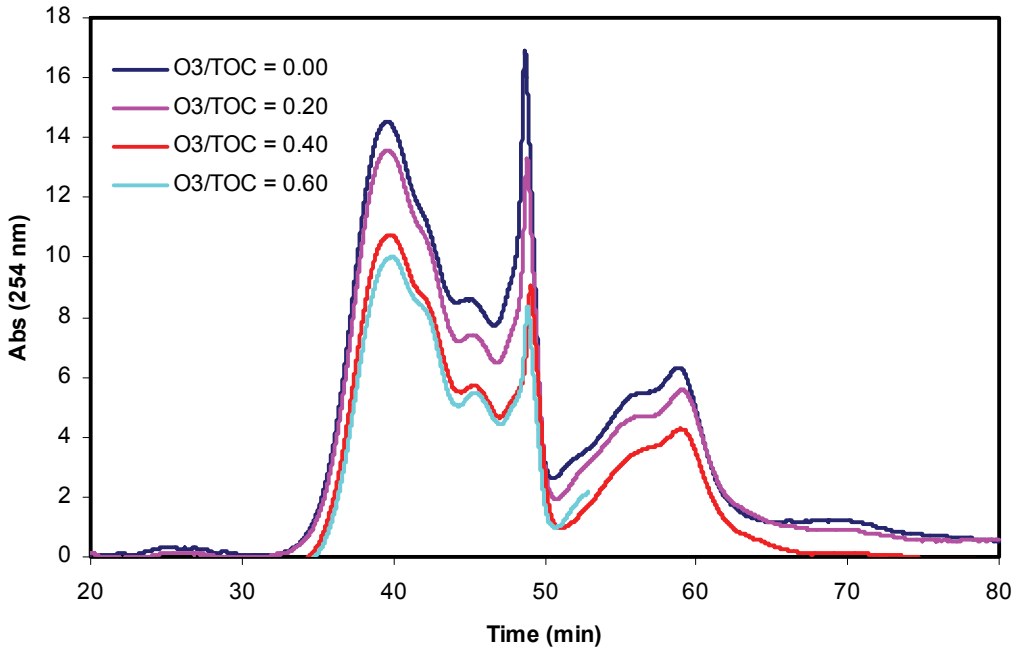

Figure 6.11. SEC results from PCFL during bench-scale experiments.

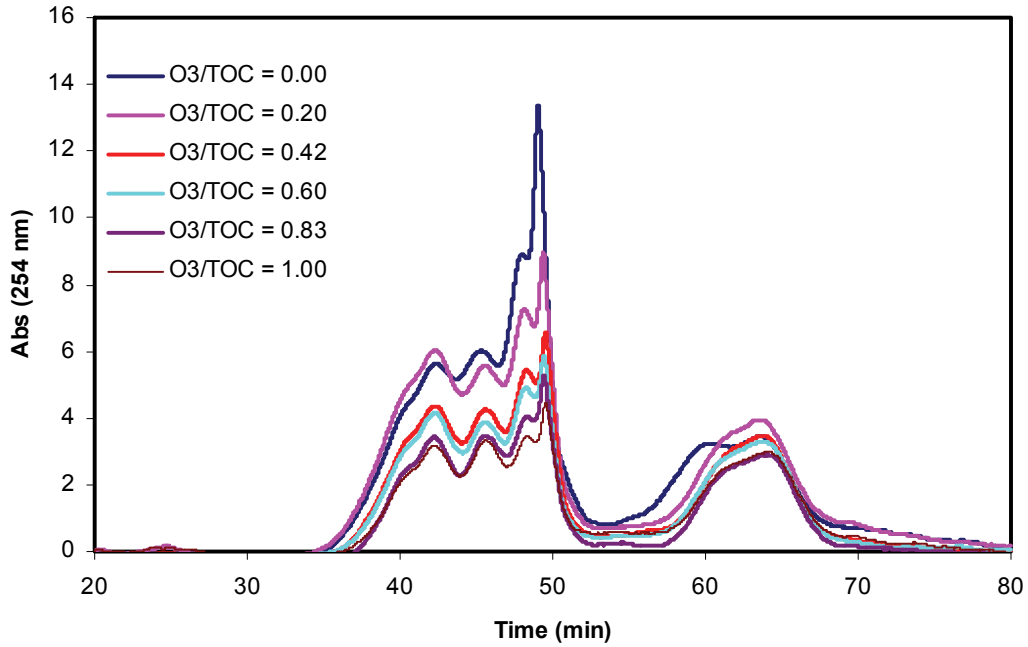

Figure 6.12. SEC results from RMCO during bench-scale experiments.

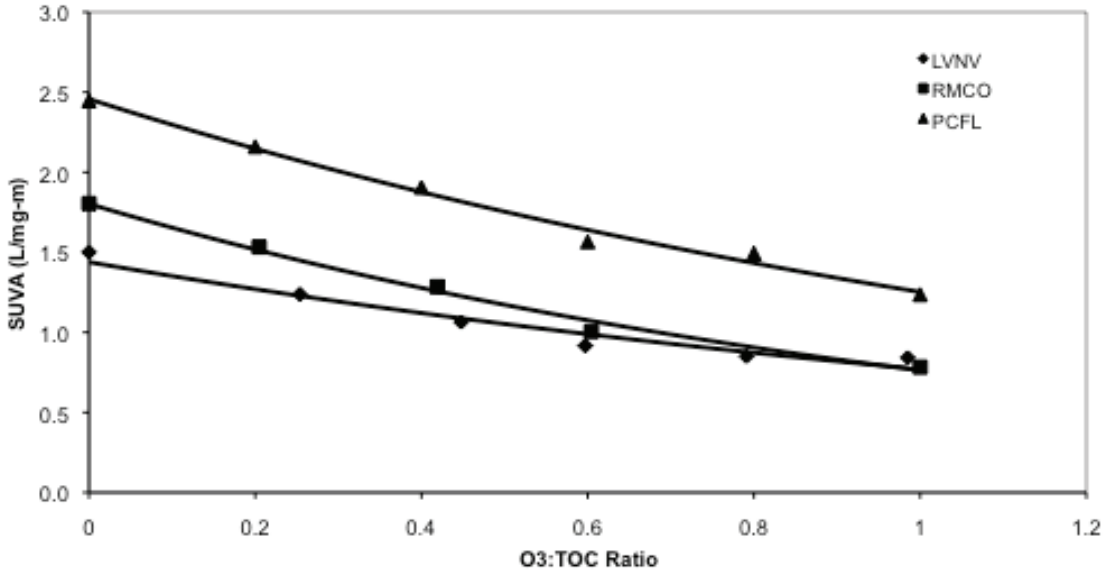

Figure 6.13. SUVA decreases with O_3/TOC ratio during bench-scale experiments.

6.4.2 Pilot-Scale Ozone

6.4.2.1 Removal of Micropollutants

The initial concentration of the micropollutants studied is shown in Figure 6.14. Removal of micropollutants that appeared to be fast-reacting with O_3 are shown in Figure 6.15. In LVNV wastewater, the O_3 demand was met using an O_3:TOC ratio of 0.2, which resulted in greater than 95% removal. The O_3 demand was not satisfied in PCFL and RMCO wastewaters explaining the 20% to 70% removal achieved. In these wastewaters, there are still O_3-EfOM reactions occurring using this O_3:TOC ratio, which consumes O_3 before it can react with these micropollutants. When the O_3:TOC ratio increased to 0.6, these compounds were greater than 95% removed in all waters.

Removal of micropollutants that appeared to be slow-reacting with O_3 and fast-reacting with $^{\bullet}OH$ are shown in Figure 6.16. Results using an O_3:TOC ratio of 0.2 show removal efficiencies varying between 0% to 60%, with most removal in the 0% to 20% range. These results demonstrate that there is little $^{\bullet}OH$ available for contaminant oxidation when using a low O_3:TOC ratio. When the ratio was increased to 0.6, the removal efficiency varied for the compounds investigated. This O_3:TOC ratio satisfied the overall O_3 demand in PCFL and exceeded the O_3 demand in LVNV and RMCO wastewaters. When the ratio was increased to 1.0, most compounds were greater than 80% removed. Meprobamate, atrazine, iopromide, TCEP, and TCPP remained between 0% to 60% removed.

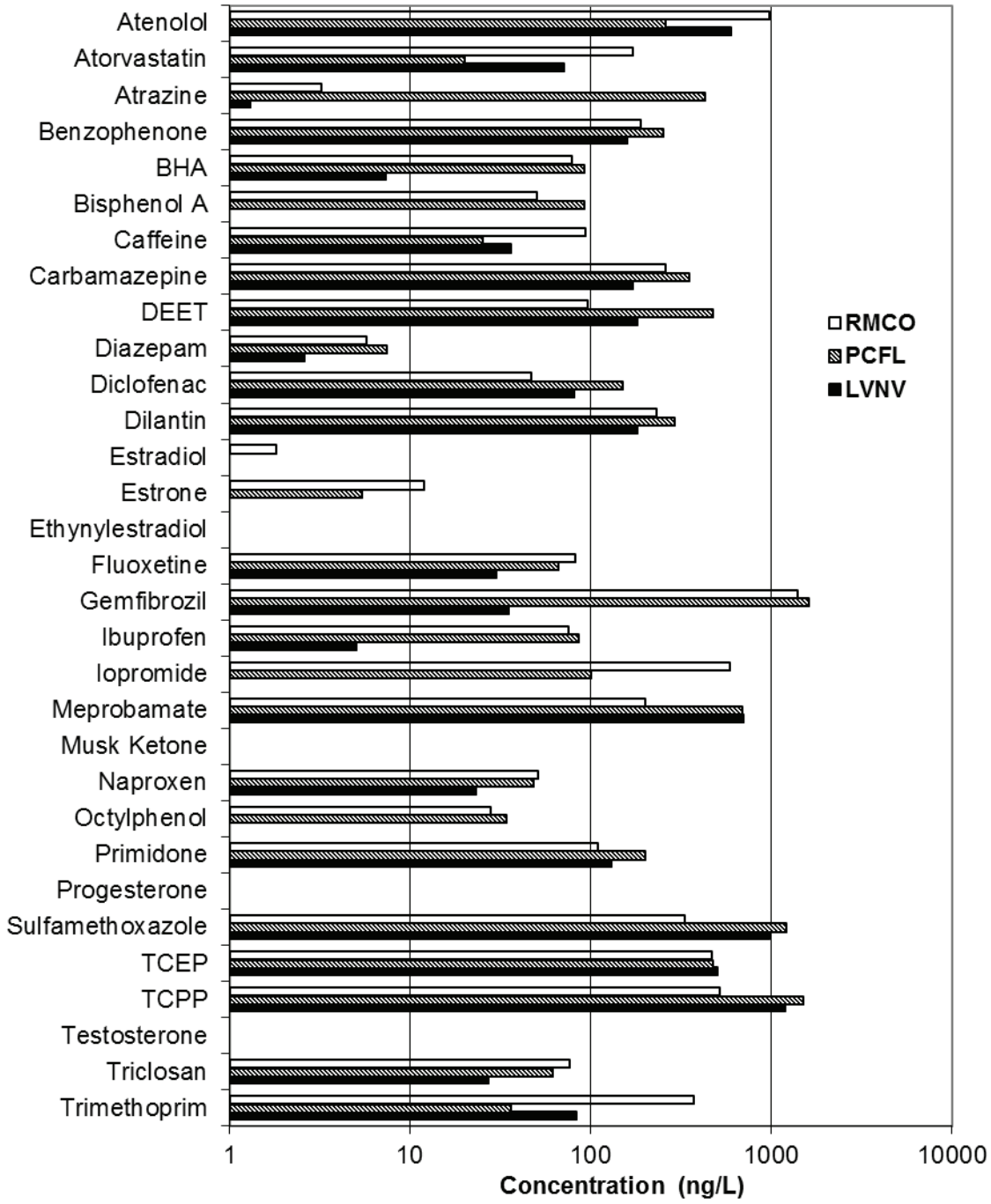

Figure 6.14. Micropollutants studied and their initial concentrations.

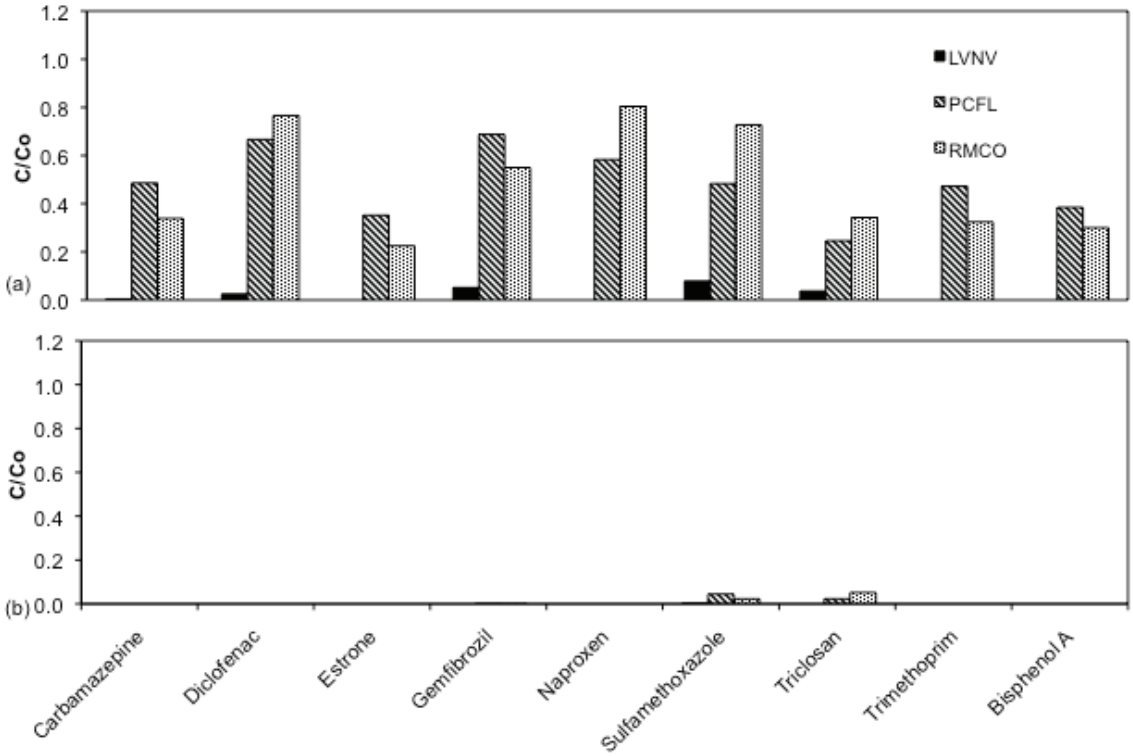

Figure 6.15. Removal of micropollutants that are fast-reacting with ozone (a) O_3:TOC=0.2 and (b) O_3:TOC=0.6.

.

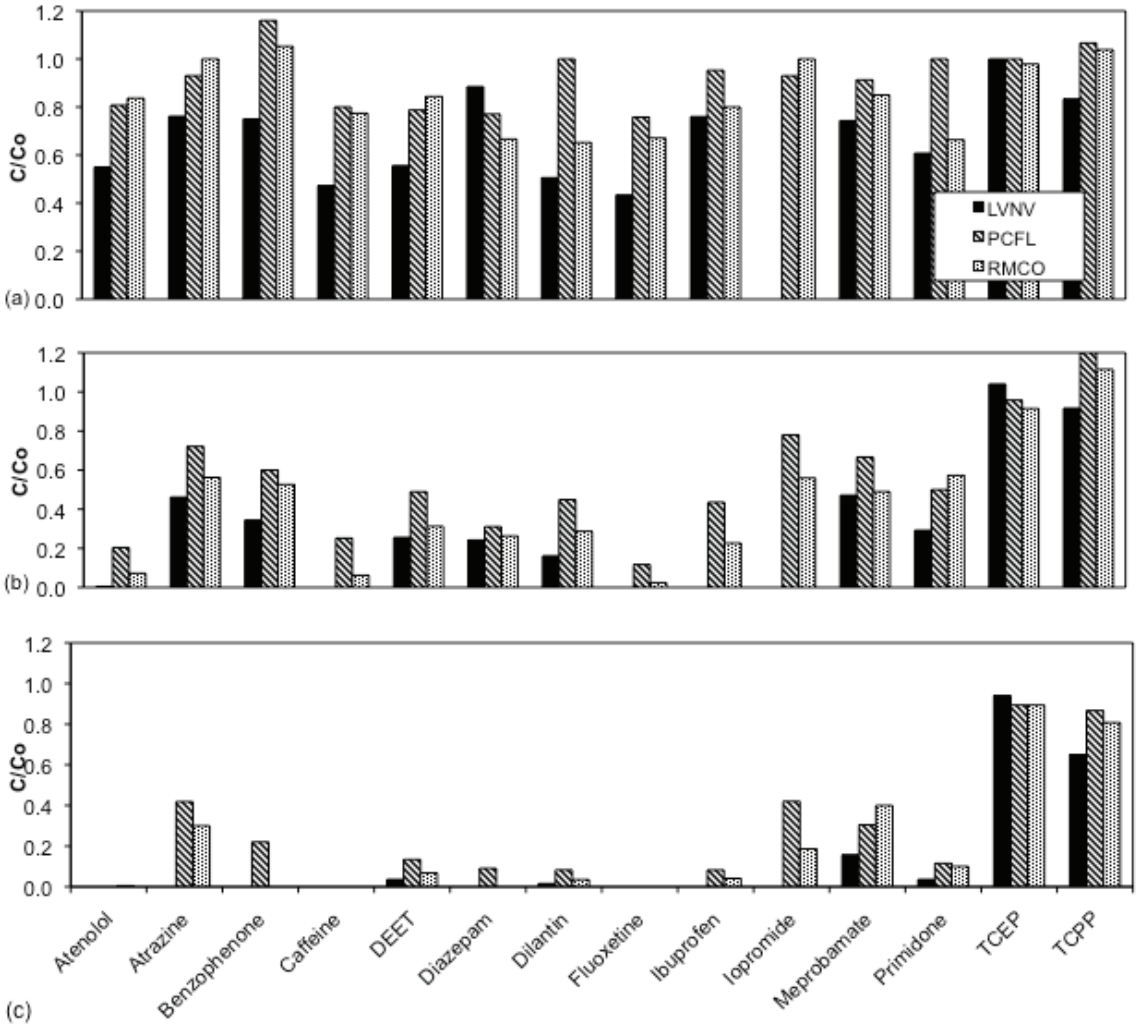

Figure 6.16. Removal of micropollutants that are slow-reacting with ozone and fast-reacting with hydroxyl radicals (a) O_3:TOC=0.2, (b) O_3:TOC=0.6, and (c) O_3:TOC=1.0.

.

6.4.2.2 Surrogate Parameters for the Application of Ozone

The removal of six specific compounds was evaluated to determine if they provided a suitable surrogate for pCBA degradation during wastewater or water reuse applications. Contaminant oxidation was compared to pCBA oxidation in all three wastewaters to determine if the correlation was linear in the three wastewaters. Caffeine reacted slightly faster than pCBA and may have been influenced somewhat by O_3 oxidation as well (Figure 6.17a). Atrazine appeared to be more slow-reacting with $^{\bullet}OH$ than pCBA (Figure 6.17c). Atrazine results were similar to meprobamate and iopromide, whereas TCPP and TCEP were extremely slow reacting with $^{\bullet}OH$. Although these compounds reacted with $^{\bullet}OH$ and correspond linearly to pCBA degradation they are not suitable surrogates for $^{\bullet}OH$ oxidation because of their occurrence at low concentrations and poor correlation to pCBA degradation. However, Dilantin, DEET, diazepam, and ibuprofen showed good correlation with pCBA destruction. Of these four compounds, DEET and dilantin were detected at concentrations greater than 100 ng/L in all three wastewaters. The correlation to pCBA coupled with occurrence at significant concentrations make these two compounds ideal surrogates to measure $^{\bullet}OH$ exposure during wastewater or water reuse applications.

The removal of UV_{254} during ozonation correlated well with the removal of various trace contaminants. Figure 6.18 illustrates the correlation of UV_{254} removal with meprobamate, dilantin, primidone, and carbamazepine. Meprobamate, dilantin, and primidone removal correlated well with UV_{254} removal between 10% to 60%. Carbamazepine removal correlated well when UV_{254} removal was between 0% to 30%. The differences can be explained by their apparent reactivity with O_3. Carbamazepine reacts rapidly with O_3, whereas meprobamate, dilantin, and primidone appear to react primarily with $^{\bullet}OH$. These results show that the removal of UV_{254} is a promising surrogate to assess contaminant oxidation by O_3.

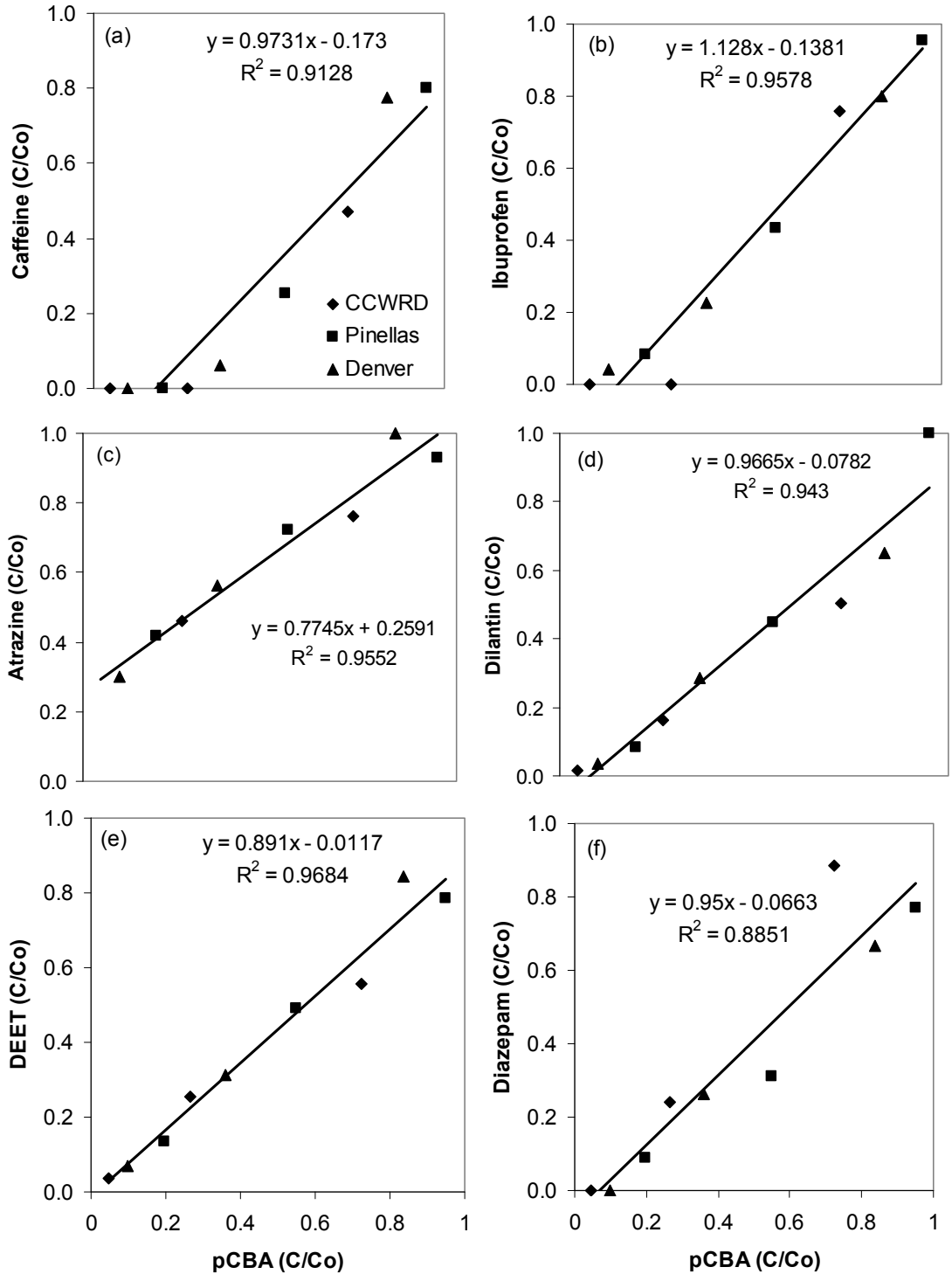

Figure 6.17. Destruction of micropollutants versus pCBA degradation for $^{\bullet}$OH-reactive compounds.

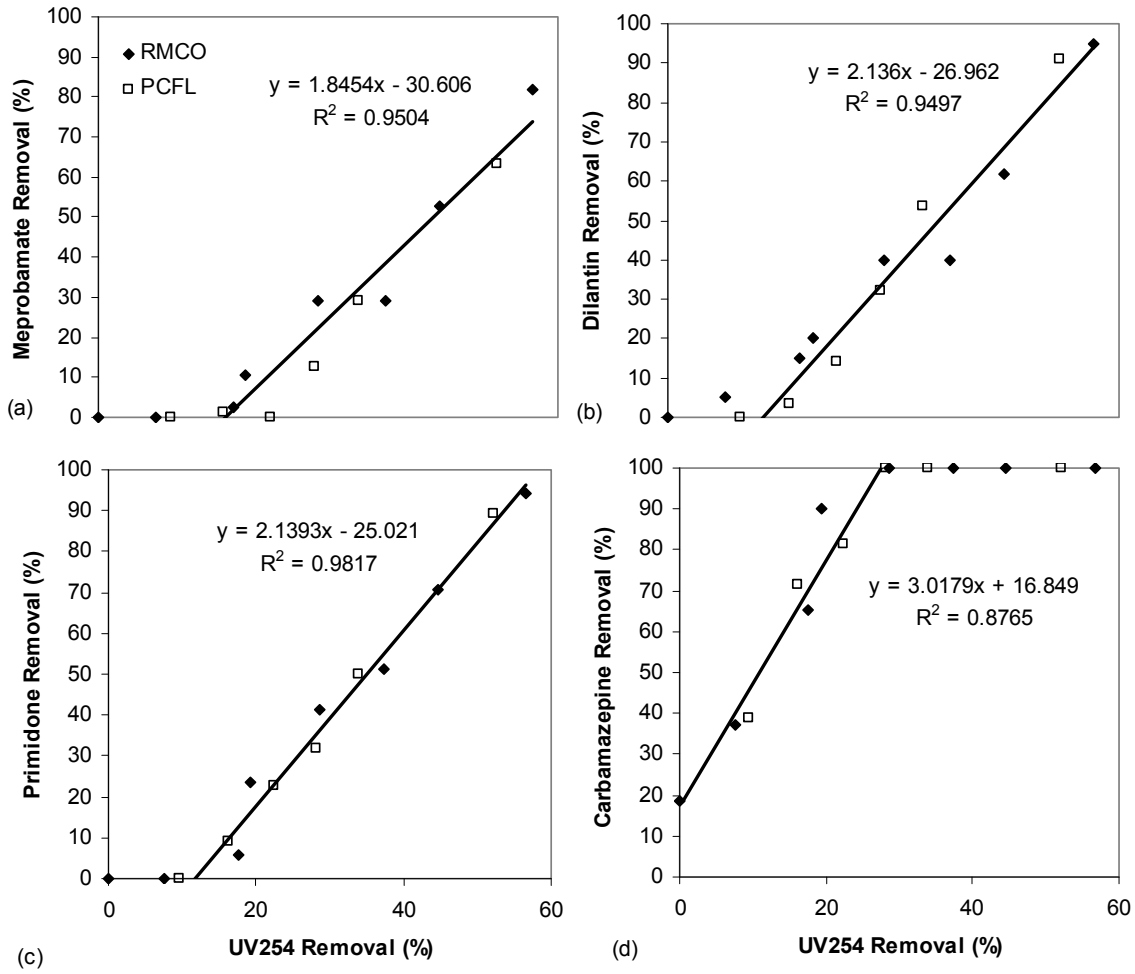

Figure 6.18. Correlations of UV_{254} removal observed during pilot-scale experiments.

6.5 Implications

The results obtained through this study examined the effect of different EfOM compositions on O_3 demand and decay rate and the corresponding $^{\bullet}OH$ exposure. Results showed that the three wastewaters evaluated performed differently based on the O_3:TOC ratio, indicating that EfOM composition has a direct impact on ozonation.

$^{\bullet}OH$ exposure, as measured by pCBA, was found to be dependent on whether or not the O_3 demand of the wastewater was met or exceeded. When operating with O_3 dosages less than the wastewater demand, there was little $^{\bullet}OH$ available for contaminant oxidation. At dosages meeting or exceeding the O_3 demand, significant $^{\bullet}OH$ exposure was observed in all three wastewaters. All three wastewaters experienced a 30% to 40% reduction in pCBA when the O_3 demand was satisfied. The addition of H_2O_2 accelerated $^{\bullet}OH$ exposure in LVNV and RMCO wastewater, but decreased exposure by 10% to 40% in the PCFL wastewater.

EfOM characterization was performed using SEC and SUVA results. SEC results showed the level of transformation of humic substances with higher molecular weight corresponded well to the amount of O_3 demand. PCFL wastewater had the greatest amount of these substances and had the greatest O_3 demand, whereas LVNV had the least amount of these substances and had the least O_3 demand. SUVA results showed that the aromatic content of all three wastewater decreased as the O_3 dose increased.

The removal of compounds that are fast-reacting with O_3 was greater than 95% when satisfying the O_3 demand of the water. When O_3 dosages were below the O_3 demand, removal of micropollutants was considerably reduced. Compounds that reacted with $^{\bullet}OH$ were poorly removed when operating below the O_3 demand of the wastewater. When slightly exceeding the O_3 demand, removal was highly variable and became the function of each individual compound's reactivity with $^{\bullet}OH$. Removal increased as the O_3 dose increased which also increased $^{\bullet}OH$ exposure. Dilantin and DEET were identified as two compounds that could be used as $^{\bullet}OH$ indicators because of the occurrence at concentrations greater than 100 ng/L and the close correlation to pCBA decomposition in all three wastewaters evaluated.

CHAPTER 7

CONCLUSIONS AND RECOMMENDATIONS

The main goal of this study was to evaluate AOP performance from the perspective of the oxidative capacity and the influence of water quality (most important EfOM) on micropollutant oxidation. One of the main advantages of the application of an AOP for water reuse is the production of radical species ($^{\bullet}OH$), which rapidly react with many micropollutants. However, the presence of EfOM will result in considerable scavenging of $^{\bullet}OH$, lowering the overall capacity to remove micropollutants and resulting in the need to reduce the concentration of EfOM via additional pretreatments. A detailed understanding of how this process occurs (in terms of EfOM properties) and how it varies at different locations (based on the fact that EfOM will vary among sites and also among different processes) would greatly enhance the capacity to model, design, and optimize an AOP.

The overall scavenging capacity of the EfOM is directly correlated to the second-order reaction rate constant between EfOM and $^{\bullet}OH$ ($k_{EfOM\text{-}OH}$). As part of this study, a detailed characterization of the $k_{EfOM\text{-}OH}$ values was conducted by measuring the absolute rate constant values from water collected at different wastewater utilities. Emphasis was placed on the quantification of $k_{EfOM\text{-}OH}$ utilizing bulk samples. This type of analysis is performed without preparative steps (i.e., isolation, desalting) and results in the evaluation of the EfOM without major modifications to the basic structure and configuration. In order to accomplish this, the team utilized the facilities of the Notre Dame Radiation Laboratory, which allows the formation of $^{\bullet}OH$ in situ permitting the quantification of $k_{EfOM\text{-}OH}$ directly. In addition, EfOM was characterized in order to evaluate EfOM properties at several WWTP sites.

The obtained kinetic results indicated that the value for the $k_{EfOM\text{-}OH}$ varied considerably among sites, from a low value of 0.27×10^9 M_C^{-1} s^{-1} to a high value of 1.21×10^9 M_C^{-1} s^{-1}. This represents a difference of a factor of almost 5, which is considerable in terms of the efficiency toward contaminant removals at different sites. These differences are attributed to variability in both the background NOM, which composes part of the EfOM, as well as in differences in the wastewater treatment and added components that compose the EfOM. Additionally, quantification of the $k_{EfOM\text{-}OH}$ for two samples collected on one site resulted in different values (0.45 and 1.21×10^9 M_C^{-1} s^{-1}), suggesting that differences in reactivity of the EfOM could be also observed as a function of process variables within a specific treatment configuration. This conclusion is also supported by the results obtained from the sampling of two treatment trains within a single wastewater facility. In this case, the measured $k_{EfOM\text{-}OH}$ rate constants were 0.27 and 1.02×10^9 M_C^{-1} s^{-1} for the two trains. One of the major differences between both trains was the operational parameters associated with the secondary biological treatment, which suggest that specific by-products associated with these processes may change the observed reactivity.

The results from the determination of the $k_{EfOM\text{-}OH}$ values indicated that there were significant variations in these waters. In order to account for these variations and to provide a mechanism to predict $k_{EfOM\text{-}OH}$ values as a function of EfOM properties, a simple correlation model was developed that considered the variability between different sites related to specific EfOM properties, including polarity, molecular weight, fluorescence index, and specific UV absorbance. The model was shown to be able to predict the variability in the rate values with an $R^2>0.99$ (n=8). Application of this model would allow utilities to estimate the overall $^{\bullet}OH$

scavenging capacity at a specific site and whether this value would change based on changes to the properties of the EfOM.

The results obtained for the quantification of the $k_{EfOM\text{-}OH}$ at different sites and the described model allows detailed analysis of the EfOM $^{\bullet}OH$ reactivity and provides detailed study of AOPs at a local level. The reported values correspond to the expected reactivity of the EfOM before an AOP has been implemented. However, during the course of an AOP, the increased oxidative capacity of the system would not only result in the oxidation of micropollutants but could also oxidize the EfOM. The effects of this oxidation on the EfOM include decreases in molecular weight, increases in the polarity of the material, and decreases in the UVA and SUVA. These properties also need to be included in any model developed to describe the $k_{EfOM\text{-}OH}$ at different sites. In order to quantitatively evaluate the effect of the EfOM oxidation on the $k_{EfOM\text{-}OH}$, one additional sample was collected at one of the sites. This sample was oxidized with several doses of O_3. The oxidative mechanisms included both direct reactions with O_3 plus oxidation via $^{\bullet}OH$ radical. After the samples were oxidized, $k_{EfOM\text{-}OH}$ was quantified to evaluate whether changes in the properties of EfOM as a result of oxidation had an effect on the values. Results indicated that oxidation had no effect on the measured $k_{EfOM\text{-}OH}$. Therefore, the measured values for $k_{EfOM\text{-}OH}$ are expected to remain constant during oxidation and that modeling of these processes should only include an initial value for $k_{EfOM\text{-}OH}$.

Based on the results obtained on the differences in scavenging capacities, the next step was to evaluate the effect of these changes in EfOM properties and how they affect O_3 and UV AOP applications with regard to the removal of micropollutants in wastewater. Three tertiary-treated wastewaters were selected based on the reactivity of the EfOM as measured by the second-order reaction rate constants, the concentration of other $^{\bullet}OH$ scavengers (alkalinity), and the ambient concentration of micropollutants (i.e., pharmaceuticals, EDCs, X-ray contrast media, and flame-retardants).

The efficacy of UV/H_2O_2 for contaminant removal for the three wastewaters was evaluated at bench-scale using a low-pressure UV collimated-beam system. For these experiments, a set of six pharmaceuticals was evaluated. The removals varied between 0% and greater than 99%, and were dependent on the EfOM chemistry and $^{\bullet}OH$ scavenging. The three sites evaluated had a range of $k_{EfOM\text{-}OH}$ between 0.68 and 2.72 x 10^{9} M_C^{-1} s^{-1}, as predicted using the developed model.

The application of O_3 was evaluated both at bench-scale and pilot-scale. Results showed that different EfOM composition had a direct impact on O_3 demand, O_3 decay rate, and corresponding $^{\bullet}OH$ exposure based on the O_3:TOC ratio. EfOM characterization was again performed using SEC and SUVA results. SEC results showed the level of transformation of humic substances with higher molecular weight corresponded well to the amount of O_3 demand. PCFL wastewater had the greatest amount of these substances and had the greatest O_3 demand, whereas LVNV had the least amount of these substances and had the least O_3 demand. SUVA results showed that the aromatic content of all three wastewater decreased as the O_3 dose increased.

When operating with O_3 dosages less than the O_3 demand of the wastewater, minimal $^{\bullet}OH$ radicals were formed for contaminant oxidation as determined by pCBA measurements. When operating at O_3 dosages meeting or exceeding the O_3 demand, significant $^{\bullet}OH$ exposure was observed in all three wastewaters. All three wastewaters experienced a 30% to 40% reduction in pCBA when the O_3 demand was satisfied. The addition of H_2O_2 accelerated $^{\bullet}OH$

exposure in LVNV and RMCO wastewater, but decreased exposure by 10% to 40% in the PCFL wastewater. These results demonstrate that fast-reacting sites within the EfOM can rapidly scavenge $^{\bullet}OH$.

Removal of micropollutants that are fast-reacting with O_3 were greater than 95% removed when satisfying the O_3 demand of the water. Compounds that reacted primarily with $^{\bullet}OH$ were less than 30% removed when operating below the O_3 demand of the wastewater. When exceeding the O_3 demand, removal became a function of each individual compound's reactivity with $^{\bullet}OH$ and overall scavenging capacity. Removal increased as the O_3 dose and corresponding $^{\bullet}OH$ exposure increased in the three wastewaters.

It is recommended that EfOM reactivity be evaluated at sites considering the implementation of AOP for micropollutant mitigation. By evaluating EfOM reactivity, the sizing/capacity of AOP systems could be better estimated in advance. When water quality is found to have large $^{\bullet}OH$ scavenging capacity, utilities should strongly consider the use of pretreatment (i.e., pre-ozonation, membranes, activated carbon) to reduce $^{\bullet}OH$ scavenging capacity. It is important that IPR systems utilize designs that maximize water quality, while minimizing energy/carbon footprint. Therefore, as shown in this study, EfOM characterization and $^{\bullet}OH$ radical scavenging capacity is critical in determining optimal barriers against emerging micropollutants.

APPENDIX A

EVALUATION OF PHOTOCATALYSIS FOR THE REMOVAL OF PHARMACEUTICALS AND ENDOCRINE DISRUPTING COMPOUNDS FROM WATER

A.1 INTRODUCTION

In addition to the evaluation of ozone, ozone/H_2O_2, and UV/H_2O_2, the efficiency of TiO_2 photocatalysis (UV/TiO_2) for the removal of 32 pharmaceuticals and EDCs was evaluated. The experiments were performed in Colorado River Water (CRW).

A.2 METHODS

A.2.1 Water Samples

For these studies, water from the Colorado River was used as the source water (Table A.1 presents the water quality parameters). The water was collected after pre-chlorination with a 0.8 mg/L dose of free chlorine (to control quagga mussel growth in the intake structures) and contained a residual less than 0.2 mg/L. The feed water was recirculated for 24 hours to remove some of the remaining chlorine residual. Afterward, the water was spiked with environmentally relevant (ng/L) concentrations of 32 pharmaceuticals and EDCs. For all experiments, the unit was operated at 24 liters per minute and samples were collected after the prefilter and following treatment with 0, 1, 2, 4, 6, 8, 16, and 32 UV lamps (0-4.24 kWh/m^3 treatment). The TiO_2 concentration in the UV reactor was approximately 50 mg/L.

Table A.1. General Water Quality Parameters of Colorado River Water

Parameter	Concentration/value
TOC (mg/L)	2.6
Alkalinity (mg/L)	137
pH	8.0
Bromide (µg/L)	100
UV254 (1/cm)	0.036

A.2.2 Photocatalytic Reactor Membrane Pilot (UV/TiO_2) Testing

Briefly, water was passed through a prefilter consisting of both a bag and cartridge filter unit having a nominal pore size of 10µm as it entered the unit. It was then mixed with a 2 liter per minute nanoparticle TiO_2-water slurry and passed through the reactor within 3 mm of 32 UV lamps, which could be individually turned on or off to alter the amount of treatment. The total amount of time that the slurry was exposed to the UV lamps was 1 to 30 seconds, depending on the number of lamps in operation. The spectral output of these lamps included bands at 254 and 185 nm. The reactor had a thin film reactor geometry, and its mixing was very

turbulent because of the plug–flow design and 3-mm sleeve. As such, comparisons with other commercially available UV reactors cannot be made. The unit's flow-through design was enabled by a patented TiO_2-recovery system. After exposure to the UV lamps, a cross-flow ceramic membrane removed the TiO_2 from the flow stream, and every 60 seconds the membrane was back-pulsed to prevent catalyst buildup. The rejected TiO_2 was returned to the head of the unit as the slurry and was mixed with influent. Thus, the unit recycled and reused all of the TiO_2, allowing for long-term operation.

A.2.3 Analytical Methods

Analytical methods (both solid phase extraction and LC-MS/MS analysis) used to measure pharmaceuticals and non-steroidal endocrine disruptors were slightly modified from published methods (Vanderford and Snyder, 2006b). A similar extraction was used for steroid hormones and PFOS/PFOA, but different LC-MS/MS methods were used for each.

A separate analytical method was employed to monitor concentrations of the nine emerging micropollutants through the photolytic and photolytic plus H_2O_2 mode experiments. This method employs an online solid phase extraction (Symbiosis, Spark Holland, Emmen, The Netherlands), followed by LC-MS/MS analysis. Although less time-consuming, this method is not as sensitive as offline extraction methods. Thus, it was necessary to spike at slightly higher concentrations. Spiked concentrations and method detection limits are presented in Table A.3. Additional details of this method are provided in supporting information.

A.3 RESULTS

The concentrations of most compounds decreased as a function of the amount of energy (Table A.1). Eleven of the 32 compounds were easily removed, with concentrations below or approaching detection limits with 0.53 kWh/m^3 (4 lamps) of treatment: estrone, estradiol, Ethynylestradiol, bisphenol A, octylphenol, butylated hydroxyanisole (BHA), atorvastatin, triclosan, diclofenac, sulfamethoxazole, and naproxen. Conversely, PFOS, tris(2-chloroethyl) phosphate (TCEP), and tris(1-chloro-2-propyl) phosphate (TCPP) were largely resistant to the photocatalytic reactor membrane experiment, exhibiting concentrations following the maximum treatment (4.24 kWh/m^3 or 32 lamps) that were still greater than 50% of their starting concentration. Their refractory nature through treatment is consistent with their chemical design: all three are used as flame-retardants or in applications requiring resistance to chemical reaction. The remaining 17 compounds were removed, although it took higher amounts of treatment (0.80-4.24 kWh/m^3 or 6-32 lamps) to achieve a greater than 70% reduction in compound concentration. In addition, no formation of PFOA was observed (data not shown)

Table A.2. Raw Data (units of ng/L) for the Removal of Micro-Pollutants Using UV/TiO_2 Photocatalysis

Compound (ng/L)	Tank	After Pre-filter	0 lamp	1 lamp	2 lamps	2 lamps - Duplicate	4 lamps	6 lamps	8 lamps	16 lamps	32 lamps	After Prefilter - 2
E_{lamps} (kWhr/m^3)	na	na	0	0.13	0.27	0.27	0.53	0.80	1.06	2.12	4.24	na
Atenolol	93	66	94	73	66	63	48	37	26	6.9	<1.0	100
Atorvastatin	130	110	100	0.65	0.83	<0.50	<0.50	<0.50	<0.50	<0.50	<0.50	120
Atrazine	140	140	140	130	120	120	99	96	82	46	18	140
Benzophenone	330	330	320	300	260	260	210	180	150	75	<50	320
BHA	190	180	180	1.1	<1.0	<1.0	<1.0	<1.0	<1.0	<1.0	<1.0	200
Bisphenol A	230	330	210	27	5.9	<5.0	<5.0	<5.0	<5.0	<5.0	<5.0	200
Caffeine	460	500	440	390	350	350	270	230	190	100	25	470
Carbamazepine	210	210	200	160	140	150	100	76	57	18	2.2	220
DEET	1400	1400	1300	1200	1100	1200	970	830	740	380	140	1500
Diazepam	240	240	230	200	190	190	150	130	110	60	20	260
Diclofenac	230	240	320	27	8	10	1.3	<0.50	<0.50	<0.50	<0.50	310
Dilantin	96	96	91	84	73	69	54	42	27	9.5	1.3	100
Estradiol	21	17	20	2.3	0.98	0.85	<0.50	<0.50	<0.50	<0.50	<0.50	18
Estrone	27	24	27	3	1.1	0.95	<0.20	<0.20	<0.20	<0.20	<0.20	27
Ethynylestradiol	160	130	160	20	7	6.2	1.1	<1.0	<1.0	<1.0	<1.0	150
Fluoxetine	33	43	65	50	44	36	27	20	11	3.4	<0.50	65
Gemfibrozil	160	160	170	140	120	120	95	78	59	28	6.9	180
Ibuprofen	170	180	170	130	120	120	98	83	64	27	7.2	160
Iopromide	480	580	480	410	330	360	250	170	140	34	<10	480
Meprobamate	330	340	330	310	300	290	250	240	230	160	90	350
Musk Ketone	<25	<25	<25	<25	<25	<25	<25	<25	<25	<25	<25	<25
Naproxen	190	210	200	66	39	37	11	2.5	0.93	<0.50	<0.50	210
Octylphenol	83	38	66	<25	<25	<25	<25	<25	<25	<25	<25	72
PFOS	400	260	360	410	310	400	290	270	310	290	280	390

Compound (ng/L)	Tank	After Pre-filter	0 lamp	1 lamp	2 lamps	2 lamps - Duplicate	4 lamps	6 lamps	8 lamps	16 lamps	32 lamps	After Prefilter - 2
Primidone	480	520	520	410	380	420	340	260	250	130	46	490
Progesterone	61	54	62	45	50	49	37	27	20	4.9	<0.50	57
Sulfamethoxazole	150	260	260	68	55	54	33	9.6	19	3.3	0.59	280
TCEP	1200	1300	1200	1300	1300	1200	1200	1200	1200	1100	1030	1300
TCPP	1000	1200	1300	1300	1200	1200	1200	1000	1100	1000	760	1400
Testosterone	290	270	280	220	170	210	140	95	63	19	1.4	290
Triclosan	33	2.6	28	1.1	<1.0	<1.0	<1.0	<1.0	<1.0	<1.0	<1.0	29
Trimethoprim	340	350	340	200	140	150	97	61	40	8.6	0.87	370

APPENDIX B

PROJECT OUTREACH

PRESENTATIONS

1. Rosario-Ortiz, F. L.; Wert, E. C.; Snyder, S. A. *Application of advanced oxidation processes for the removal of pharmaceuticals.* WateReuse Research Conference, Huntington Beach, CA, May 18–19, 2009.
2. Wert, E. C.; Rosario-Ortiz, F. L.; Snyder, S. A. *Application of ozone for contaminant oxidation in wastewater.* IOA & IUVA North American Conference, Boston, MA, May 4–5, 2009.
3. Rosario-Ortiz, F. L.; Wert, E. C.; Snyder, S. A. *Evaluation of the removal efficiency of pharmaceuticals during UV advanced treatment as a function of the water quality*. AWWA Research Symposium on Emerging Organic Contaminants, Austin, TX, February 12–13, 2009.
4. Trenholm, R. A.; Rosario-Ortiz, F. L.; Snyder, S. A. *Analysis of the formation of formaldehyde during advanced oxidation treatment using on-fiber derivatization SPME GC-MS.* AWWA WQTC, Cincinnati, OH, November 16–20, 2008.
5. Rosario-Ortiz, F. L.; Mezyk, S.P.; Doud, D.; Snyder, S. A. *Quantification of the hydroxyl radical scavenging capacity during advanced oxidation treatment.* AWWA WQTC, Cincinnati, OH, November 16–20, 2008.
6. Rosario-Ortiz, F. L., Snyder, S. A.; Mezyk, S. P. *Use of fluorescence to understand the reactivity of effluent organic matter with $^{\bullet}OH$.* AGU Chapman Conference on Organic Matter Fluorescence. Birmingham, UK, October 20–23 2008.
7. Rosario-Ortiz, F. L.; Mezyk, S. P.; Doud, D.; Snyder, S. A. *Quantitative correlation of absolute hydroxyl radical rate constants with non-isolated effluent organic matter bulk properties in water.* IWA NOM Conference, Bath, UK, September 2–4, 2008.
8. Snyder, S. A.; Vanderford, B. J.; Rosario-Ortiz, F. L. *Evaluation of $^{\bullet}OH$ quantification methods for advanced oxidation processes.* IOA, Orlando, FL, August 24–26, 2008.
9. Rosario-Ortiz, F. L.; Mezyk, S.P.; Doud, D.; Snyder, S. A. *Quantification of the hydroxyl radical scavenging capacity during advanced oxidation treatment*. IOA, Orlando, FL, August 24–26, 2008.
10. Mezyk, S. P.; Doud, D. F. R.; Singh, M. K.; Rosario-Ortiz, F. L; Snyder, S. A. *Absolute rate constant measurement for $^{\bullet}OH$ reaction with effluent organic matter*. 236th ACS Meeting, Philadelphia, PA, August 17–21, 2008.
11. Rosario-Ortiz, F. L.; Mezyk, S.; Vanderford, B.; Snyder, S. *Evaluation of $^{\bullet}OH$ quantification methods for advanced oxidation processes.* 22nd WateReuse Symposium, Tampa, FL, September 9–12, 2007.
12. Rosario-Ortiz, F. L.; Suffet, I. H.; Snyder, S. *Effect of ozone on the chemical and physical characteristics of natural organic matter.* IOA-IUVA World Congress, Los Angeles, CA, August 27-29, 2007.

CONFERENCE PROCEEDINGS

1. Rosario-Ortiz, F. L.; Wert, E. C.; Snyder, S. A. *Application of advanced oxidation processes for the removal of pharmaceuticals.* WateReuse Research Conference, Huntington Beach, CA, May 18–19, 2009.
2. Wert, E. C.; Rosario-Ortiz, F. L.; Snyder, S. A. *Application of ozone for contaminant oxidation in wastewater.* IOA & IUVA North American Conference, Boston, MA, May 4–5, 2009.
3. Rosario-Ortiz, F. L.; Mezyk, S. P.; Doud, D. F. R.; Snyder, S. *Quantification of the hydroxyl radical scavenging capacity during advanced oxidation treatment*. AWWA WQTC, Cincinnati, OH, November 16–20, 2008.
4. Rosario-Ortiz, F. L.; Mezyk, S. P.; Doud, D. F. R.; Snyder, S. A. *Quantification of the hydroxyl radical scavenging capacity during advanced oxidation treatment*. IWA Conference; NOM: From Source to Tap. Bath, UK, September 2–4, 2008.
5. Snyder, S. A.; Vanderford, B. J.; Rosario-Ortiz, F. L. *Evaluation of $^{\bullet}OH$ quantification methods for advanced oxidation processes.* International Ozone Association Pan American Group Meeting, Orlando, FL, August 24–27, 2008.
6. Rosario-Ortiz, F. L.; Mezyk, S. P.; Doud, D. F. R.; Snyder, S. A. *Quantification of the hydroxyl radical scavenging capacity during advanced oxidation treatment*. International Ozone Association Pan American Group Meeting, Orlando, FL, August 24–27, 2008.
7. Rosario-Ortiz, F. L.; Mezyk, S. P.; Vanderford, B. J.; Snyder, S. *Evaluation of $^{\bullet}OH$ quantification methods for advanced oxidation processes.* WateReuse Annual Meeting, Tampa, FL, September 10–12, 2007.
8. Rosario-Ortiz, F. L.; Suffet, I. H.; Snyder, S. *Effect of ozone on the chemical and physical characteristics of natural organic matter.* Proceedings of the IOA-IUVA International Conference. Los Angeles, CA, August 27–29, 2007.

PEER-REVIEWED PUBLICATIONS

1. Rosario-Ortiz, F. L.; Wert, E. C.; Snyder, S. A. Evaluation of the efficiency of UV/H_2O_2 treatment for the oxidation of pharmaceuticals in wastewater. *Water Research* **2010**, *44* (5), 1440–1448.
2. Wert, E. C.; Rosario-Ortiz, F. L.; Snyder, S. A. Using UV absorbance and color as surrogates to evaluate trace contaminant oxidation during the ozonation of wastewater, *Environmental Science and Technology* **2009**, *43*, 4858–4863.
3. Benotti, M. J.; Stanford, B. D.; Wert, E. C.; Snyder, S. A. Evaluation of a photocatalytic reactor membrane pilot system for the removal of pharmaceuticals and endocrine disrupting compounds from water. *Water Research* **2009**, *43* (6), 1513–1522.
4. Wert, E. C.; Rosario-Ortiz, F. L.; Snyder, S. A. Effect of ozone exposure on the oxidation of trace organic contaminants in wastewater. *Water Research* **2008**, *43* (4), 1005–1014.

5. Trenholm, R. A.; Rosario-Ortiz, F. L.; Snyder, S. A. Analysis of formaldehyde formation in wastewater using on-fiber derivatization solid phase extraction gas chromatography mass spectrometry. *Journal of Chromatography A* **2008**, *1210* (1), 25–29.
6. Rosario-Ortiz, F. L.; Mezyk, S. P.; Wert, E.; Snyder, S. A. Effect of pre-oxidation on the absolute rate constants between hydroxyl radical and effluent organic matter. *Journal of Applied Oxidation Technologies* **2008**, *11* (3), 529–535.
7. Rosario-Ortiz, F. L.; Mezyk, S. P.; Doud, D. F. R.; Snyder, S. A. Quantitative correlation of absolute hydroxyl radical rate constants with non-isolated effluent organic matter bulk properties in water. *Environmental Science and Technology* **2008***, 42* (16), 5924–5930.

APPENDIX C

REFERENCES

Acero, J. L.; Stemmler, K.; Von Gunten, U. Degradation kinetics of atrazine and its degradation products with ozone and OH radicals: A predictive tool for drinking water treatment. *Environmental Science & Technology* **2000,** *34,* 591–597.

Acero, J. L. and Von Gunten, U. Characterization of oxidation processes: Ozonation and the AOP O-3/H2O2. *Journal of American Water Works Association* **2001,** *93,* 90–100.

American Public Health Association (APHA). Standard Methods for the Examination of Water and Wastewater, 20th ed. American Public Health Association, American Water Works Association,Water Environment Federation: Washington DC, 1998.

Bader, H. and Hoigne, J. Determination of ozone in water by the indigo method: A submitted standard method. *Ozone: Science and Engineering* **1982,** *4,* 169–176.

Baker, A. Fluorescence excitation-emission matrix characterization of some sewage-impacted rivers. *Environmental Science and Technology* **2001,** *35,* 948–953.

Becker, W. C. and O'Melia, C. R. Ozone, oxalic acid, and organic matter molecular weight—Effects on coagulation. *Ozone-Science & Engineering* **1996,** *18,* 311–324.

Benitez, F. J.; Acero, J. L.; Real, F. J. Degradation of carbofuran by using ozone, UV radiation and advanced oxidation processes. *Journal of Hazardous Materials* **2002,** *B89,* 51–65.

Bolton, J. R.; Bircher, K. G.; Tumas, W.; Tolman, C. A. Figures-of-merit for the technical development and application of advanced oxidation technologies for both electric- and solar-driven systems (IUPAC Technical Report). *Pure and Applied Chemstry* **2001,** *73,* 627–637.

Bolton, J. R. and Linden, K. G. Standardization of methods for fluence (UV dose) determination in bench-scale UV experiments. *Journal of Environmental Engineering* **2003,** *129,* 209–215.

Buffle, M.-O.; Schumacher, J.; Meylan, S.; Jekel, M.; von Gunten, U. Ozonation and advanced oxidation of wastewater: Effect of O_3 dose, pH, DOM and HO Scavengers on ozone decomposition and HO generation. *Ozone: Science and Engineering* **2006a,** *28,* 247–259.

Buffle, M.-O., Schumacher, J., Salhi, E., Jekel, M. and von Gunten, U. Measurement of the initial phase of ozone decomposition in water and wastewater by means of a continuous quench-flow system: Application to disinfection and pharmaceutical oxidation. *Water Research* **2006b,** *40,* 1884–1894.

Buffle, M. O.; Schumacher, J.; Meylan, S.; Jekel, M.; von Gunten, U. Ozonation and advanced oxidation of wastewater: Effect of O_3 dose, pH, DOM and $HO^{\bullet}$ scavengers on ozone decomposition and $HO^{\bullet}$ generation. *Ozone-Science & Engineering* **2006c,** *28,* 247–259.

Buxton, G.V.; Greenstock, C. L.; Helman, W. P.; Ross, A. B. Critical review of rate constants for reactions of hydrated electrons, hydrogen atom and hydroxyl radicals

(·OH/·O-) in aqueous solutions. *Journal of Physical and Chemical Reference Data* **1988,** *17,* 513–886.

Elovitz, M. S. and von Gunten, U. Hydroxyl radical ozone ratios during ozonation processes. I. The R_{ct} concept. *Ozone-Science & Engineering* **1999,** *21,* 239–260.

Hengesbach, B.; Schoenen, D.; Hoyer, O.; Bernhardt, H.; Mark, G.; Schuchmann, H. P.; Von Sonntag, C. UV disinfection of drinking water—The question of bacterial regrowth and the photolytic degradation of biogenic high-molecular-weight substances. *Journal of Water Supply: Research and Technology-AQUA* **1993,** *42,* 13–22.

Hesse, S.; Kleiser, G; Frimmel, F. H. Characterization of refractory organic substances (ROS) in water treatment. *Water Science and Technology* **1999,** *40,* 1–7.

Huber, M. M.; Canonica, S.; Park, G. Y.; Von Gunten, U. Oxidation of pharmaceuticals during ozonation and advanced oxidation processes. *Environmental Science & Technology* **2003,** *37,* 1016–1024.

Huber, M. M.; Gobel, A.; Joss, A.; Hermann, N.; Loffler, D.; McArdell, C. S.; Ried, A.; Siegrist, H.; Ternes, T. A.; von Gunten, U. Oxidation of pharmaceuticals during ozonation of municipal wastewater effluents: A pilot study. *Environmental Science & Technology* **2005a,** *39,* 4290–4299.

Huber, M.M., Korhonen, S., Ternes, T.A. and von Gunten, U. Oxidation of pharmaceuticals during water treatment with chlorine dioxide. *Water Research* **2005b,** *39,* 3607–3617.

Huber, S.A. Evidence for membrane fouling by specific TOC constituents. *Desalination* **1998,** *119,* 229–234.

Jansen, R. H. S.; Zwijnenburg, A.; Van Der Meer, W. G. J.; Wessling, M. Outside-in trimming of humic substances during ozonation in a membrane contactor. *Environmental Science & Technology* **2006,** *40,* 6460–6465.

Klassen, N.V.; Marchington, D; McGowan, H. C. E. H_2O_2 determination by the I_3^- method and by $KMnO_4$ titration. *Analytical Chemistry* **1994,** *66,* 2921–2925.

Larson, R. A. and Zeep, R. G. Reactivity of the carbonate radical with aniline derivatives. *Environmental Toxicology and Chemistry* **1988,** *7,* 265–274.

Lee, N.; Amy, G.; Croué, J.; Buisson, H. Identification and understanding of fouling in low-pressure membrane (MF/UF) filtration by natural organic matter (NOM). *Water Research* **2004,** *38,* 4511–4523.

Lopez, A.; Bozzi, A.; Mascolo, G.; Ciannarella, R.; Passino, R. UV and H_2O_2/UV degradation of a pharmaceutical intermediate in aqueous solution. *Annali Di Chimica* **2002,** *92,* 41–51.

Lopez, A.; Bozzi, A.; Mascolo, G.; Kiwi, J. Kinetic investigation on UV and UV/H_2O_2 degradations of pharmaceutical intermediates in aqueous solution. *Journal of Photochemistry and Photobiology A: Chemistry* **2003,** *156,* 121–126.

MacDonald, B. C.; Lvin, S. J.; Patterson, H. Correction of fluorescence inner filter effects and the partitioning of pyrene to dissolved organic carbon. *Analytica Chimica Acta* **1997,** *338,* 155–162.

McKnight, D. M.; Boyer, E.W.; Westerhoff, P. K.; Doran, P. T.; Kulbe, T.; Andersen, D. T. Spectrofluorometric characterization of dissolved organic matter for indication of precursor organic material and aromaticity. *Limnology and Oceanography* **2001,** *46,* 38–48.

Meulemans, C. C .E. The basic principles of UV disinfection of water. *Ozone: Science and Engineering* **1987,** *9,* 299–314.

Park, J. S.; Choi, H.; Cho, J. Kinetic decomposition of ozone and para-chlorobenzoic acid (pCBA) during catalytic ozonation. *Water Research* **2004,** *38,* 2285–2292.

Pi, Y.; Schumacher, J.; Jekel, M. The use of para-chlorobenzoic acid (pCBA) as an ozone/hydroxyl radical probe compound. *Ozone-Science & Engineering* **2005,** *27,* 431–436.

Rosario-Ortiz, F. L.; Mezyk, S. P;, Doud, D. F. R.; Snyder, S. A. Quantitative correlation of absolute hydroxyl radical rate constants with non-isolated effluent organic matter bulk properties in water. *Environmental Science & Technology* **2008,** *42,* 5924–5930.

Rosario-Ortiz, F. L.; Snyder, S.; Suffet, I. H. Characterization of dissolved organic matter in drinking water sources impacted by multiple tributaries. *Water Research* **2007a,** *41,* 4115–4128.

Rosario-Ortiz, F. L.; Snyder, S.; Suffet, I. H. Characterization of the polarity of natural organic matter under ambient conditions by the polarity rapid assessment method (PRAM). *Environmental Science & Technology* **2007b,** *41,* 4895–4900.

Rosenfeldt, E. J. and Linden, K. G. Degradation of endocrine disrupting chemicals bisphenol A, ethinyl estradiol, and estradiol during UV photolysis and advanced oxidation processes. *Environmental Science & Technology* **2004,** *38,* 5476–5483.

Rosenfeldt, E. J. and Linden, K. G. The $R_{OH,UV}$ concept to characterize and the model UV/H_2O_2 process in natural waters. *Environmental Science & Technology* **2007,** *41,* 2548–2553.

Rosenfeldt, E. J.; Melcher, B.; Linden, K. G. UV and UV/H_2O_2 treatment of methyllisoborneol (MIB) and geosmin in water. *Journal of Water Supply Research and Technology-Aqua* **2005,** *54,* 423–434.

Sachse, A.; Babenzien, D.; Ginzel, G.; Gelbrecht, J.; Steinberg, C. E. W. Characterization of dissolved organic carbon (DOC) in a dystrophic lake and an adjacent fen. *Biogeochemistry* **2001,** *54,* 279–296.

Sachse, A.; Henrion, R.; Gelbrecht, J.; Steinberg, C. E. W. Classification of dissolved organic carbon (DOC) in river systems: Influence of catchment characteristics and autochthonous processes. *Organic Geochemistry* **2005,** *36,* 923–935.

Sharpless, C. M. and Linden, K. G. Experimental and model comparisons of low- and medium-pressure Hg lamps for the direct and H_2O_2 assisted UV photodegradation of N-nitrosodimethylamine in simulated drinking water. *Environmental Science & Technology* **2003,** *37,* 1933–1940.

Shon, H. K.; Vigneswaran, S.; Snyder, S. A. Effluent organic matter (EfOM) in wastewater: Constituents, effects, and treatment. *Critical Reviews in Environmental Science and Technology* **2006,** *36,* 327–374.

Snyder, S. A.; Wert, E. C.; Lei, H.; Westerhoff, P; Yoon, Y. Evaluation of conventional and advanced treatment processes for the removal of endocrine disruptors and pharmaceutically active compounds. AWWARF: Denver, CO, 2007.

Snyder, S. A.; Wert, E. C.; Rexing, D. J.; Zegers, R. E.; Drury, D. D. Ozone oxidation of endocrine disruptors and pharmaceuticals in surface water and wastewater. *Ozone: Science and Engineering* **2006,** *28,* 445–460.

Trenholm, R. A.; Vanderford, B. J.; Snyder, S. A. On-line solid phase extraction LC-MS/MS analysis of pharmaceuticals indicators in water: A green alternative to conventional methods. *Talanta* **2009,** *79,* 1425–1432.

Vanderford, B. J.; Rosario-Ortiz, F. L.; Snyder, S. A. Analysis of p-chlorobenzoic acid in water by liquid chromatography/tandem mass spectrometry. *Journal of Chromatography A* **2007,** *1164,* 219–223.

Vanderford, B. J. and Snyder, S. Analysis of pharmaceuticals in water by isotope dilution liquid chromatography/tandem mass spectrometry. *Environmental Science & Technology* **2006a,** *40,* 7312–7320.

Vanderford, B. J. and Snyder, S. A. Analysis of pharmaceuticals in water by isotope dilution liquid chromatography/tandem mass spectrometry. *Environmental Science & Technology* **2006b,** *40,* 7312–7320.

von Gunten, U. Ozonation of drinking water: Part I. Oxidation kinetics and product formation. *Water Research* **2003,** *37,* 1443–1467.

von Sonntag, C. The basics of oxidants in water treatment. Part A: OH radicals reactions. *Water Science and Technology* **2007,** *55,* 19–23.

von Sonntag, C. and Schuchmann, H.-P. UV disinfection of drinking water and by-product formation—Some basic considerations. *Journal of Water Supply: Research and Technology* **1992,** *41,* 67–74.

Vuorio, E.; Vahala, R.; Rintala, J.; Laukkanen, R. The evaluation of drinking water treatment performed with HPSEC. *Environment International* **1998,** *24,* 617–623.

Weishaar, J. L.; Aiken, G. R.; Bergamaschi, B. A.; Fram, M. S.; Fujii, R.; Mopper, K. Evaluation of specific ultraviolet absorbance as an indicator of the chemical composition and reactivity of dissolved organic matter. *Environmental Science & Technology* **2003,** *37,* 4702–4708.

Wert, E. C.; Rosario-Ortiz, F. L.; Drury, D. D.; Snyder, S. A. Formation of oxidation byproducts from ozonation of wastewater *Water Research* **2007,** *41,* 1481–1490.

Westerhoff, P.; Mezyk, S. P.; Cooper, W. J.; Minakata, D. Electron pulse radiolysis determination of hydroxyl radical rate constants with Suwannee River fulvic acid and other dissolved organic matter isolates. *Environmental Science & Technology* **2007,** *41,* 4640–4646.

Whitham, K.; Lyons, S.; Miller, R.; Nett, D.; Treas, P.; Zante, A.; Fessenden, R. W.; Thomas, M. D.; Wang, Y. Linear accelerator for radiation chemistry research at Notre Dame, *Proceedings from the Particle Accelerator Conference*, Dallas, TX, 1995.

Zhang, H.; Yamada, H.; Tsuno, H. Removal of endocrine-disrupting chemicals during ozonation of municipal sewage with brominated byproducts control. *Environ. Sci. Technol.* **2008,** *42,* 3375–3380.

Advancing the Science of Water Reuse and Desalination

WATEREUSE RESEARCH

1199 North Fairfax Street, Suite 410
Alexandria, VA 22314 USA
(703) 548-0880
Fax (703) 548-5085
E-mail: Foundation@WateReuse.org
www.WateReuse.org/Foundation